THE MUON COMPONENT OF EXTENSIVE AIR SHOWERS

by

J. C. EARNSHAW, B.Sc.

A Thesis submitted to the University of Durham
in accordance with the Regulations for
the Degree of Doctor of Philosophy

Department of Physics
University of Durham

August 1968

ABSTRACT

This thesis describes the determination of various characteristics of the muon component of extensive air showers (EAS) using the magnet spectrograph situated at the British Universities joint air shower array at Haverah Park, near Harrogate.

After an introduction concerning the relevance of muon studies to current problems in the studies of air showers (Chapter 1), the air shower arrays and the magnet spectrograph are briefly described and a summary given of the analysis of the data from each (Chapters 2 and 3).

The lateral density distribution of muons of momentum above 1 GeV/c is determined (Chapter 4) for use in the normalization of the measured momentum spectrum of muons. The dependence of the number of muons on shower size is found to be constant over a wide range of size.

The momentum spectrum of muons in air showers is determined as a function of distance from the shower core. The variation of spectrum with shower size and zenith angle is also investigated. These measurements extend beyond previous experimental work (Chapter 5), and do not agree with theoretical predictions. All the features can be accounted for by a careful treatment of air showers initiated by primary particles of mass greater than ten (Chapter 6), provided the multiplicity of pions follows an $E^{0.5}$ law for high energy.

The average heights of origin of muons of various momenta are determined by two different methods. It is further shown that the muons originate at heights compatible with the modified model (Chapter 7).

The implications of these observations are discussed in Chapter 8 and, finally, experiments are suggested which might confirm the proposed model.

PREFACE

This thesis contains an account of work done at Haverah Park by the author, a research student in the Physics Department of the University of Durham, under the supervision of Professor G. D. Rochester, F. R. S.

Extensive air showers are detected at Haverah Park by arrays of Cherenkov detectors. The larger arrays are operated by workers from Leeds University and measure the characteristics of rather large showers.

The main experimental equipment used in the present work, the magnet spectrograph, was designed and constructed by Professor G. D. Rochester and Dr. K. E. Turver in 1964, and the two smaller EAS arrays were built by Dr. K. E. Turver and Mr. A. B. Walton in 1965. These workers were joined by Mr. K. J. Orford and the author in September, 1965.

Reports of the work were presented at the International Conferences on Cosmic Rays held in London (1965) and Calgary (1967), and also in the Proceedings of the Physical Society in 1967.

The author assisted Mr. A. B. Walton in the development of the simplified method of EAS analysis described in Section 2-2.3, and was entirely responsible for the work presented in Chapter 4. Together with his colleagues the author shared responsibility for the routine operation of the spectrograph and the treatment of the data.

Mr. K. J. Orford derived the muon momentum spectrum as a function of distance from the shower core. The checks on the EAS analysis (5-3.1) and the analysis of the momentum spectrum as a function of shower size and zenith angle were carried out by the author. Mr. A. B. Walton and Dr. K. E. Turver calculated the geomagnetic deflection of muons and their work was extended by the author. The analysis of the angular deviation of muons from the core direction was carried out by the author.

CONTENTS

Page

CHAPTER 1

INTRODUCTION TO EXTENSIVE AIR SHOWERS

1-1. Introduction

1-1.1 Cosmic Rays

The earth is continuously exposed to radiation varying widely in origin and in nature. That portion of this radiation called 'cosmic rays' is essentially particulate, the particles being atomic nuclei. The primary cosmic rays interact strongly with the nuclei of the atoms in the atmosphere. The study of these interactions and the secondary cosmic rays to which they give rise can yield information about the character of the interactions and the nature and properties of the primary particles themselves.

1-1.2 Extensive air showers

The secondary particles from the interaction of a primary particle may initiate further interactions by a cascade process which continues until the energies of the strongly interacting particles are too low to initiate further interactions. If the primary particle is of sufficient energy, the cascade of particles will continue to sea level and form an 'extensive air shower' which may contain millions of particles spread over an area of several square kilometers.

The particles produced in the nuclear interactions comprise pions, kaons and baryons. They are mainly confined to a region

rather close to the axis of the shower, known as the core. These particles have nuclear interaction lengths in air of about 100 gm cm^{-2} and they may either initiate further nuclear interactions, thus continuing the cascade, or decay to other types of particles, which do not contribute to the further development of the nuclear cascade.

The charged pions and kaons decay to muons. Because of relativistic time dilation the probability of pion or kaon decay is greatest at low atmospheric densities, and thus the muons tend to originate rather early in the nuclear cascade, and because of their low probability for decay they mainly survive to the bottom of the atmosphere. The muons suffer Coulomb scattering in the atmosphere and are deflected by the geomagnetic field, but the probability of catastrophic collision is very low and thus the muons, especially those of high energy, retain information about their point of production.

Neutral pions have an extremely short lifetime and, even when moving with velocities close to 'c', decay promptly into photons which initiate electromagnetic cascades, whose development is characterised by a 'radiation length' of 38 gm cm^{-2} in air. As long as the nuclear-active particles are sufficiently energetic to initiate further interactions, the nuclear cascade injects energy into the electron-photon component of the shower via neutral pions.

1-2. Current problems in the study of E.A.S.

1-2.1 The primary spectrum

The energy spectrum of primary cosmic rays extends from some few GeV to a hitherto undetected upper limit larger than 10^{19} eV. This vast energy range cannot all be surveyed by one technique. At energies of a few GeV the spectrum is well defined by the limitation of the flux by the earth's magnetic field, while above this region the interactions of the primary particles may be observed in nuclear emulsions until, at energies above some 10^{14} eV the flux of particles becomes so low that direct observation becomes almost impossible. The primary energy spectrum may also be estimated by studying the secondary cosmic rays comparatively deep in the atmosphere. High energy particles cause extensive air showers deep in the atmosphere. Given a sufficient understanding of the processes involved in the evolution of an air shower, its size can yield an estimate of the energy of the initiating particle. Thus for energies above 10^{14} eV, the energy spectrum of cosmic rays may be deduced from the size spectrum of air showers. This estimation is open to systematic errors resulting from an incomplete knowledge of the processes involved in the shower, but despite these difficulties a wide measure of agreement has been reached on the form of the spectrum. Most estimates agree that for showers at maximum development the primary energy in GeV is numerically equal to twice the number of particles in the shower.

An alternative approach is to estimate the energy carried by the

shower at the observation level from the measured energy spectra of the various components. The energy lost by the shower above the observation level may be estimated from observations on the atmospheric Cherenkov light emitted by the relativistic shower particles. For example Zatsepin et al. (1964) deduced that a shower containing 3.5×10^5 particles at mountain altitudes corresponded to a primary energy of $(6 \,^{+\,1.8}_{-\,1.1}) \times 10^{14}$ eV, but a major uncertainty in this estimation was the lack of detailed knowledge of the muon energy spectrum at energies above 20 GeV.

The primary spectrum shown in Figure 1.1 has been deduced from all available date (Greisen 1966a). Above 10^{14} eV the spectrum is a reflection of the number spectrum of air showers. The change of slope at a shower size corresponding to a primary energy of some 10^{15} eV is now well established experimentally. The reversion of the energy spectrum to a lower gradient at energies above about 5×10^{18} eV is much less well established and is currently being examined by several groups.

The lower inflexion has been explained as a result of a failure in the containment of cosmic rays by the magnetic field of the galaxy, occurring at a constant magnetic rigidity. Linsley (1964) suggests that the upper change of gradient may be due to the total failure of the galactic containment leading to a predominance of extra-galactic cosmic rays. Alternative explanations of the lower 'kink' have been proposed, such as a fundamental change in the

FIGURE 1.1

The integral spectrum of primary cosmic rays (Greisen 1966a).

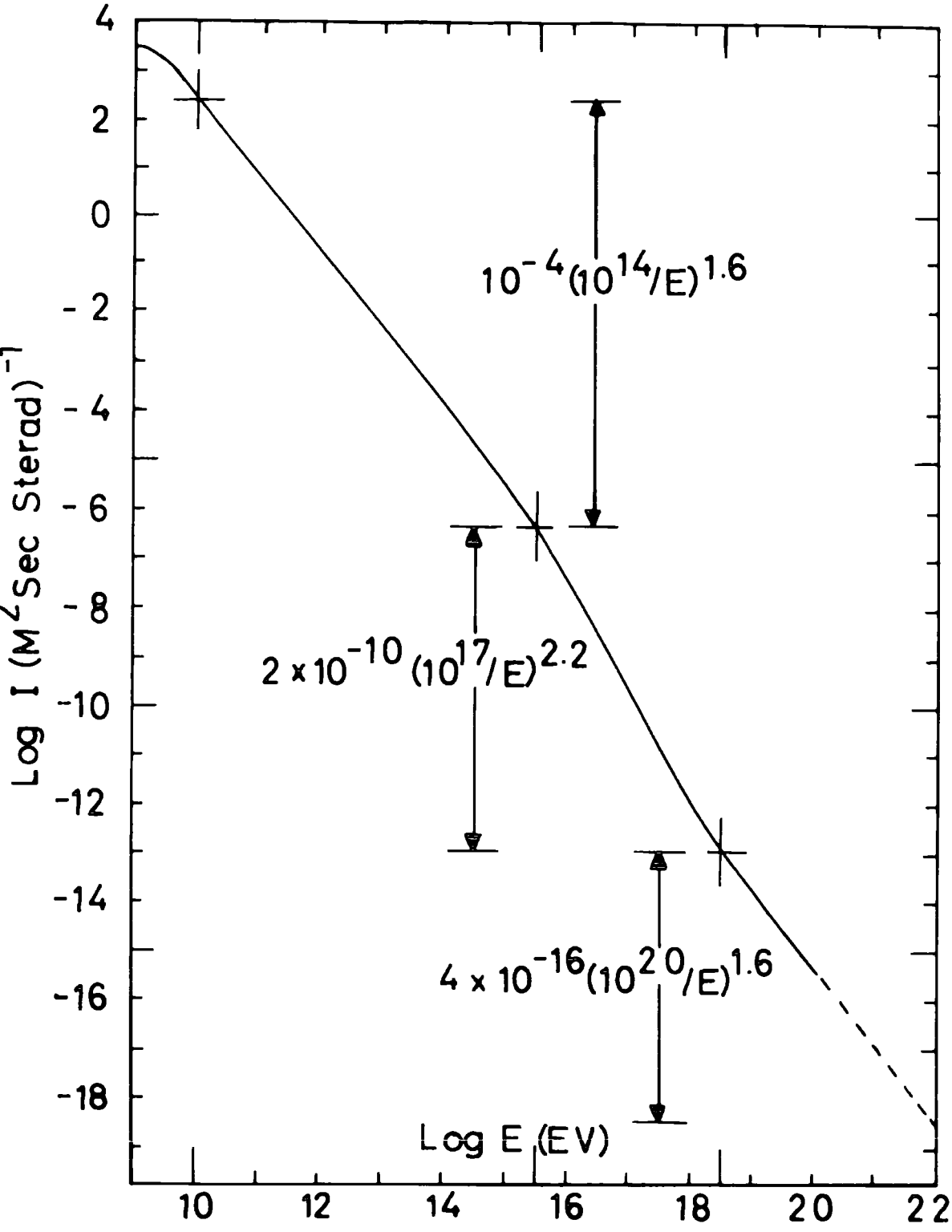
4
2
0
- 2
- 4
- 6
- 8
-10
-12
-14
-16
-18
Log I (M^{2}Sec Sterad)$^{-1}$
$10^{-4}(10^{14}/E)^{1.6}$
$2 \times 10^{-10}(10^{17}/E)^{2.2}$
$4 \times 10^{-16}(10^{20}/E)^{1.6}$
Log E (EV)
10
12
14
16
18
20
22

nuclear interactions at energies above 10^{13} eV (Nikolskii 1967).

The discovery of an isotropic universal black-body radiation of temperature approximately 3°K (e.g. Roll and Wilkinson 1967) has placed all these explanations in doubt. Greisen (1966b) has placed a rather firm estimate on the maximum energy which a cosmic ray may possess, rendering the observation by Linsley of a flattening of the energy spectrum and of one event of energy 10^{20} eV rather surprising. Hillas (1967a,b) suggests that if current theories on the evolution of the universe are correct this black-body radiation may also explain the irregularities in the primary energy spectrum.

The choice of which, if any, of these suggestions is correct depends on the detailed observation of the characteristics of air showers over the region of primary energy covering the 'kinks'. Any information on the mass composition of the primary cosmic rays at the relevant energies would be of great interest in this context, as the predictions of the various models are rather different.

1-2.2 The primary composition

At energies below the air shower region the mass composition of the primary particles has been determined by many workers by direct observation using nuclear emulsions (see Table 1.1, after Ginzburg and Syrovatskii 1964). Observations of events of extreme energies in emulsions indicate that the primary composition may be largely unchanged for particles of energy up to 2×10^{14} eV (McCusker et al. 1968).

TABLE 1.1

COMPOSITION OF PRIMARY COSMIC RAYS

Group	Ā	Percentage of nuclei with a fixed energy per nucleon
P	1	93
α	4	6.3
L	10	0.14
M	14	0.42
H	31	0.14
VH	51	0.04

At greater energies definite conclusions cannot be drawn at the present time. However, the current picture of the composition of the primary beam is as follows. The composition remains substantially unchanged from that shown in the table to primary energies of about 2×10^{15} eV. As the energy rises above this value the magnetic containment of the cosmic rays within the galaxy breaks down and first protons and then particles of progressively greater mass can escape, until at about 10^{17} eV it is thought that even the heaviest nuclei are not trapped in the galaxy. Beyond this energy the metagalactic cosmic rays predominate, giving a pure beam of protons.

These conclusions are rather tentative and the experimental

basis for them will now be examined. The constancy of the gradient of the number spectrum of air showers to a size equivalent to a primary energy of some 10^{15} eV indicates that the composition must be largely unchanged, whilst the change in gradient at such a size is that expected on the hypothesis of a magnetic rigidity cut-off in the primary cosmic rays. This is supported by observations of the density spectrum of air showers which exhibits a steepening at large densities (Swinson and Prescott 1966). The variation with altitude of the 'join point' of this spectrum is consistent with the behaviour expected if the energy per nucleon available to the primary particles terminates at about 2×10^{15} eV (Norman 1956, McCusker et al., 1968).

Further evidence of the constancy of the composition to energies of 10^{15} eV is provided by an analysis of the fluctuations in the intensity of atmospheric Cherenkov light associated with air showers of primary energy less than 10^{15} eV, observed at mountain altitudes by Zatsepin et al. (1964).

Showers with multiple cores have been studied experimentally and theoretically by several groups (e.g. Bray et al., 1966, Matano et al., 1967, Shibata et al., 1966, Thielheim and Karius 1966). The theoretical studies suggest that such showers could be due to primary particles of large atomic weight. The observation of an increasing proportion of showers with multi-core structure as the primary energy increases beyond about 10^{15} eV (McCusker et al., 1968) may then be

interpreted as evidence for the variation of composition with energy outlined above. However the experimental results show a very wide degree of discord, apparently dependent to a large extent upon the method of detection. Thus it is not possible at present to deduce unambiguous information from the work on this phenomenon.

From an analysis of the fluctuations of the numbers of muons in showers initiated by primary particles of energy greater than 10^{16} eV, Hasegawa et al. (1962) find that an appreciable number of the primary particles are heavy nuclei. It will be shown later in this thesis (Chapter 6) that an interpretation of the results of the present experiment indicates that the effective atomic mass of particles of energy 2×10^{17} eV is probably greater than 10.

Turning now to primary energies greater than about 10^{17} eV, two groups have examined the fluctuations in the proportion of muons in showers at maximum development (Linsley and Scarsi 1962a, Toyoda et al., 1966) and conclude that the experimental data is incompatible with that expected for the composition of Table 1.1, while it is compatible with a pure beam of protons or particles of greater mass. By a consideration of the fluctuations of the age parameter of the showers, Linsley and Scarsi ruled out heavy particles, for which these fluctuations should be much narrower than observed. It has thus been concluded that at these great energies the primary cosmic rays are protons.

A comparison of the cosmic ray abundances of Table 1.1 with the

so-called 'cosmic abundances' (Suess and Urey 1956) indicates that the cosmic rays are much richer in nuclei heavier than helium. Colgate (1966) predicts that supernovae should accelerate particles to give an abundance similar to cosmic rays up to iron. Beyond this element the abundances of the cosmic rays should be similar to the 'cosmic abundances', a prediction confirmed by the measurements of Fowler et al. (1967).

1-2.3 Nuclear interactions at air shower energies

The nuclear cascade plays an essential role in air showers, but, due to the complexity of the phenomenon, it is very difficult to deduce the nature of the nuclear interactions from the characteristics of air showers. However, a measure of agreement has been reached on some features of very high energy interactions.

Estimates of the mean free path for nuclear interaction of protons in air give a value of about 80 gm cm^{-2} (Matano et al., 1964). The distribution of transverse momentum and its mean value observed for high energy hadrons (Hasegawa et al., 1966) is similar to that found for pions in accelerator experiments and also in cosmic ray jets (Imaeda 1967). Occasionally very large values of transverse momentum are observed, an observation perhaps connected with the fact that the surviving nucleon can have great transverse momentum (Akashi et al., 1966). The inelasticity of the collisions of nucleons with air nuclei has been shown to be distributed from 0.2 to 0.9, with a mean value of 0.54 (Winn et al., 1965); the inelasticity of

collisions of pions with air nuclei appears much closer to unity. The data available to date on high energy interactions suggest that a fireball model with some contribution to the pion population from baryon isobars is most likely.

Extrapolation of the information on nuclear interactions available at lower energies to air shower energies is hazardous in view of the vast energy range involved. Interactions in the region of energy studied using accelerators or cosmic ray jets in emulsion stacks give rise to most of the particles in an air shower, but very high energy particles or those particles originating from the first interactions of the cascade will be produced in ultra-high energy interactions and will thus be subject to the extrapolation problems mentioned above.

1-3 The muon component of air showers

New data about the primary particles or nuclear interactions can only be inferred from the study of air showers by comparison of experimental data with the predictions of theories based upon many uncertainly known parameters. The muons in air showers are closely related to the secondaries of the nuclear interactions, and, while they constitute only a few per cent of all the particles in a shower, they carry much of the energy of the shower and are relatively numerous at distances of several hundred metres from the core. Muons are easily distinguished from the electrons at these distances by their superior penetrating power but nearer the core there is some danger of confusion with the nuclear interacting component.

If the mass of the primary particles varies as suggested above, one consequence will be a variation in the proportions of muons in showers of various energies. Hillas (1966) suggests that the densities of high energy muons may be very sensitive to the primary mass. Such high energy muons will be secondary to particles produced in the very high energy interactions in the core of the shower. Thus the muon component is potentially most informative of the characteristics of the shower, the nature of the primary and the nuclear cascade. These facts have for some time stimulated studies, both experimental and theoretical.

The theoretical studies have become comprehensive in recent years and predict average lateral distributions for varying energy thresholds, energy spectra at various distances and heights of origin of the muons. The fluctuations in these and other parameters have also been estimated. To date, the experimental measurements have been rather restricted, lateral distributions or energy spectra being measured over restricted distance or energy ranges. These measurements have succeeded in reaching some agreement, but comparison with theoretical predictions shows discrepancies throughout the regions of distance and energy expected to be influenced strongly by the nuclear cascade. As the distance from the core increases the energy of the muons falling at this distance and originating high in the atmosphere decreases (Hillas 1966), and thus at any distance it is possible to define energies above which the muon component

should be related directly to the very early interactions of the nuclear cascade.

For the fullest use to be made of such comparisons of measurements on the muon component with theoretical suggestions, and hence with the assumed natures of the nuclear interactions and the primary particles, detailed information on the characteristics of muons of different energies is needed over wide ranges of various shower parameters. At Haverah Park showers of a wide range of size are detected and in 1964 a magnet spectrograph was constructed there for the primary purpose of measuring the momentum spectrum of muons between 1 and 100 GeV/c at distances varying from 10 m to 1000 m from the cores of showers of size between 10^5 and 2×10^8 particles.

In addition to this principal measurement several other aspects of the muon component have been studied with this instrument. The lateral distribution of muons with momentum greater than 1 GeV/c has been determined to distances such that it becomes sensitive to the upper portion of the nuclear cascade. Again, the heights of origin of muons detected at distances from the core greater than 100 m have been investigated for large showers by two different techniques.

CHAPTER 2

THE DETECTION OF EXTENSIVE AIR SHOWERS AT HAVERAH PARK

2.1 The Extensive Air Shower Arrays

The air shower arrays at Haverah Park are assemblies of deep diffused Cherenkov light detectors (Tennent 1967, a, b). The main 500 m array consists of four units of 34 m^2 of detector, three of which are placed symmetrically round a circle of 500 m radius centred on the fourth unit. The two smaller arrays are of similar geometry of spacing 50 m and 150 m respectively, each having 4.5 m^2 detector area at the outer stations and utilizing 9 m^2 of the centre detector of the 500 m array as the central detector. A recent development is a large array, consisting of six arrays (50 m and 150 m spacings), of similar geometry to that described above, distributed about the circumference of a circle of radius 2 km centred on the 500 m array. The situation of these detectors is shown in Figure 2.1, relative to the coordinate system used.

The individual detectors are of area 2.25 m^2 and are 120 cm deep, filled with clear water and lined with white Darvic to diffuse the Cherenkov light, which is detected by a photomultiplier. These detectors present large areas and depths to air showers from all directions, resulting in very small fluctuations in the detected signal. The detectors are sensitive to both the penetrating and the soft components of air showers; the dynamic range of the response which can be recorded

FIGURE 2.1

The Haverah Park extensive air shower arrays.

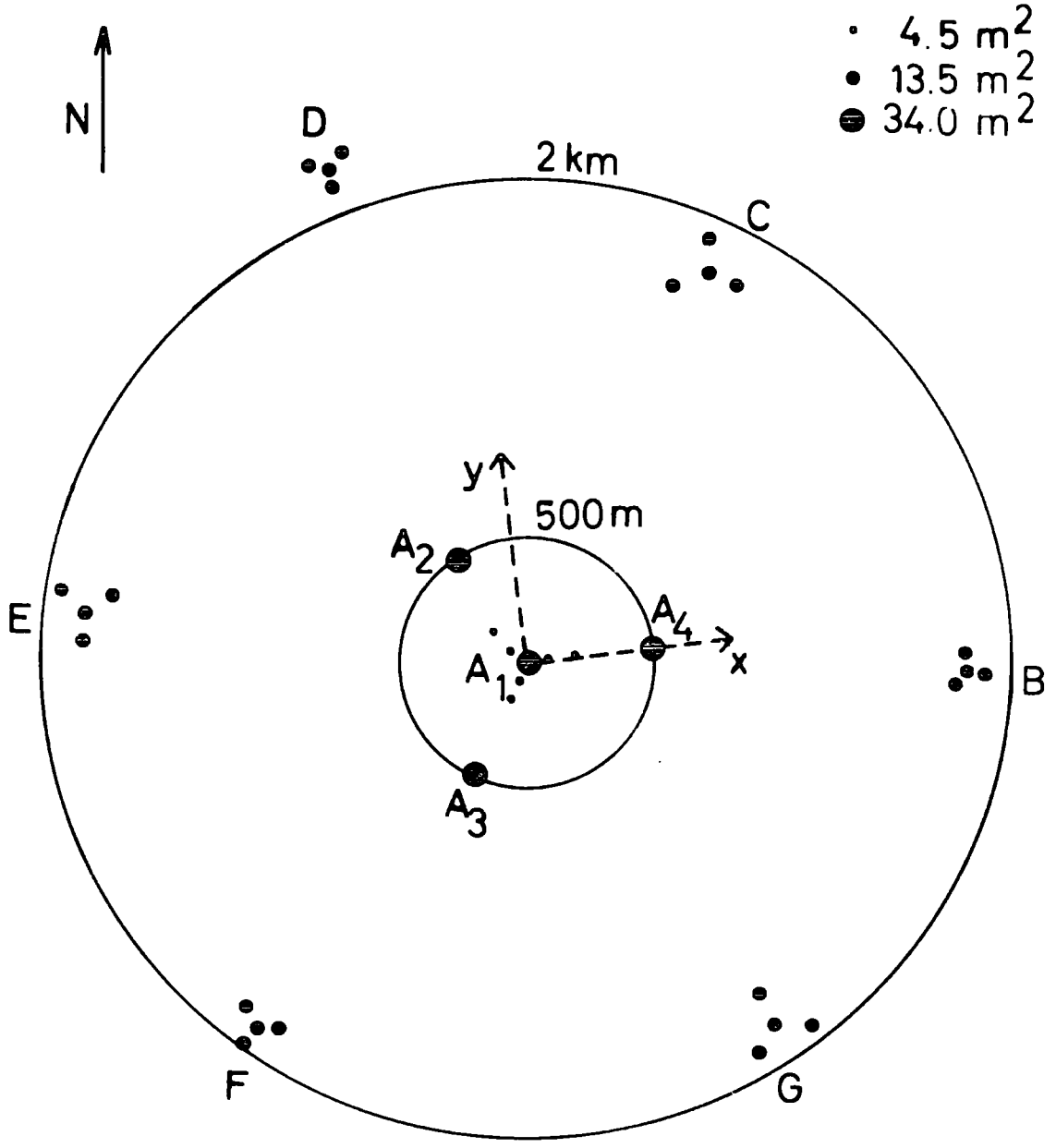
4.5 m2
13.5 m2
34.0 m2
N
D
2 km
C
y
500 m
A2
A4
x
E
A1
B
A3
F
G

is very large. The pulse height of the Cherenkov output is calibrated in terms of the output due to a single vertically incident relativistic muon and is stated in terms of 'equivalent muons'. Whenever a three-fold coincidence above the required trigger level occurs the amplitudes and relative times of arrival of the responses from all the detectors of the array are recorded photographically together with the solar time of occurrence.

Over the period of operation of the muon experiment the 500 m array has maintained an 85% efficiency, recording 43 showers per day, mainly between 10^{17} eV and 10^{18} eV. The zenith angle distribution is rather broad, but only showers with zenith angles less than 40° are used in the muon studies. Such showers form 66% of all showers and have a mean zenith angle of 25°, rather similar to the mean angle of 22° found for the showers accompanying muons measured in the present study. The azimuthal distribution of the showers is slightly asymmetric as the array is tilted from the horizontal 2° towards the north.

2.2 The Analysis of air showers

The 500 m array is triggered whenever the centre detector and two of the outer detectors record more than ten'equivalent muons'. A criterion imposed on the data prior to full analysis, which has recently been removed from the treatment, was that any two of the detectors should have recorded more than 15 equivalent muons. Much of the muon data of the present work has been recorded before this removal.

The full analysis carried out by workers at Leeds University is highly sophisticated and accurate, but this limitation prevented some 40% of the showers with zenith angles less than 40° being analysed. To enable such events to be used in this experiment a simple analysis based on the method of intersecting loci (Allan et al., 1960) has been developed for these unanalysed events. A similar method has been applied to the showers recorded by the two smaller arrays.

2.2.1 The lateral distribution of Cherenkov response

To enable a shower to be analysed the lateral structure function of the detector response must be established. While this can be done for each shower, the individual best fit structure functions have been shown by Suri (1966) to differ only by fluctuations from the mean values. Thus a knowledge of the average structure function is sufficient, this average function being known in the region of distance greater than 150 m from the core from many previous analyses of 500 m showers and at closer distances from the results from several smaller arrays.

The average lateral distribution of the response of the detectors used at Haverah Park is shown in Figure 2.2, where the density of Cherenkov response is related to shower size by

$$D = N \; j(r) \qquad (2.1)$$

the normalization being made at distances from the core less than 20 m by Lillicrap (1963) by a comparison with densities recorded by Geiger counters. For the purposes of shower analysis it is convenient

FIGURE 2.2

The lateral structure function of the response of the Cherenkov detectors.

$$\Delta = Nj\,(r)$$

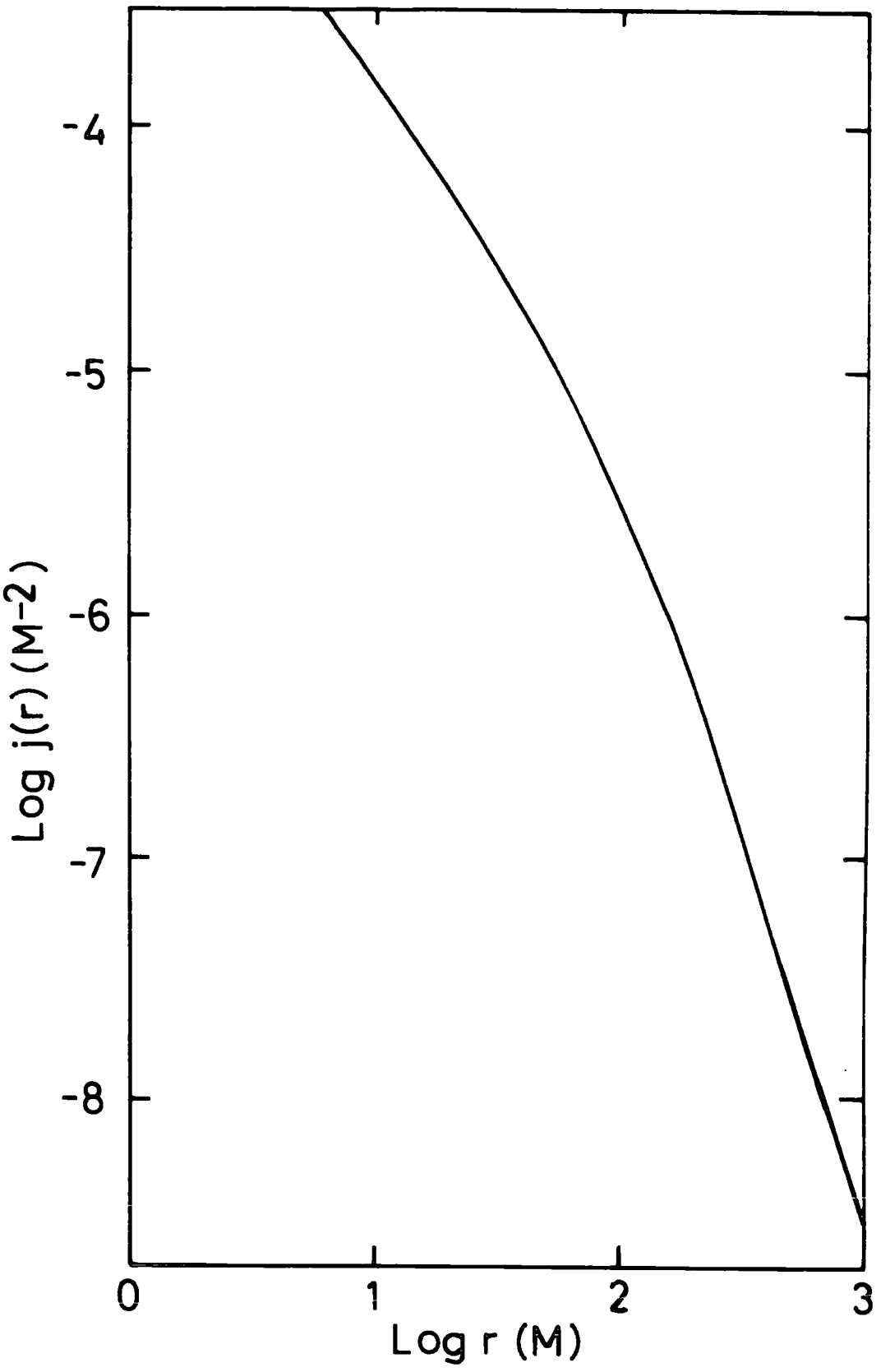
-4
-5
-6
-7
-8
Log j(r) (M-2)
0
1
2
3
Log r (M)

to represent this relation over a restricted range of distance by a power law, as

$$j(r) = K r^{-n} \qquad (2.2)$$

This is a good representation for distances greater than 150 m from the core of the shower, and at these distances the exponent in relation 2.2 varies strongly with zenith angle and less strongly with shower size (Tennent 1967,b).

For the distance and size range covered by the smaller arrays it is convenient to adopt a two exponent form, the median exponent being 2.05 for distances less than 150 m and 2.75 for greater distances for vertical showers. Only showers near the zenith need be considered because of the restrictions on the zenith angles of showers set by the acceptance of the spectrograph.

2.2.2 The Leeds analysis of showers detected by the 500 m array

A brief synopsis only of the full analysis of the showers detected by the 500 m array is given since a more detailed account has been published by Tennent (1967, a).

The direction of the axis of the shower and the radius of curvature of the shower front at the array are found from the relative times of arrival of the pulses at the four stations. Using the average exponent appropriate to the zenith angle of the shower the core position and the constant K in equation 2.2 are optimized.

The estimation of the size of the shower presents many difficulties as the arrays at Haverah Park sample the shower in a quite different fashion from any other arrays. In principle the size is determined by

the normalization constant K, which has been determined under the assumption of a constant power law structure function between 100 and 1000 metres from the core. A quantity, E_{100}, may be defined as the energy lost by the shower on passing through 120 cm depth of water between 100 and 1000 m from the core, that is,

$$E_{100} = \beta K \int_{100}^{1000} 2\pi \; r \; r^{-n} \, dr \quad GeV \qquad \beta = GeV/particle$$

E_{100} can be related to primary energy either by a comparison of rates or by detailed calculation of the development of the shower. Such a calculation has been carried out for a primary proton of a unique energy of 9×10^{16} eV, the primary energy being found for a vertical shower to be $160 \times E_{100}$ (Baxter 1968). A comparison of rates with the primary energy spectrum of Bradt et al. (1966) would suggest a factor of 140, varying somewhat with energy. More extensive calculations will be of great importance in establishing the close connection between E_{100} and primary energy suggested by Suri (1966).

For purposes of comparing characteristics of showers measured at Haverah Park with results from arrays using other detectors, a conversion of E_{100} to shower size (N_e) would be useful. Suri (1966) has compared rates of arrival of showers with those found by Delvaille et al. (1962) and he finds:-

$$N_e \; \alpha \; E_{100}^{1.195}$$

While this is true on average, the wide fluctuations expected in shower size will be absent from E_{100}. Thus effects due to fluctuations will largely be absent from any variation of a parameter with shower size as used in this thesis.

2-2.3 The Durham analysis of showers

The method used to analyse the showers recorded by the smaller arrays and some of the showers detected by the 500 m array is based on the method of intersecting loci. A detailed account of the procedure is given by Walton (1966).

This method can be expressed analytically in very simple terms by virtue of the power law structure function and the geometry of the array. It can be shown that the core position determined by this formulation of the method is liable to errors due to fluctuations in the lowest observed density. However, such erroneous analyses produce very poor fits between expected and observed densities and are thus rejected.

The results of this method of analysis for both the 500 m and 50 m arrays have been checked against the results of the more sophisticated method. The showers triggering the 150 m array have only been analysed by the simpler method, but comparison may be made for showers which trigger both the 150 m array and one of the other two arrays with the analysis of the densities recorded by the other array. The core location for individual showers can fluctuate randomly by about ± 20% from the results of the more accurate analysis, but on average the two methods agree. A comparison of the lateral distributions of muons of momentum greater than 1 GeV/c for 500 m showers of size between 10^7 and 2×10^7 particles which (a) have been accepted for analysis under the criterion mentioned in section 2-2 or which (b) have been rejected on this criterion confirms that the simple

method agrees with the Leeds analysis, on average.

The sizes of the showers detected by the small arrays have been computed using relation 2.1 where j(r) has been normalized after Lillicrap. The timing measurements have proved sufficiently accurate only to distinguish vertical and non-vertical showers. For these showers the cores often fall within 100 m of the array centre and the displacement of the spectrograph from the centre of the array becomes important. This is allowed for in the analysis of these showers.

2-3 Errors in the analysis of showers

In the present work systematic and random errors in air shower analysis must be considered carefully. The random errors of core location are important to the present work as it has been pointed out by many workers that such errors could, if sufficiently large, cause systematic hardening of the momentum spectra of muons at various distances from the core. The errors in the direction of the shower axis are most important in the study of the direction of motion of the muons within the shower.

2-3.1 Systematic errors in core location

For a shower falling closer to a detector in the 500 m array than about 200 m the straight line approximation to j(r) will force the computed core location away from this detector. The magnitude of this effect varies from zero at 200 m from the hut to 20 m at 100 m. Showers falling so near one of the outer huts are unlikely to be

displaced along a line from this hut to the central detector and thus any systematic effect will be small compared to the distance of the core to the centre of the array, which is more than 300 m from the core for such showers. This effect occurs most frequently near the central detector.

At distances from the core less than 150 m, the muon momentum spectrum is changing very slowly with distance and thus the spectrum will be unaffected by this effect. The lateral distribution of muons of momentum above 1 GeV/c derived using the 500 m array will, however, be altered inside 200 m from the core and this effect has been included in the analysis (Chapter 4).

2-3.2 The accuracy of core location

Baxter (1967) has carried out a very detailed analysis of the errors for the 500 m array. A sample of artificial showers with random core location, azimuth and shower size was generated. The particle numbers contributing to the Cherenkov response from the muon and electron-photon components were allowed to fluctuate in a Poissonian fashion and the total Cherenkov response was then subject to random 'errors in measurement'. Baxter concludes that for showers at a zenith angle of 20°, falling not further than 500 m from the centre of the array and not closer than 150 m to any of the detectors the accuracy is ± 40 m. For showers falling further from the centre of the array than 500 m the error is expected to be much larger than this.

2-3.3 Core direction accuracy

Baxter includes in his analysis a timing uncertainty to allow for the sampling of particles in a diffuse shower front by a detector of finite area. He estimates that the uncertainties in determining zenith (θ) and azimuth (ϕ) angles at zenith angles about 20° are:-

$$\sigma_{\theta} = 2.2^{\circ} \quad , \sigma_{\phi} = 7.3^{\circ} \qquad (2.3)$$

These calculations, while intended only to be approximate estimates, are in fact compatible with the observed errors in determining the angular separation of the shower axis and muons.

2-4 Summary

It is seen that for showers detected by the 500 m array a very sophisticated analysis provides rather accurate estimates of the core location, the shower size and the direction of the axis. The errors in the core location are too small to markedly affect the measured muon momentum spectra. In the case of the smaller arrays the core location, and hence the shower size, can be determined to some accuracy, whilst the zenith angle of the shower can only be used to distinguish vertical or non-vertical cases.

CHAPTER 3

THE HAVERAH PARK MUON SPECTROGRAPH

3-1 The spectrograph

The magnet spectrograph used at Haverah Park to measure muons in extensive air showers is broadly similar to those developed by the Durham and Nottingham groups (e.g. Bull et al., 1965 a, Ashton and Wolfendale, 1963) adapted to give a higher area and a wider angle for efficient acceptance of a low flux of air showers. These increases in acceptance necessarily lead to a reduction in the resolving power of the instrument. The spectrograph is shown in Figure 3.1 and is fully described by Walton (1966).

Four trays of visual detectors are situated in pairs above and below a solid iron magnet, enabling incident and emergent directions to be determined for particles traversing the magnet. The instrument is shielded by 5 cm of lead to reduce the contamination of the spectrograph records by electrons. The spectrograph is situated adjacent to the central detector of the 500 m array (at coordinates $x = -5$ m and $y = 10$ m), with the plane in which projected angles can be measured oriented parallel to the line between detectors A1 and A2 of this array.

3-1.1 Description of the magnet

The solid iron magnet is in the form of a rectangular picture frame of low carbon steel plates, with the inside corners of the frame rounded off to extend the region of uniform magnetic field. The area

FIGURE 3.1

The Haverah Park muon spectrograph. The dotted lines across the magnet in the side view indicate the extent of the usable volume of magnetic field.

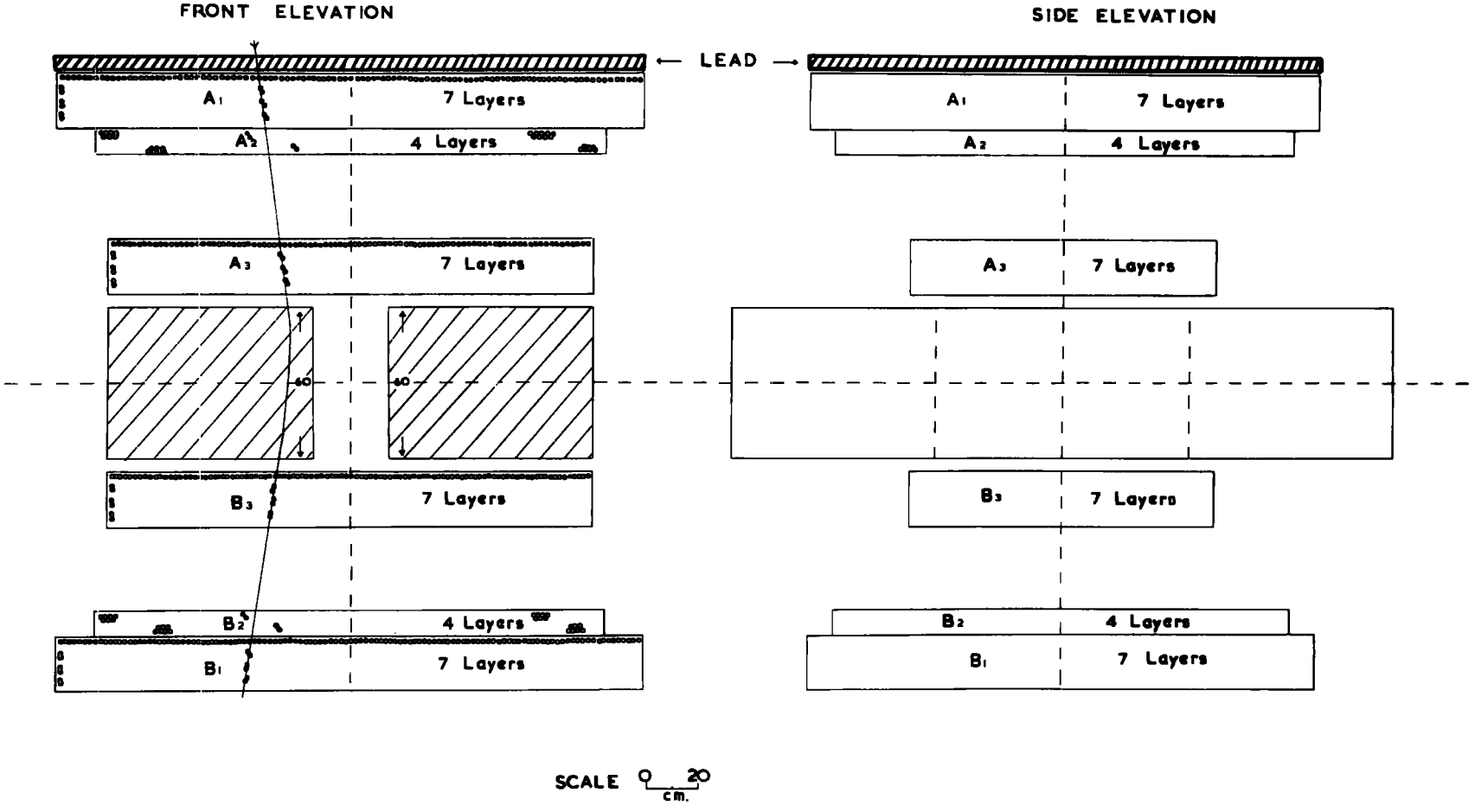
FRONT ELEVATION
SIDE ELEVATION
LEAD
A1
7 Layers
A2
4 Layers
A3
7 Layers
60
60
B3
7 Layers
B2
4 Layers
B1
7 Layers
A1
7 Layers
A2
4 Layers
A3
7 Layers
B3
7 Layers
B2
4 Layers
B1
7 Layers
SCALE 0 20
cm.

presented to vertically incident particles is 1.8 m^2. The magnet comprises 60 cm (474 gm cm^{-2}) thickness of iron. The magnetising field is produced by 325 turns of 14 s.w.g. wire on each arm of the magnet, the windings being connected in series to give a total resistance of 10.7 ohms. A current of 13.9 amps passes through the coils, giving an average field of 14.6 ± 0.1 kilogauss. This field is effectively constant over all the region used in the deflection of particles, the uncertainties being largely due to the lack of uniformity in the thicknesses of the iron plates. The ripple on the field is less than 0.2%.

3-1.2 The visual detectors

The visual detectors used in the spectrograph are flash tubes of internal diameter 1.6 cm filled to a pressure of 600 torr with '98% commercial neon'. They are identical with the 'EAS tubes' developed by Wolfendale and co-workers (Coxell 1961). As it is necessary to allow the air shower arrays to complete their recording before the high voltage pulse is applied to the flash tubes, this pulse is delayed by a passive delay of 20 microseconds. The images of the flash tubes are recorded on a single frame of fast 35 mm film.

The tubes are located in six trays, three above and three below the magnet. Four of these trays (the 'momentum trays', A_1, A_3, B_1, B_3) contain seven layers of tubes each, arranged normal to the front view of the spectrograph in Figure 3.1. This plane is defined as the 'measuring plane' of the spectrograph as it forms the plane

of the magnetic deflection of muons. Within each of these trays four layers of tubes are located in accurately milled dural supports and the lower three of these layers each serves to locate another layer of tubes. The two outer trays, A_1 and B_1, contain tubes of length 200 cm while the inner trays, A_3 and B_3, contain 120 cm tubes.

The other two trays (the 'direction trays', A_2 and B_2) each contain 400 tubes, 200 cm long, arranged in two double layers, skewed at an angle of $3\frac{1}{2}^{\circ}$ to the normal to the measuring plane. This arrangement, intended to facilitate the assessment of the distance of a particle from the front of the spectrograph in the back-front direction and assist in the correct connection of upper and lower half-tracks in events where two or more muons pass through the apparatus with small projected separation, has been found to be of limited usefulness only.

The wall thickness of a flash tube is 1 mm and the electrodes placed between each double layer of tubes are made of 24 gauge aluminium sheet. Thus the amount of matter presented to a particle by the visual detectors is about 25 gm cm^{-2}; by comparison with the magnet, the trays give rise to a negligible degree of Coulomb scattering.

The polar angle of light emitted by the tubes is very narrow, decreasing for longer tubes (Coxell et al., 1961). Thus it is important that the light path length is as long as possible to decrease the angle subtended by the extreme corners of the trays at the camera, enabling light from tubes in these portions of the spectrograph to be recorded.

The light path is in fact 40 ft. long, giving an angle of nearly 6^{o} and hence leading to some fall in the intensity of the images of these flash tubes on the recording film. This effect must be taken into account in determining the acceptance function of the instrument.

3-1.3 The acceptance function of the spectrograph

Muons have a probability of traversing all four momentum trays of flash tubes and the sensitive volume of the magnet which depends on their incident direction and their deflection in the magnet. This variation in probability, the acceptance of the spectrograph, has been determined as a function of the incident direction both in the measuring plane (ψ_o) and normal to this plane (ϕ_o) and the deflection in the measuring plane ($\Delta\psi$).

The acceptance function, $A(\psi_o, \Delta\psi)$, in the measuring plane and the acceptance in the back-front plane, $B(\phi_o)$, are shown in Figure 3.2. $B(\phi_o)$ has been evaluated neglecting any deflection in the back-front plane. The effects of this simplification have been estimated to include a 5% rise in muon densities at 1 GeV/c, a 1% rise at 10 GeV/c and no change at 100 GeV/c. The functions $A(\psi_o, \Delta\psi)$ and $B(\phi_o)$ may be combined to give the probability of acceptance of a muon incident with any zenith and azimuth angles (θ,ϕ) and having deflection of absolute value $\Delta\psi$. The variation of this probability with θ and ϕ for one value of deflection is shown in Figure 3.2.

As mentioned in section 3-1.2, the intensity of light from the neon flash tubes depends on the angle to their axis at which they are

FIGURE 3.2

The acceptance function of the spectrograph in the measuring plane and the back-front plane (A and B).

The probability of acceptance of muons of zero deflection as a function of zenith and azimuth angles.

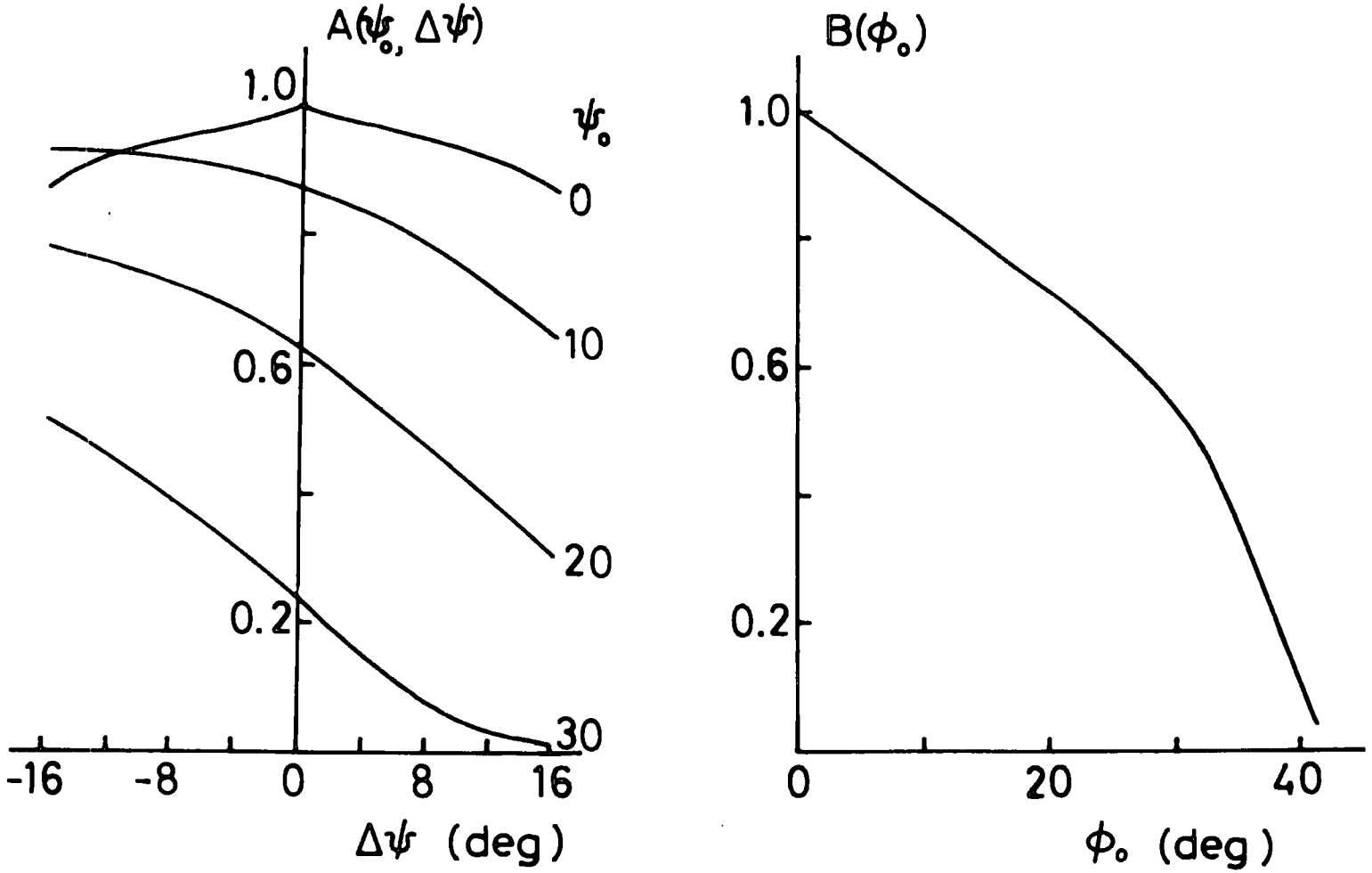
A(ψ₀, Δψ)
1.0
0.6
0.2
ψ₀
0
10
20
30
-16
-8
0
8
16
Δψ (deg)
B(φ₀)
1.0
0.6
0.2
0
20
40
φ₀ (deg)

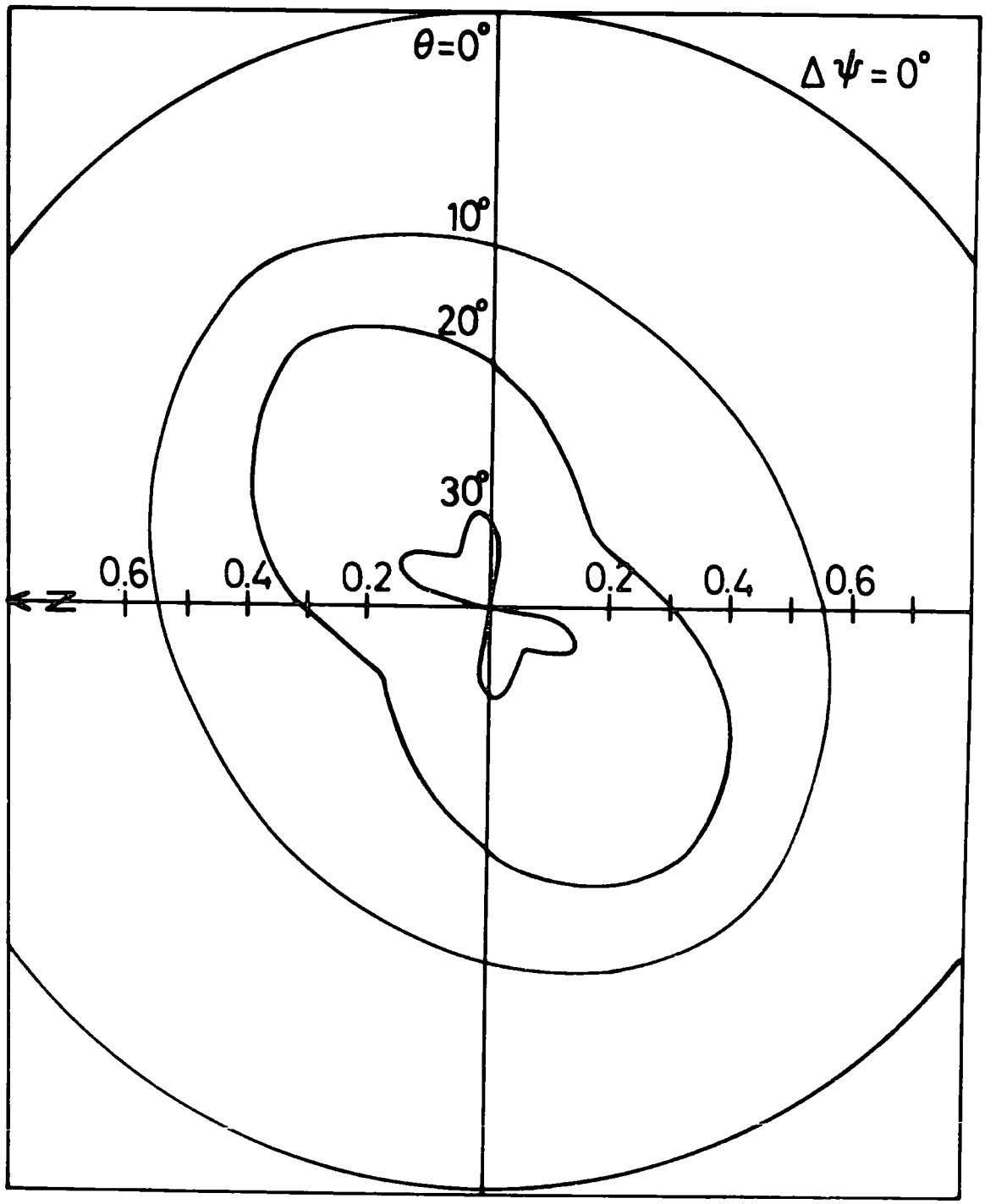
θ=0°
Δψ=0°
10°
20°
30°
0.6
0.4
0.2
0.2
0.4
0.6
Z

viewed. As a consequence of this the efficiency of the visual detectors is expected to fall towards the corners of the trays. This effect has been examined in the two momentum trays above the magnet and the mean number of tubes observed in a track crossing a tray falls from five at the centre to three at the corners of the trays. There is only a small probability that a track will pass through inefficient regions in both of these trays and a careful check is made on the slightest suspicion that a track may be present. Thus any effect on the spectrum will be reduced considerably, and there is a very marginal effect even under the assumption that the chance of selecting a track is proportional to the number of flashed tubes constituting it.

3-1.4 Spectrograph measurements

The flash tube trays contain neon flash tubes mounted in two distinct fashions. About 60% of all the tubes are located in accurately machined grooves in dural supports, enabling their positions to be determined to within 0.2 mm. The rest of the tubes lie on these tubes and are thus less accurately located, due to variations in the diameters of the lower tubes. Measurements have been made of the horizontal positions of certain key flash tubes in each tray referred to a vertical plane defined by four plumb lines at one side of the magnet, and the vertical positions of the trays.

The tube alignment procedure and the absence of any tilting of the spectrograph over the period of operation may be checked by an

examination of the distribution of incident directions of muons. No asymmetry in this distribution has been found, giving confidence on these two points.

3-2 The treatment of the data

3-2.1 The selection procedure

The spectrograph is triggered whenever an air shower is recorded and the neon flash tubes are photographed on a single frame of 35 mm film. The film is subsequently scanned visually for tracks above and below the magnet which appear likely to intersect. The selected frames are then re-projected and the flash tube images marked on a scale drawing of the spectrograph. A further visual examination of these drawn events is carried out to eliminate those events in which the 'half-tracks' above and below the magnet will obviously not intersect, and those in which the particle traverses the sides of the sensitive volume of the magnet. Any doubtful 'events' are passed on to the next stage of the analysis. A typical drawn event containing one useful muon and a muon which has partially passed through the magnet is shown in Figure 3.3.

3-2.2 The simulation of the particle trajectory

The selected events are 'simulated' on an 8/10 scale drawing of the two arms of the spectrograph. The tubes which have flashed are marked and the most probable trajectory for the particle is estimated, making allowance for the variation in flashing probability with the

FIGURE 3.3

A drawn-out event, showing a typical low deflection muon.

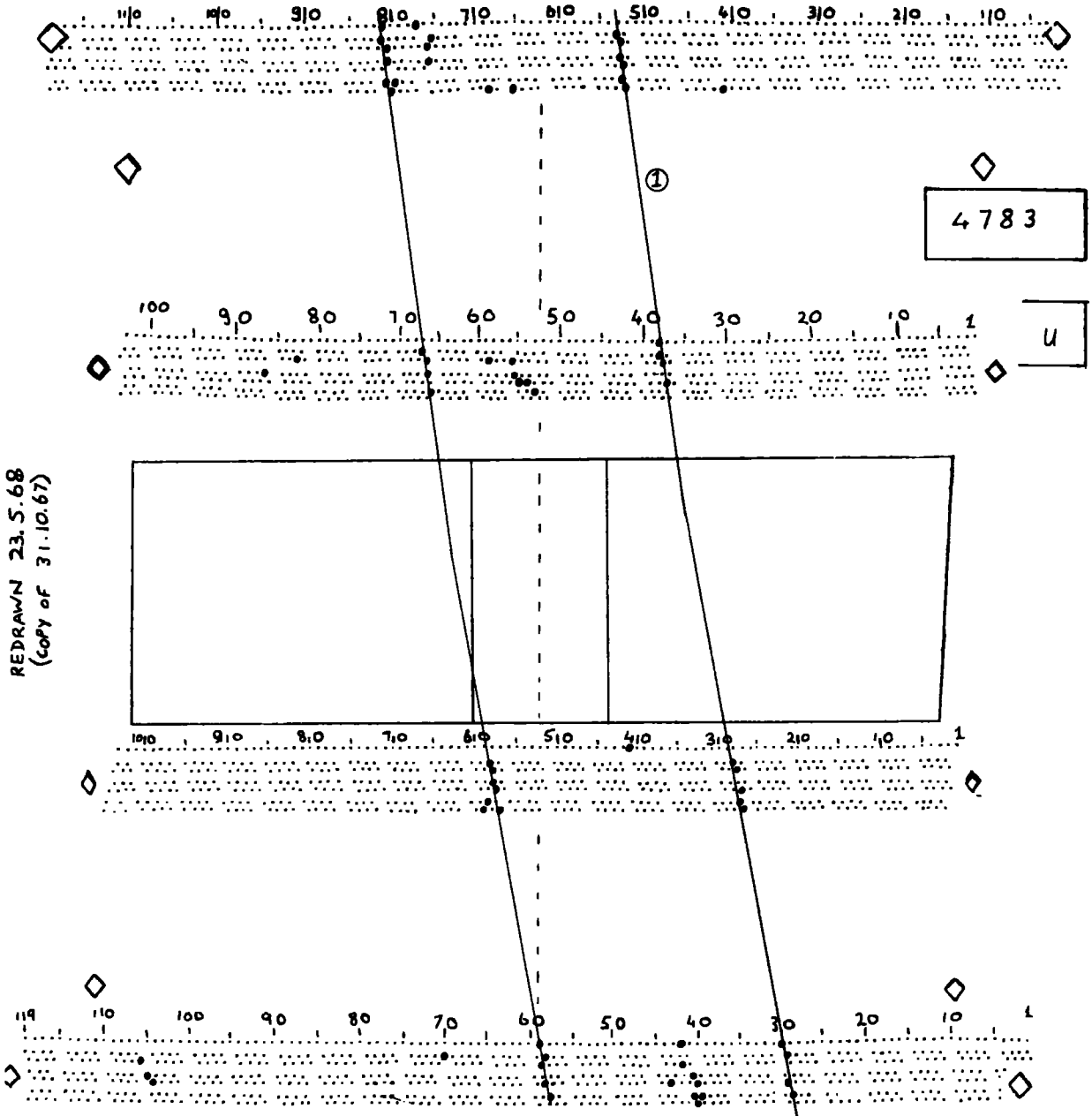

				1															
					A	B													
F280	TRIG	500		L_1	11·1	12·6													
	N	$1{\cdot}7_{10}{}^{7}$		L_2	5·45	7·0													
H+	r_1	304m		N'	23	18													
	Θ	13°																	
663631	Φ	296°		$\dot{m}$	-11·45														
	X	-317		$\Delta\dot{m}$	0·10														
	Y	4																	
	L/R	1·9																	

position of the track across the tube diameter. Whilst this method of simulation is necessarily somewhat subjective, an attempt to replace it by more objective computer based methods has not met with great success (Maslin, G.C., private communication), because of two basic difficulties.

(1) Comparisons of hand and computer simulations of the same events show that the two methods are not in serious discord for momenta below about $\frac{2}{3}$ of the m.d.m., when the computer finds a Gaussian fit to the positions of the flashed tubes. But for higher momenta the results are critically affected by the variation across the tube diameter of the probability of flashing assumed in the computer analysis. This probability function must be established with the same precision as the spectrum under analysis. A further difficulty is that the probability function implicitly used in the hand simulation is non-analytic, in that a non-flashed tube is ignored if the weight of evidence from the flashed tubes dictates a line passing through it.

(2) In the case of air shower events the accompaniment to the muon may be large, and is clearly correlated to both muon energy and distance from the shower core. The computer is therefore at present unable to analyse the complex pictures obtained in a time commensurate with analysis by a skilled observer.

3-2.3 The determination of the angles of the track

The drawings of the spectrograph arms used in the simulation process have measuring levels set 28 inches apart, outside the two

flash tube trays. The coordinates of the best estimates of the two half-tracks may be read on these scales to ± 0.05 inches. These coordinates are then analysed by a computer programme which calculates the incident angle and deflection of the muon, its electric charge and tests whether the intersection of the two half-tracks could take place within the limits of the magnetic cross-section. The errors in determining the angles of the two half-tracks cause the intersection point to be uncertain. If the uncertainty in the height of intersection of a high energy muon (deflection less than 2°) corresponding to one standard deviation of these errors extends within the magnet volume, the track is accepted. Muons which pass through the sides of the magnet cross-section are rejected.

3-3 Spectrograph noise

A knowledge of the error in the measured deflection of a muon due to the inherent errors of the track-fitting procedure is vital to the determination of the momentum spectrum of the muons from the deflections. The 'noise' has been determined by several different methods which are treated in detail by Walton (1966). Here only a summary will be presented, together with details of recent improvements.

3-3.1 The repeated assessments of angle

From a consideration of the accuracy with which half-tracks can be simulated a value of the error in the deflection of $(0.256 \pm 0.017)^{\circ}$ was found.

As a check upon this procedure 24 tracks, each of deflection

less than 1°, were simulated five times, without the knowledge of the operative. The high average momentum of these particles will minimise scattering in the trays. From these measurements, the standard deviation of the error in the deflection was found to be $(0.25 \pm 0.03)^{\circ}$.

3-3.2 Muons which traverse the magnet hole

For events recorded in air showers 67 muons passing through the magnet hole were selected, using information from the direction trays to reject muons likely to have struck the magnet iron. These muons were simulated and the resultant distribution in deflection was fitted by a Gaussian distribution, using a χ^2 minimization procedure. The value of the noise so determined was $(0.325 \pm 0.033)^{\circ}$.

3-3.3 The interpretation of Δy_m

The computer programme by which the angles of the two half-tracks are calculated also gives the linear separation of the two half-tracks when extrapolated to the mid-plane of the magnet, a quantity signified as Δy_m. For high energy muons this separation should reflect the spectrograph noise.

For muons of deflection less than 0.72° the distribution of Δy_m can be fitted for Δy_m less than 12 mm by a Gaussian curve of standard deviation 6 mm. However, muons of low momenta scattered to small deflections typically have large values of Δy_m, and thus the observed numbers of particles at Δy_m greater than 12 mm are greater

than the numbers predicted by this Gaussian curve. The standard deviation of 6 mm leads to an estimate of simulation error of 0.32^{o}, when allowance is made for the scattering of high energy particles.

3-3.4 The 'no-field' tracks

Many previous workers have analysed the deflections of muons by the magnet in the absence of any magnetic field to estimate the track-fitting errors in their experiments. The total width of the observed distribution of deflections is compounded quadratically of Coulomb scattering in the magnet iron and the errors in track location. The method is not very reliable because the contribution of the errors to the total width is not large.

The spectrograph was triggered on unaccompanied muons prior to switching on the magnetic field and the analysis of the data gives an estimate of the simulation error in agreement with the results of the other methods.

3-4 The Performance of the spectrograph

For muons incident with a distribution of zenith angles similar to that observed at Haverah Park, the mean energy required to penetrate the magnet and the lead shielding is 940 MeV (Sternheimer 1959). Muons of energy less than about 1.1 GeV are, however, prevented by the magnetic field from emerging from the volume of the magnet. Thus the lowest detectable momentum is about 1.1 GeV/c. The signal to noise ratio defined as the ratio of the magnetic deflection of a muon to the r.m.s. angle of Coulomb scattering for

this muon is approximately three. An indication of the range of momentum measurable by the spectrograph is given by the maximum detectable momentum (m.d.m.) which may be defined as the momentum for which a vertically incident muon is magnetically deflected by an amount equal to the noise of the instrument. The noise is a combination of the scattering in the magnet iron and the errors in measurement of the incident and emergent angles. Since the noise of the instrument is about 0.3°, the m.d.m. is about 60 GeV/c.

CHAPTER 4

THE LATERAL DENSITY DISTRIBUTION OF MUONS ($p > 1 GeV/c$) BY AN ABSORPTION TECHNIQUE

4-1 Introduction

The treatment of the magnetic deflections of the muons only yields the shapes of the momentum spectra at various distances from the core. Normalization of these shapes to a known absolute density at some fixed momentum would enable the muon densities for various momenta to be derived, such densities being then directly comparable with theoretically predicted values.

For this reason an analysis has been made of the number of muons traversing the flash tube tray B_3, immediately under the magnet iron. The showers examined had zenith angles less than 40°, as this angle is approximately the limit beyond which particles cannot usefully pass through the spectrograph, and also because the variation in depth of atmosphere penetrated by showers of such a range of zenith angle is rather restricted. The method of analysis follows that described by Allan et al. (1966).

4-2 The sensitive area of the detector

The use of the same instrument to measure densities and momentum spectra offers great advantages, as the threshold energy for muon number determination is closely similar to that imposed on the momentum measurements. Muons which have traversed only a portion of the thickness

of the magnet due to the inclination and position of their tracks must not be included. Areas of the flash tube tray B_3, which could be traversed by an undeflected muon which had passed through a depth of iron in the projected plane at least equal to the vertical thickness of the magnet, were found geometrically for four projected incident directions (5^o, 15^o, 25^o, 35^o), the centres of the four cells of incident direction used in the analysis. The areas of these portions of the trays were then corrected to give the areas perpendicular to the incident direction of the shower projected into the measuring plane of the spectrograph.

These areas, shown in the second column of Table 4.1, must be corrected for two effects, details of which are given below. The final column of Table 4.1 shows the areas corrected for these two effects.

4-2.1 The back-front correction

The corrections for this effect differ from the back-front acceptance corrections for the derivation of momentum spectra as there is no necessity in the analysis of densities for the muons to pass through the magnetized volume of the iron. A study of Figure 3.1 will show that in the back-front plane the magnet overhangs tray B_3 sufficiently to reduce the necessary correction to cos (ϕ_o).

The incident directions in both the measuring plane (ψ_o) and the back-front plane (ϕ_o) corresponding to each point of a matrix

TABLE 4.1

AREAS FOR DENSITY DETERMINATION

Incident direction	Uncorrected areas (m^2)	Back-front correction factor	Acceptance factor	Final areas (m^2)
5^o	1.692	0.886	0.989	1.482
15^o	1.442	0.911	1.000	1.313
25^o	1.163	0.932	1.000	1.083
35^o	0.907	0.976	1.000	0.885

of zenith angle and azimuth (spaced by 5^o in zenith and 10^o in azimuth) were computed. Those points of the matrix with ψ_o within one of the cells used were grouped together and the mean correction to the area appropriate to this cell was found from the corresponding values of ϕ_o. Each point was weighted according to the observed zenith angle distribution of air showers, azimuthal symmetry being assumed. Each of the cells of incident direction was treated in this way, giving the results in Table 4.1.

4-2.2 The acceptance correction

The magnetic field will deflect particles both into and out of the areas defined above. For the four incident directions this acceptance was investigated as a function of deflection, using an analogue method. To be accepted a track must enter the tray B_3 within the areas defined for the value of ψ_o in question. Except for large deflections at the

lowest value of ψ_o the probability of detection did not change with deflection. To obtain an average correction factor the probabilities for various deflections must be weighted in accordance with the chance of such a deflection occurring. This latter probability was found by unfolding the acceptance used in measurements of deflection (section 3-1.3) from the observed deflection spectra. Using the deflection spectrum observed in all the events recorded in showers triggering the 500 m array there is only a 1% change in the area for the lowest ψ_o.

The variation of the deflection spectrum with distance from the shower core, which will lead to a decrease in this correction for distances less than about 300 m and an increase above this distance, has been neglected. Also it is possible for muons included in the density measurements to penetrate none or a part only of the 'magnetized volume', when the deflections in the measuring plane will be less than for muons penetrating the full depth of the field. The correction given above will decrease for these muons. Averaged over all incident directions this is a very small effect indeed and thus these small errors in this treatment may be neglected.

4-3. The analysis of the data

Spectrograph records for showers with zenith angles less than 40° were examined and the mean projected incident angle of the particles observed in the upper part of the spectrograph was estimated. In those events in which the flash tubes above the magnet were

saturated, the angle of incidence was determined by the angle of the electrons at the side of the magnet in the lower half of the spectrograph. The number of muons passing through the area appropriate to this mean angle was then determined. This caused little difficulty except in those cases where an interaction occurs in the iron producing a burst in the visual detectors below the magnet. In such cases, if the picture is otherwise unambiguous and if the burst appears unlikely to obscure another muon, the data for the event is recorded with one muon attributed to the burst. In some few cases the event cannot be interpreted, due either to obscuration by a burst or to a very great density of penetrating particles; such occurrences are noted.

This procedure is subjective to some degree, but the majority of events are quite unambiguous, leaving only a small fraction where observer bias may affect the results. Two checks suggest that this bias is acceptable. Three separate batches of data of equivalent size were read at widely separated times and the mean number of muons observed per frame was found to be the same for all three batches. On two occasions the same data was scanned by two independent observers to check this subjectivity and in both cases no difference was found.

It is of interest to note the rate of detection of muons by the spectrograph. Table 4.2 shows the mean numbers of muons seen in the spectrograph in showers triggered by each of the arrays.

TABLE 4.2

SUMMARY OF MUON NUMBER DATA

Array	Number of showers analysed	Mean muon number	Fraction of frames with no muons
50	640	1.1	50%
150	435	1.5	33%
500	2371	1.4	44%

The accumulated data for many showers have been subdivided into intervals of size and distance. Those intervals containing indecipherable events of the kinds mentioned above have not been used, in order to avoid wrongly estimating the muon densities. Four estimates of the muon density (Δ_μ) are available in each of these intervals, one from each of the four cells of incident direction used. If each of these estimates is weighted according to the number of events included in it, we can write

$$\Delta_\mu = \frac{\Sigma_i \mu_i/A_i}{\Sigma_i n_i} \pm \frac{\Sigma_i \left(\mu_i/A_i^2\right)^{\frac{1}{2}}}{\Sigma_i n_i} \qquad (4.1)$$

where A_i is the area appropriate to the i th cell of incident direction, and μ_i is the total number of muons observed in that area in n_i showers. The errors quoted are standard errors on the mean of a Poisson distribution and for very small samples are replaced by the Poisson fiducial limits (Regener 1951).

FIGURE 4.1

A comparison of an observed distribution of numbers of muons and that predicted assuming Poisson statistics.

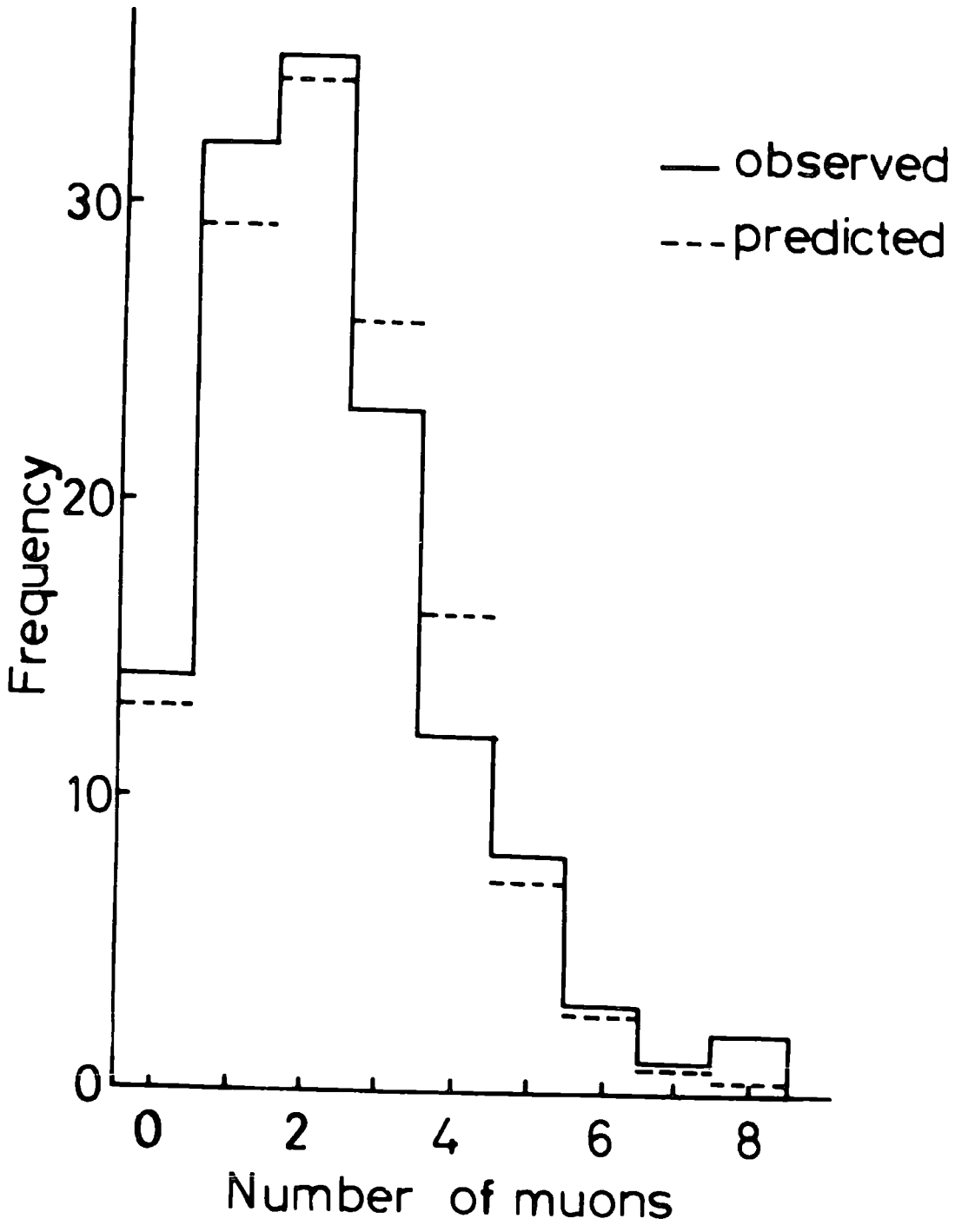
$1 \times 10^7 \leq N < 2 \times 10^7$
$150 \leq r < 200$ M
observed
predicted
Frequency
30
20
10
0
0
2
4
6
8
Number of muons

The assumption that the numbers of muons are distributed according to Poisson statistics has been examined for all those intervals of size and distance which contain more than 100 showers. In all cases the frequency distribution of the numbers of muons is consistent with a Poisson distribution of mean equal to that determined using equation 4.1. A typical comparison of observed events with the predicted distribution is shown in Figure 4.1.

4.4. The lateral density distribution of muons

Data have been obtained from all three arrays, the different size and distance ranges covered by the different arrays overlapping to some extent, thus providing checks of the consistency of the results derived from each of the arrays. The results are summarized in Figures 4.2 to 4.4 and only the most important features will be discussed.

The function $f_\mu(r)$ describing the lateral distribution of muons of momentum greater than 1 GeV/c about the shower core does not vary with shower size. This function appears, to a sufficiently close approximation, to be identical in shape to that deduced by Greisen (1960) for muons of energy above 1 GeV:-

$$f_\mu\ (r, \geq 1\ \text{GeV/c}) \quad \alpha \quad r^{-0.75}(1 + r/320)^{-2.5} \qquad (4.2)$$

The lateral distributions for three different intervals of shower size for data from the 500 m array are shown in Figure 4.2, compared with the above function normalized to fit the data. Similar agreement at

FIGURE 4.2

The lateral distribution of muons of momentum greater than 1 GeV/c in three different ranges of shower size.

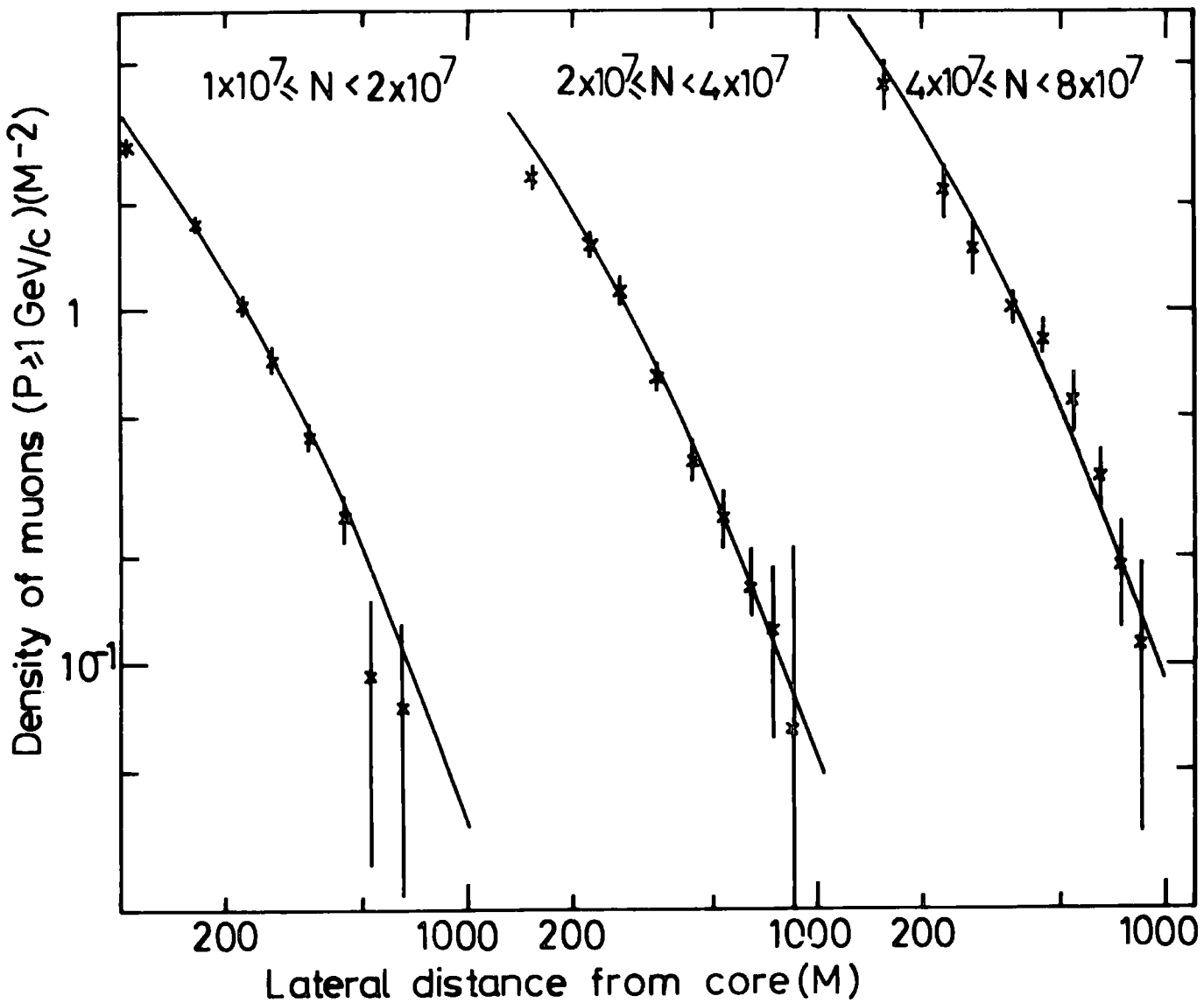
1x10^7 ≤ N < 2x10^7
2x10^7 ≤ N < 4x10^7
4x10^7 ≤ N < 8x10^7
Density of muons (P≥1 GeV/c)(M^-2)
1
10^-1
200
1000
200
1000
200
1000
Lateral distance from core (M)

FIGURE 4.3

The variation with shower size of the muon density above 1 GeV/c at 300 m from the shower core. The straight line which is the best fit to the data is shown.

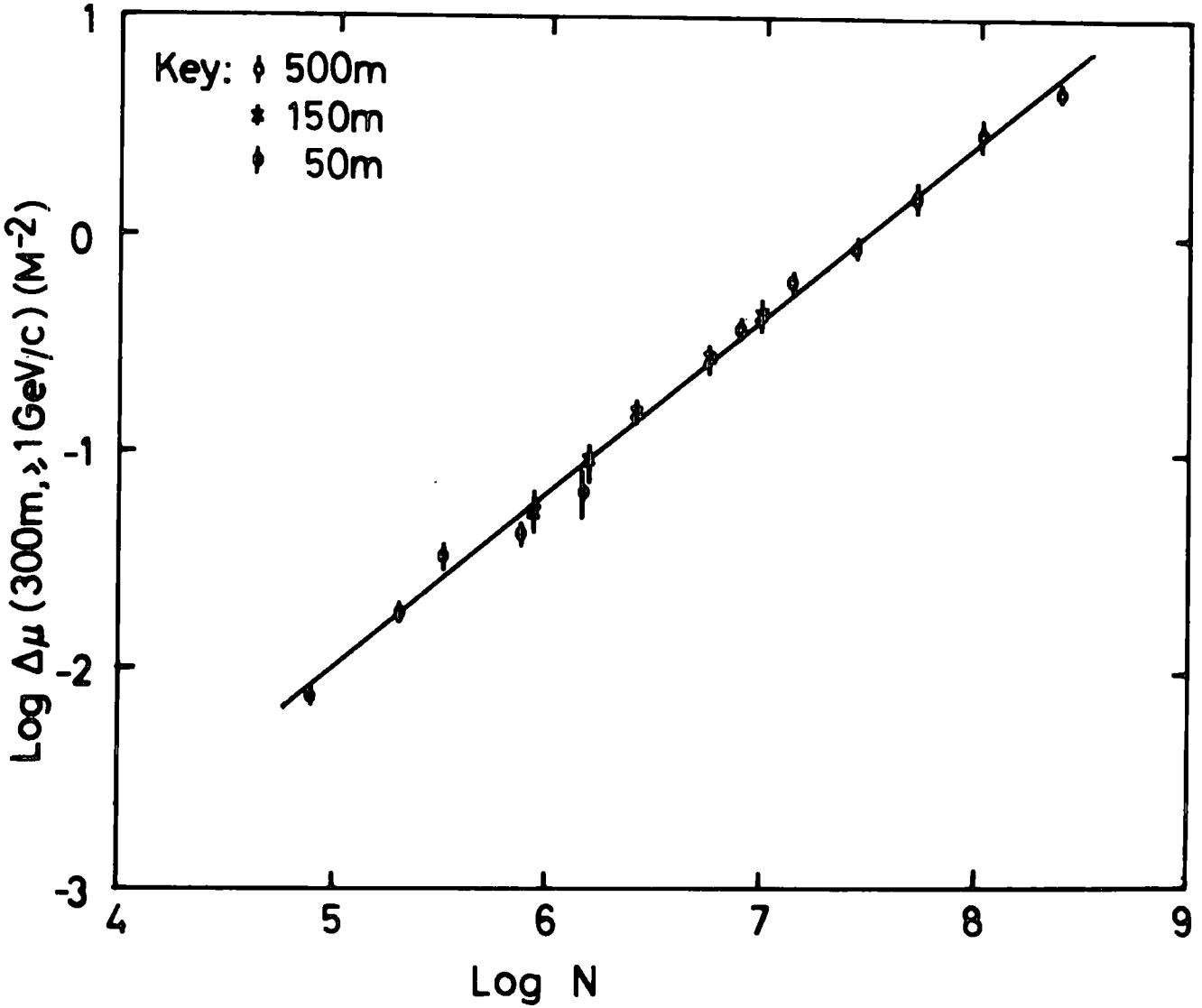
Key: 500m
150m
50m
Log Δμ (300m, ≥1GeV/c) (M⁻²)
Log N
1
0
-1
-2
-3
4
5
6
7
8
9

the relevant distances is found for all other intervals of shower size, within the statistical limitations of the data.

For the data from each of the arrays the variation of muon density with shower size can be estimated by plotting the density at some distance in the middle of the range covered by the array as a function of shower size. The distances chosen for the three arrays are 30 m, 100 m, and 300 m, for the 50 m, 150 m and 500 m arrays respectively. These relations are all similar within the errors to a power law of exponent about 0.8. If the lateral structure function is assumed constant and unchanging with shower size, normalization of this function to fit the data in each of the intervals of size, using a least squares fitting procedure, enables the densities of muons at 300 m from the core for showers of the average sizes of the various intervals to be estimated. The variation with size of the muon density at 300 m from the core is shown in Figure 4.3. The fractional errors on the mean densities at 300 m have been found as the standard errors of the distribution of the ratio of observed density to that predicted by the normalized $f_\mu(r)$. It can be seen that no significant departure from the relation

$$\Delta_\mu \ (300 \text{ m}, \geq 1 \text{ GeV/c}) \propto N^{0.78 \pm 0.05} \qquad (4.3)$$

is observable, over a range of size from 8.75×10^4 to 2.6×10^8 particles. The errors on the exponent are those involved in fitting a straight line to experimental data using a least squares procedure.

Using relation 4.3, the densities from the various intervals of size can be scaled to a common size to enable a more accurate check of the form of $f_\mu(r)$ to be made. The size selected is 2×10^7, the median size of the showers detected by the 500 m array. This lateral distribution of muon densities from the three arrays is shown in Figure 4.4, the points being the weighted mean densities with associated standard errors. The curve plotted is of the form of $f_\mu(r)$ from equation 4.2 suitably normalized. It may be seen to be a reasonable representation of the data.

The densities of muons of momentum above about 1 GeV/c for showers of zenith angle less than 40° can be expressed by the formula,

$$\Delta_\mu (r,N, \geq 1 \text{ GeV/c}) = 26.0 \pm 1.15\left(\frac{N}{10^6}\right)^{0.78\pm0.05} r^{-0.75}(1+r/320)^{-2.5} \quad (4.4)$$

for a range of shower sizes between 8.75×10^4 and 2.6×10^8 and distances from 10 m to 1100 m from the cores.

4.4.1 The variation of muon density with zenith angle

For showers recorded by the two smaller arrays the timing measurements were only sufficiently accurate to provide an indication of whether the zenith angles of the showers were greater or less than 40°. The zenith angle distributions of these small showers are, however, very steep and thus this lack of information should not lead to serious errors. In the case of the 500 m array the zenith angles of the showers have been measured accurately and thus a

FIGURE 4.4

The lateral distribution of muons of momentum greater than 1 GeV/c in a shower of size 2×10^7.

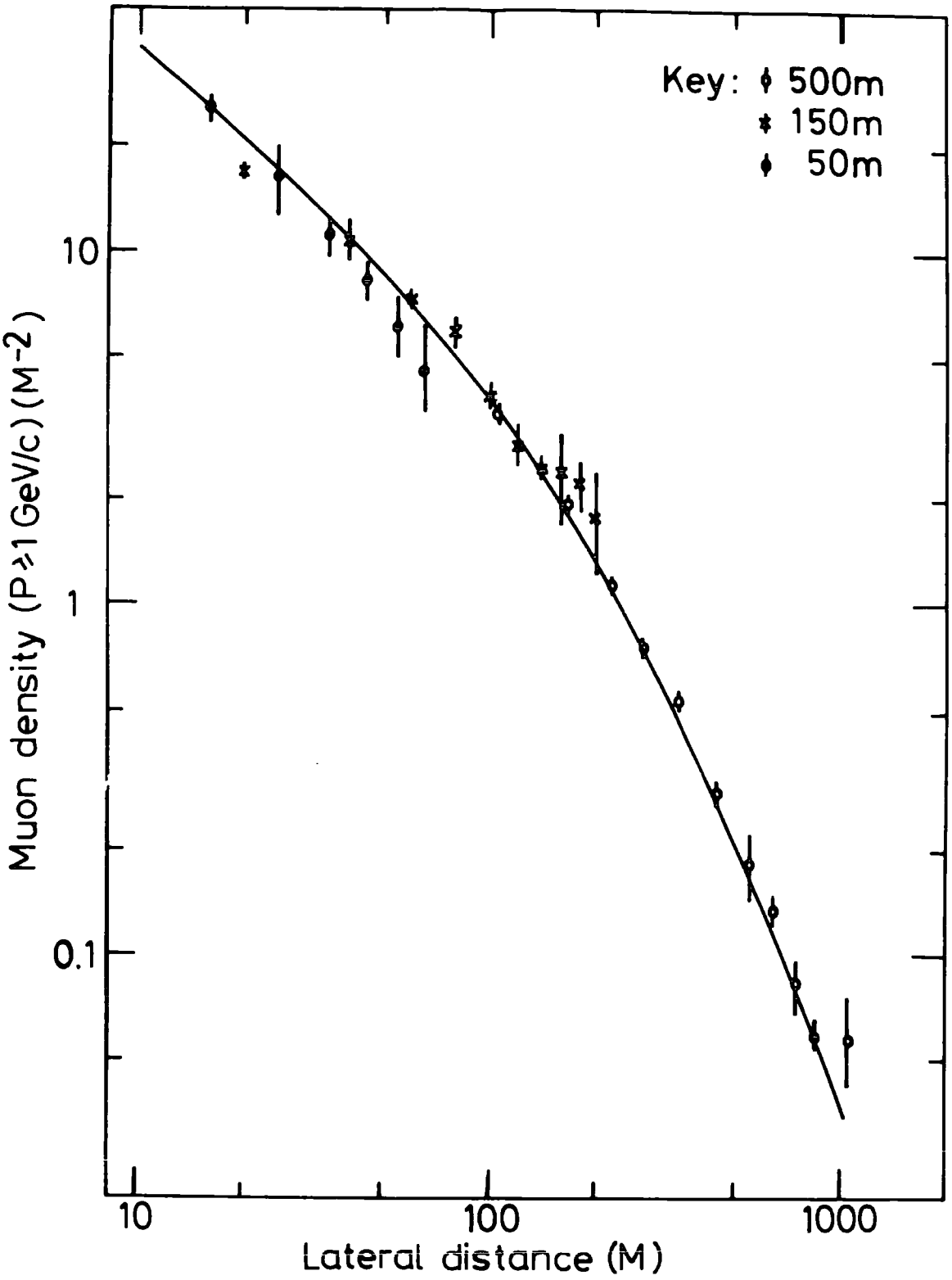
Key: 500m
150m
50m
10
1
0.1
Muon density (P≥1 GeV/c) (M⁻²)
10
100
1000
Lateral distance (M)

subdivision of the data to examine the variation with zenith angle of the lateral distribution is possible.

The data were divided into two sets, one for zenith angles above and the other for those below 20°. The densities at a given distance, normalized to a size of 2×10^{7}, for the larger zenith angle events were found to be systematically 25% higher than for the lower angles, although the densities were not separated by more than one standard error. The lateral distributionscould both be fitted quite well over the distance range available to study by the form of $f_{\mu}(r)$ given in equation 4.2.

For the total 500 m data for showers of zenith angle less than 40°, it may be remarked that for all the intervals of shower size above 2×10^{7}, the mean zenith angle remains constant at about 21°. The mean zenith angle increases for the two intervals at smaller size, being 25° for the interval of mean size 1.4×10^{7} and 31° for that of mean 8.0×10^{6}. From the above conclusions on the variation of muon density with zenith angle it appears that this will cause a slight flattening of the plot of the muon density at 300 m from the core against shower size in this region of size. The measured exponent of the variation of Δ_{μ} with N for the 500 m data is 0.75, and when corrected for this effect this becomes 0.77. The appropriate points plotted in Figure 4.3 have not been corrected for this effect.

4-5 Discussion of the results

At all distances from the core the lateral distribution of muons of energy above about 1 Gev is in good agreement with other measurements (Clark et al., 1958, Abrosimov et al., 1960, etc.). However, the densities of muons found in the present work for a shower of given size are 45% greater than those given for a shower of similar size by the formula of Greisen (1960), which is based upon the results of Clark. A comparison of the lateral distribution found in the present experiment with that measured at Haverah Park by Allan et al. (1967) for muons of energy greater than 0.35 GeV shows that the densities found in that experiment for distances greater than 250 m from the shower axis are consistently about 30% higher than those found in the present work. This can be understood as a result of the difference in the threshold muon energies in the experiments. Due to the changing momentum spectrum of the muons as the distance from the core increases, this excess is expected to increase for larger distances. However, the present densities, while tending in the right direction, are insufficiently accurate to quantify this trend at the necessarily large distances.

The observed increase with zenith angle of muon densities at a fixed distance in a shower of given size is the same as that determined by Allan et al. The increase in muon densities as the zenith angle increases can be ascribed to a lateral spreading of the muons as they traverse greater distances before observation, and also

to an increase in the energy of the primary particle initiating a shower of fixed size at sea level, due to the absorption of the electromagnetic component of the shower in the extra thickness of atmosphere at larger zenith angles.

Under the assumption of a constant lateral distribution function the density of muons at a fixed distance has been taken as typifying the number of muons in a shower. If we write the relation between the number of muons (N_μ) and shower size (N) as

$$N_\mu(\geq p) \propto N^\alpha \qquad (4.5)$$

a comparison of the value of α derived in the present work shows it to be in good agreement with other experimental data (e.g. Allan et al., 1967, Linsley et al., 1962b, Clark et al., 1958). The lateral distribution function has been seen to be independent of shower size and thus can be used to normalize the muon momentum spectra to give absolute densities for given distance and shower size. For muons of large threshold energy the value of α in the relation 4.5 is not well established and thus caution is necessary in such scaling. For muons of energy greater than 5 GeV and 10 GeV, Khrenov (1962) found a value of α of 0.85. For very high energies the only experimental evidence (Barrett et al., 1952, Chatterjee et al., 1966) seems to indicate that α may be much lower. An interpretation of Barrett's data by Greisen (1960) indicates that α may be 0.7 over the region of shower size of interest in the present work. In the following chapter evidence will be presented which suggests that for muons of

great threshold energies the value of α is approximately equal to that determined in the present experiment for muons above 1 GeV/c.

CHAPTER 5

THE MOMENTUM SPECTRUM OF MUONS IN EAS

5-1 The Selection and treatment of the data

In a previous chapter (section 3-2) the treatment of the spectrograph records was briefly summarized. This procedure will now be examined in view of the possibility of introducing biases.

5-1.1 Selection biases

The film record of one run of 450 events has been carefully drawn in its entirety to check this procedure. An ordinary visual scan noted 73 potentially useful events, whereas 78 were selected from the drawn records of the whole film. Of the extra five events, only one was accepted as a muon, the other four being rejected for various reasons. It is of interest to note that this one event did not fall in the corners of the flash tube trays where the light intensity falls off.. While the sample of events is insufficient to detect any momentum bias due to this effect, it can be concluded that the scanning of the films is quite efficient.

5-1.2 The effect of simulation quanta

The simulation precedure is limited at each measuring level to scale divisions of 0.05 inches. As the levels are set 28 inches apart, the angular increments vary from 0.102° for vertically incident particles to 0.075° at an incident angle of 30° and 0.06° at 46°. The effect of these 'quanta' will be very small at large deflection,

and at low deflection the maximum effect has been shown to be a 1% raising of the integral spectrum at 60 GeV/c (Orford, private communication).

5-1.3 The rate of recording of single muons

The flash tubes retain a layer efficiency greater than 50% for about 50 microseconds after the passage of a charged particle. Thus they will 'remember' the passage of an ionizing particle during this time prior to the application of the EHT pulse. Wolfendale (1963) gives the vertical intensity of the penetrating component of cosmic rays as 0.83×10^{-2} cm^{-2} sec^{-1} sterad^{-1} and from this value the probability of a particle striking the magnet area during the sensitive time of the flash tubes is about 0.45×10^{-2} per exposure. Such a rate is confirmed by the observation of two possibly acceptable events in a film of 446 randomly triggered spectrograph events. This rate will be an overestimate of the flux of true unassociated events as these particles must then satisfy all the criteria imposed on the observed muons.

5-1.4 Final classification

The analysed events are subjected to a final scrutiny and are only accepted subject to several criteria. These are detailed below, with a discussion of the possible biases introduced by each criterion. Three criteria are rigidly enforced.

(1) The two half-tracks above and below the magnet must intersect within the magnet cross-section. Muons of low deflection are accepted

if the intersection lies within the limits set by the measuring errors (Section 3-2.3). Low energy muons scattered to small deflections and large lateral separations may be rejected on this criterion, but there will be less than a 1% effect at 1 GeV/c.

(2) The entire track must lie within the limits of the spectrograph defined by the acceptance function. At least half of the depth of each flash tube tray must be traversed by the particle, which must not pass through the sides of the magnet volume. No bias is introduced by this criterion as full allowance is made for it in the analysis.

(3) The angle of incidence and the deflection must be within the limits of the acceptance function (Section 3-1.3). The cut-off in deflection is of no consequence as the predicted deflection spectra are similarly cut-off, but if the momentum spectrum varies strongly with zenith angle, a bias might be introduced by the limit imposed on incident angle as showers with large zenith angles are accepted preferentially for small values of incident angle.

The potentially useful muons are examined on the basis of further, less stringent criteria, viz:-

(4) The track must not be confused by neighbouring tracks. This will cause a bias against dense spectrograph records and thus will affect the mean size and distance attached to a spectrum. Confusion is most likely to arise for low energy (large deflection) muons.

(5) The particle must have a path length within non-flashed tubes less than 2 tube diameters in each arm of the spectrograph. As a

re-scan of the film is carried out in any dubious cases, this should not lead to the rejection of an event due to the erroneous omission of a tube in drawing. The high energy muons should be least affected as the energy loss rises with energy and the probability of producing a knock-on electron capable of flashing a tube also rises with energy.

(6) The particle must have the same general direction of incidence ($\pm 20^{o}$) as the rest of the shower particles recorded by the spectrograph. Thus unassociated muons within this angle will be included in the spectra, and shower muons at high angles to the shower will be excluded. It can be shown that such shower muons must have low energies; this source of loss will be offset by the single muons included in the data.

The tracks are checked for errors after examination of a final point.

(7) A muon of low deflection is expected to have a value of Δy_m less than 12 mm (Section 3-3.3). If such a muon has a greater value of Δy_m the event is checked for any evidence of spurious association of half-tracks. If no such evidence is present the event is accepted as part of the expected tail of the distribution due to scattered low energy muons. Experience shows that the probability of a spurious event having such a low Δy_m is small.

Before leaving this consideration of the validity of the muon data it should be noted that, if a muon is observed with two possible half-tracks in one arm of the spectrograph, the mean of the angles is taken if this does not markedly affect the deflection. Such events

will more commonly be accepted if they are low energy muons, but any excess thus introduced will tend to offset the losses of low energy muons due to confusion of tracks.

5-2 The derivation of the momentum spectrum of muons

The conversion of an observed spectrum of deflections into the momentum spectrum of muons at a given distance from the shower core is not straightforward because of the scattering in the magnet. The shape of the spectrum is only known approximately from previous analyses and thus methods based on the optimisation of some parameter in a previously known spectrum are not of great usefulness. Iterative methods starting from an arbitrary trial spectrum and giving a unique solution are preferable.

Two distinct approaches to this problem have been used, one of which is an adaptation of that used by the workers at Durham and Nottingham (e.g. Bull et al., 1965b). This method, which starts with an assumed momentum spectrum, predicts a deflection spectrum which may then be compared with the observed spectrum. This inductive method has been developed extensively for use with the momentum spectra found in air showers by Orford (private communication). The second, deductive, method, developed for use with the present spectrograph by Walton (1966), involves the evaluation of the probability distributions of momentum appropriate to the incident angles and deflections of the individual muons.

For each muon there is available the incident direction and deflection in the measuring plane (ψ_o, $\Delta\psi$) and from the associated air shower direction the incident direction in the back-front plane of the spectrograph (ϕ_o) is also known. Ignoring Coulomb scattering the deflection can be related to momentum by the formula derived by Bull et al (1965a):-

$$p = \frac{\ell \; K(1 + \epsilon^2/K^2) \sec \phi_o}{\exp\left\{ (\epsilon/K)\Delta\psi \right\} (\sin \psi_1 + (\epsilon/K)\cos\psi_1) - (\sin\psi_o + (\epsilon/K)\cos\psi_o)} \qquad (5.1)$$

where ℓ is the thickness of the magnet in cm, ϵ is the specific energy loss in MeV cm^{-1} of a muon of momentum p (Ashton and Wolfendale, 1963), K is three hundred times the magnetic flux density and ψ_1, given by

$$\psi_1 = \psi_o + \Delta\psi$$

is the angle of emergence from the magnet of the particle.

A muon of momentum p suffers Coulomb scattering in the iron magnet and the r.m.s. angle of this scattering about the magnetic deflection is

$$\alpha_s = \sqrt{\left\{ \frac{E_s^2 \; s}{2\, p(p - \epsilon' s)} \right\}} \qquad (5.2)$$

Here E_s is a constant (21 MeV), s is the thickness of iron in radiation lengths and ϵ' is the energy loss of a muon of momentum p per radiation length.

On the basis of these two relations the momentum spectrum appropriate to a sample of muons can be derived. The two methods of derivation of the spectrum are discussed below.

5-2.1 The derivation of a deflection spectrum from an assumed momentum spectrum

The assumed momentum spectrum, $S(p)\,dp$, is evaluated for values of momentum corresponding to the centres of the cells of deflection. The contributions to each of the deflection intervals from these momenta are then evaluated and, after weighting according to $S(p)\,dp$, are summed. If the contribution to the interval of deflection of median value Δ_j from momentum p_i is $W(\Delta_j, p_i)$, the expected number of events in this deflection interval can be written -

$$N_j = \Sigma_i\, W(\Delta_j, p_i)\, S(p_i)\,d\,p_i \qquad (5.3)$$

The derivation of the factors W is carried out as follows. The distribution of incident directions (ψ_o, ϕ_o) characteristic of the muons composing the spectrum of deflections at a given distance from the core varies only slightly with distance. Thus the average characteristics of showers accompanying the measured muons in events triggered by the 500 m array are used for all the intervals of distance. If the distributions are $M_1(\psi_o)$ and $M_2(\phi_o)$, they can be corrected for the acceptance function of the spectrograph $\times (p_i, \psi_o, \phi_o)$ to give the distribution $M(\psi_o, \phi_o)$ for muons of momentum p_i :-

$$M(\psi_o, \phi_o) = \times(p_i, \psi_o, \phi_o)\, M_1(\psi_o)\, M_2(\phi_o)$$

Using the median values of the cells of the distribution M_1 and M_2, $(\psi_o)_k$ and $(\phi_o)_\ell$, we can use the relation 5.1 to find the deflections $\Delta\psi$ of a muon of momentum p_i due to the magnetic field. Now a muon of momentum $p_i (\psi_o)_k$ and $(\phi_o)_\ell$ suffers Coulomb scattering in the

magnet given by equation 5.2. The total scattering is compounded of this scattering and the error in track location (σ_e) :-

$$\sigma = \sqrt{\left\{ (\sigma_s)^2_{i,k,\ell} + \sigma_e^2 \right\}} \qquad (5.4)$$

Using this, the probability $G(i,j,k,\ell)$ of a muon of p_i incident with $(\psi_o)_k$ and $(\phi_o)_\ell$ appearing with deflection Δ_j can be evaluated, and the weighting factors found from

$$W(\Delta_j, p_i) = \Sigma_k \Sigma_\ell M_i (k,\ell) G(i,j,k,\ell)$$

Using relation 5.3 the assumed momentum spectrum, of arbitrary shape, is converted to a deflection spectrum which can be compared with the observed distribution. The differences between the observed and predicted deflection spectra are caused both by the finite numbers of muons and by the inappropriateness to the data of the assumed momentum spectrum. The effect of the numbers of muons will be seen in the errors placed upon the spectrum, and the differences due to the assumed spectrum can be utilized to alter the assumed momentum spectrum to a shape close to that appropriate to the data. The ratios R_j of the observed to predicted numbers of particles in each deflection interval are used to give a new form of $S(p_i)dp_i$

$$S'(p_i)dp_i = \Sigma_j R_j W(\Delta_j, p_i) S(p_i)dp_i$$

Because of the non-unique relation between observed deflections and muon momentum, this procedure is iterative. Unique convergence has been demonstrated by using widely differing trial spectra to

derive the same final momentum spectrum (Orford private communication).

5-2.2 The derivation of the momentum spectrum from the observed deflections

For individual particles detected by the spectrograph values are determined for the incident angle in the measuring plane, the deflection of the muon by the magnet in this plane, and, in combination with the air shower directions, the incident angle in the back-front plane. For each event the magnetic deflection ($\Delta\psi_m$) appropriate to a selected momentum p_i can be found using relation 5.1. The probability $G(p_i, \Delta)$ of a muon of momentum p_i being scattered to the observed deflection, $\Delta\psi$, where

$$\Delta = \Delta\psi - \Delta\psi_m \ ,$$

can be found from equation 5.4. Such a probability distribution assumes that the muon has equal a priori probability of possessing any momentum, which is not the case. Corrections for the momentum spectrum $S(p)dp$, and for the acceptance of the spectrograph $\chi(\Delta\psi, \psi_o, \phi_o)$, must be made, giving the final probability of a muon of momentum p_i having deflection $\Delta\psi$ as

$$P_i = \frac{G(p_i, \Delta)\ S(p_i)dp_i}{\chi(\Delta\psi, \psi_o, \phi_o)\int_a^b G(p_i, \Delta)\ S(p_i)dp_i}$$

where a is the lowest momentum accepted by the spectrograph and b is arbitrarily set at twice the upper limit of the results quoted ($b = 200$ GeV/c).

The distributions appropriate to a number of particles are summed to give the differential momentum spectrum corresponding to the sample of events. The spectrum thus deduced is corrected for the loss of low momentum particles due to the probability of such particles being scattered beyond the limits of ψ_o at 30^o and $\Delta\psi$ at 16^o, but no correction is made for the absorption of particles of momentum less than 1.5 GeV/c in the iron. The spectrum below this point is found using the previous methods of analysis by a systematic relaxation of the shape of $S(p)dp$ below 1.5 GeV/c.

This method is iterative in nature, the length of the iteration procedure being dependent upon the closeness of the assumed form of $S(p)dp$ to that appropriate to the data. The uniqueness of the spectrum derived by this procedure has been checked by tests commencing with widely different trial spectra. One such test is described in section 5-3.3.

5-2.3 A comparison of the two methods of deriving a momentum spectrum

The treatment of an assumed momentum spectrum to predict a spectrum of deflections to be compared with the observed data is to be preferred for numerically large samples of data in that the values of ψ_o and $\Delta\psi$ need not be treated individually. The cells of deflection have been chosen so that muons at distances of about 300 m from the core of an air shower have roughly equal numbers in each of fifteen cells. The cell of smallest deflection covers the range 0^o

to 0.72^{o} and has been split into two at 0.36^{o}, giving sixteen cells in all, to enable more information to be derived for momenta near the m.d.m. A limitation on this method of analysis is that the weighting factors have only been computed for the normal population of ψ_o and Φ_o, appropriate to data subdivided by distance from the core.

The second method of analysis is much more lengthy and is better for small samples (but see section 5-3.3) or for data which has abnormal distributions of ψ_o and Φ_o. Such a case is the spectrum as a function of zenith angle. For these cases the low energy correction discussed above cannot be carried out, as the weighting factors will be inappropriate.

Treatment of the same sample of data by both methods indicates that they are quite compatible (Walton, 1966).

5-2.4 Biases in the spectra

Several sources of error in the momentum spectrum of muons derived at Haverah Park have been discussed (section 5-1) and numerical estimates of the effect of these given wherever possible. Two other effects must be considered:-

(1) The spectrograph is shielded by 5 cm of lead to reduce contamination of the flash tube records by the electromagnetic component. Muons penetrating the magnet will have lost some 100 Mev in this lead, so that the observed momentum spectrum will be displaced by

0.1 GeV/c towards higher momenta.

In considering muon energy loss, no allowance has been made for the loss of a large amount of energy in one collision. Such a process is more likely at high energies and thus the spectra deduced will be slightly underestimated at large momenta (Orford, private communication).

The overall bias in the spectrum at any distance will result in a slight steepening of the true spectrum.

5-3 The momentum spectrum of muons as a function of the distance from the core

The records from the spectrograph from May 1965 to May 1967 have been analysed, yielding 2774 'useful' muons from showers triggering the 500 m array. Shorter runs have been made by triggering the spectrograph on the two smaller arrays; 1762 muons have been analysed from triggers on the 50 m array and 814 muons from the 150 m array. In a previous analysis (Earnshaw et al., 1967a) the results from the 50 m array were used to derive spectra for four mean distances from 20 m to 100 m from the core. These spectra differed only very slightly from each other and so in the present analysis the data from each of the small arrays have been combined to form more significant spectra placed at typical distances for the individual arrays. For the 500 m array the range in distance covers a much wider variation in muon momentum spectrum and therefore the data have been sub-divided into six ranges of distance. The various distance ranges for which the momentum spectra have been derived are shown in Table 5.1,

FIGURE 5.1

Distributions of shower size and zenith angle for a typical interval of distance.

200≤ r< 250 M

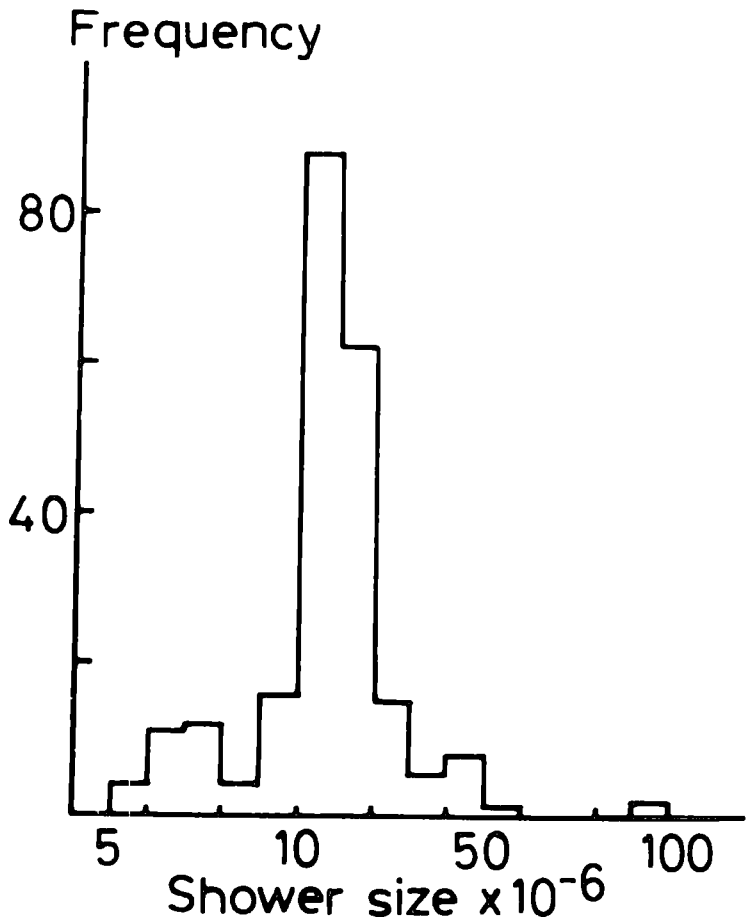
Frequency
80
40
5
10
50
100
Shower size x10^-6

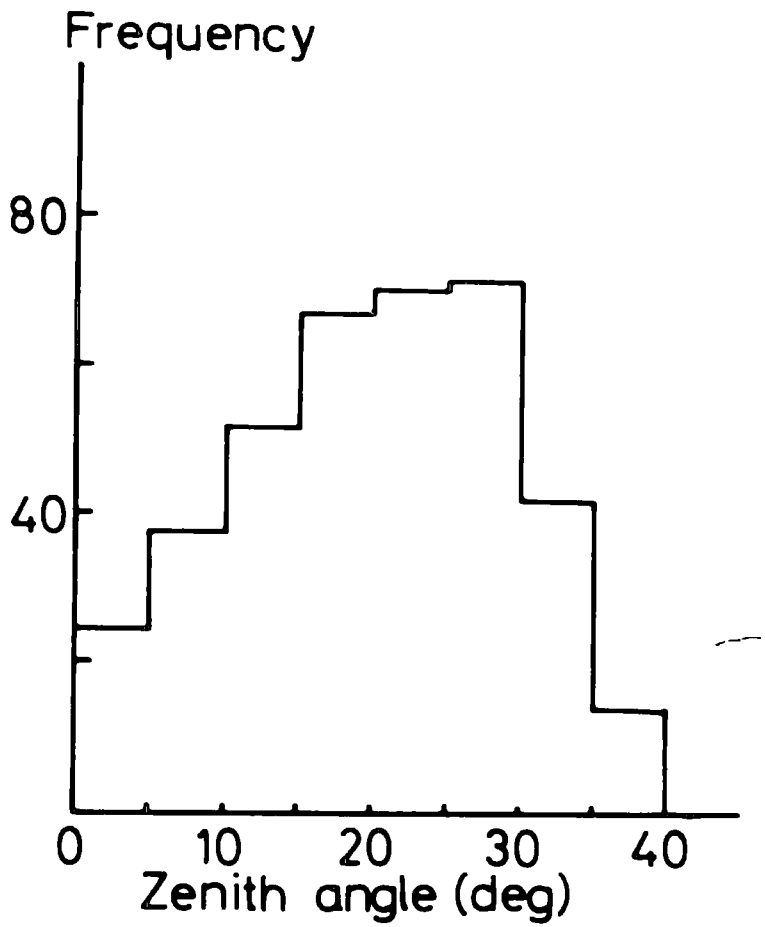
Frequency
80
40
0
10
20
30
40
Zenith angle (deg)

with the median distances and sizes appropriate to each spectrum.

TABLE 5.1

DISTANCE INTERVALS

Array	Range of distance (m)	Median distance (m)	Median size (No. of Particles)
50 m	10-70 (about)	50	4×10^5
150 m	20-210 (about)	100	2×10^6
	100-200	155	1.53×10^7
	200-250	225	2.26×10^7
500 m	250-350	300	2.80×10^7
	350-450	380	2.91×10^7
	450-600	520	4.55×10^7
	> 600	700	9.51×10^7

Typical distributions of shower size and zenith angle for one such distance interval are shown in Figure 5.1.

The data in each of these ranges, except the interval furthest from the core of 500 m showers, have been treated by using a spectral shape to predict a deflection spectrum. The fit of the predicted distribution of deflections to that observed is shown in Figure 5.2 for a typical case. The sole remaining interval has been analysed

FIGURE 5.2

A typical observed distribution of deflection and the distribution predicted using the momentum spectrum derived for this data.

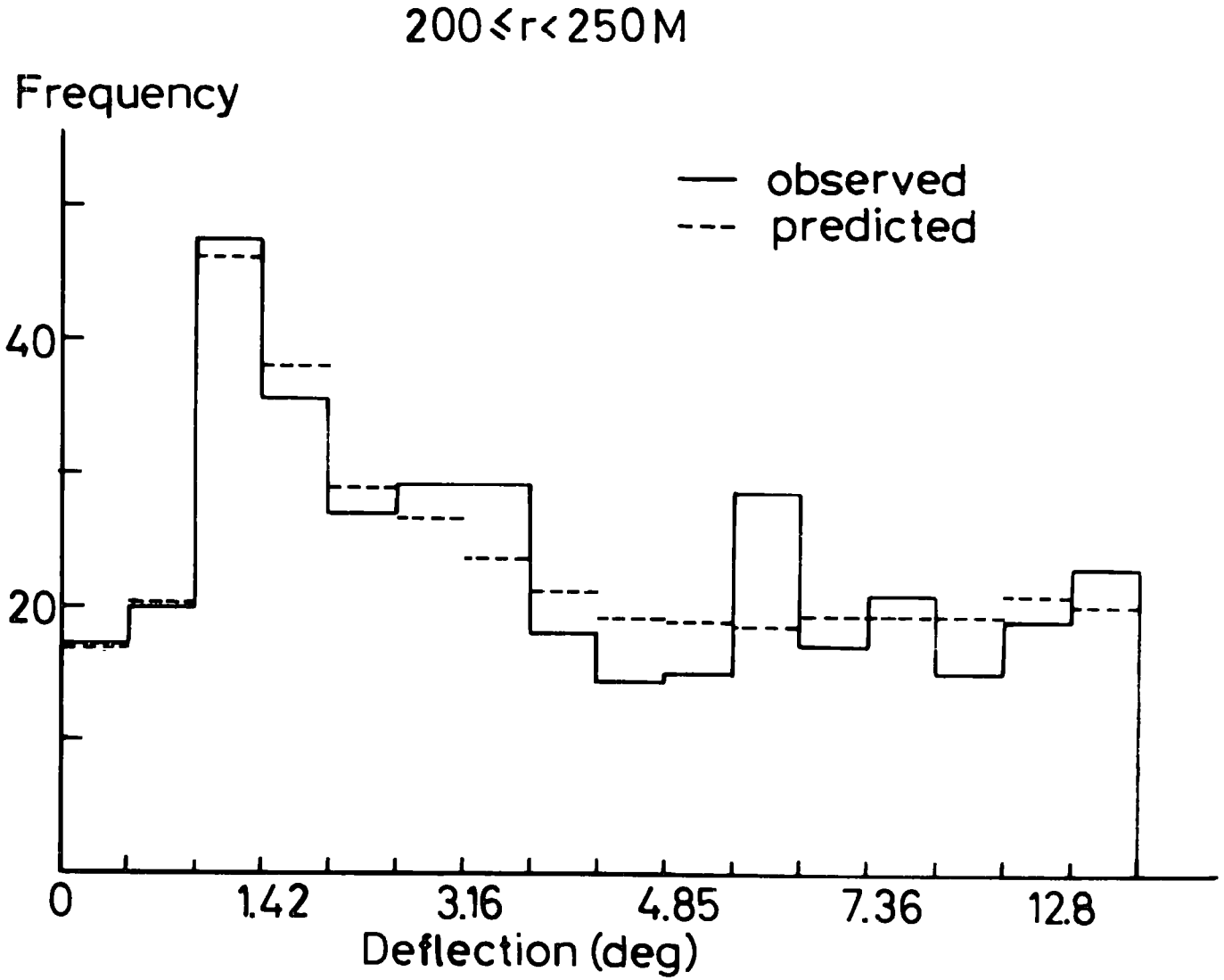
200≤r<250M
Frequency
observed
predicted
40
20
0
1.42
3.16
4.85
7.36
12.8
Deflection (deg)

by treatment of the individual deflections, because of the paucity of the data. Both procedures yield the differential shape of the momentum spectrum appropriate to the data, which may be integrated from 1 GeV/c to a momentum (500 GeV/c), which is sufficiently high for the integral intensity of muons above it to be negligible compared to the integral intensity at the upper momentum for which a value is quoted in this work. The differential spectrum can be integrated to give the integral intensities of muons above various momenta. The spectrum is normalized so that the integral intensity of muons of momentum above 1 GeV/c is equal to the density found by the absorption measurement, for a shower of size 2×10^7 particles at a distance from the core equal to the median of the interval in question.

The errors placed on the momentum spectra have been derived from the Poisson fiducial limits (Regener 1951) on the data in each cell of deflection allowing for the error on the lateral distribution of muons above 1 GeV/c. The extreme limits of the shape of the spectrum will correspond to the upper and lower fluctuations of the data in the two cells of deflection at the opposite ends of the distribution. These cells are allowed to fluctuate by the Poisson fiducial limits and the fluctuations of the intermediate cells are determined from the appropriate Poisson fiducial limits by percentile interpolation.

The normalization to a common size of 2×10^7 particles mentioned above involves the assumption that the muon densities above any

momentum can be scaled using

$$N_\mu (\geq p) \propto N_e^{0.78}$$

which, as we have seen, may not be the case for large momenta. However, the mean sizes for the different distance intervals within the 500 m data do not vary very widely except at large distances from the core, and the spread about these mean sizes is quite small. The error involved in the adopted procedure is thus very small, leading possibly to a slight underestimate of the densities of high energy muons at great distances. For the spectra from the smaller arrays the range of size is greater and thus any error will be greater. Evidence presented in section 5-3.2 suggests that normalization as $N^{0.78}$ is a reasonable procedure.

5-3.1 Comments on the air shower analysis and selection

It is important that muons be ascribed to the correct interval of distance from the core, and thus the possibility of errors in air shower analysis must be examined. As discussed above, inaccuracies in the air shower analysis for the two smaller arrays are unimportant and thus only checks upon the showers detected by the 500 m array will be considered.

(a) Air shower selection

Air showers may be considered in three categories, (1) those fully analysed by the Leeds group, (2) those partially analysed and subsequently analysed by the Durham procedure, and (3) those which

cannot be analysed. The last category comprises less than 0.2% of all showers and may be neglected. The best fit momentum spectra derived by the inductive method of analysis for the muons in showers in the first two categories have been compared for two distance ranges, centred about 300 m and 400 m from the core. There are fewer muons in the second category, but there is no difference between the spectra derived for the two categories at either distance, within the errors, confirming that the two methods of analyses agree on average (section 2-2.3).

Despite the evidence that the two methods of analysis agree on average, it is necessary to check that the analyses of individual events are not in error. Such errors will be most important for showers associated with muons of high energy, and these showers have been checked in several ways, detailed below.

(b) The analysis of showers associated with fast muons

The showers associated with muons of deflection less than 0.72° in these two spectra have been inspected. Those which have been analysed by the sophisticated method but which had a poor goodness-of-fit parameter and those which have been analysed by the simple method have been re-examined using the analogue method of intersecting loci.

In the case of the 300 m spectrum, out of 47 events one, which had been analysed by the simple method, apparently fell between 150 m

and 200 m from the spectrograph, depending on the structure function used in the analysis.

For the 380 m spectrum four dubious events, apparently nearer 200 m from the core, were found out of a total of 20 events. Each of these events had been treated by the simple analysis and further, each had one density unreadably low on the film record of the air shower densities. The method of analysis is known to be very sensitive to the smallest density observed and thus fluctuations in these low densities could lead to very large errors. The momentum spectra of muons in showers of the first two categories mentioned above are quite similar and hence it is not thought that all of these dubious events are in error.

(c) The numbers of flashed tubes

The total number of flashed tubes observed in a record of a shower triggering the spectrograph may be correlated with the shower size and the distance of the core from the spectrograph. The numbers of flashed tubes were counted for many showers and the data subdivided by size and distance from the core, and it was found that the distributions of these numbers were restricted to values not greater than twice the mean of the distributions. This restriction was the same for the individual flash tube trays and for all the trays summed. Thus the number of flashed tubes observed in the spectrograph may be used to place upper limits on distance from the core and shower size although no physical significance has been attached to this number.

The events with deflection less than 0.72^{o} in the 300 m and 380 m spectra have been examined with this criterion in mind, and only one event in each spectrum has been rejected as inappropriate to the relevant band of distance. These events also appeared from the analyses using the analogue method to be much closer to the core than originally estimated.

From the above it was concluded that the spectra at 300 m and 380 m each contained one fast particle spuriously placed at these distances. These events were not included in the deflection spectra used to derive momentum spectra. As such errors will be independent of muon momentum, and erroneous events have only been rejected for muons of low deflection, it is expected that the spectra deduced will be lower estimates.

(d.) The selection of showers by the spectrograph

Showers containing muons of low deflection (less than 1.42^{o}), between 250 m and 450m from the shower core, detected by the spectrograph may be compared with all showers, in this distance range and with zenith angles less than 40^{o}, detected by the array at Haverah Park. As the two samples of showers have rather similar mean sizes and zenith angles, the structure function exponents in the two cases should be the same if there is no causal relation between muon densities and this exponent. The distributions of best fit structure function exponent for the two classes are very similar,

the mean values being -

'Muon showers' mean exponent = 3.04 ± 0.34

All showers mean exponent = 3.13 ± 0.15

From this comparison it may be concluded that showers containing fast muons are not flatter than typical showers recorded at Haverah Park.

(e) The variation of shower parameters with deflection

If the air shower data cause any biases in the momentum spectrum of the muons, this fact will be reflected in the variation of the various shower parameters with muon deflection.

The variation with deflection of shower size, zenith and azimuth angles and radius of curvature of the shower front has been examined for the 300 m and 380 m data. No significant variation has been found, implying that, at least in first order, the muon deflection spectra are independent of these parameters.

5-3.2 Muon momentum spectra

The derivation of the absolute differential and integral spectra has been discussed above, and the checks carried out upon the data ensure assignation of events to the correct interval of distance from the core.

The absolute differential momentum spectra for the various distances for a shower of size 2×10^7 particles are shown in Figure 5.3 and the corresponding integral spectra in Figure 5.4. It must

be remembered that the spectra shown at 50 m and 100 m from the core are in fact normalized from much smaller showers. These integral densities enable the lateral distributions of muons above various fixed momenta to be drawn (Figure 5.5). These have been extrapolated as shown and the total numbers of muons of momentum greater than various thresholds in a shower of 2×10^7 particles can be found by evaluating:-

$$N_\mu (\geq p) = \int_1^{1000} f_\mu (r, \geq p)\, 2\pi r\, dr$$

These muon numbers are plotted against $(p + 2)$ in Figure 5.6, where it can be seen that they follow a line of the form

$$N_\mu (\geq p) = (7.32 \pm 0.80) \times 10^5 \, (p + 2)^{-1.3 \pm 0.1} \qquad (5.5)$$

The total number of muons in the shower is $(1.8 \pm 0.2) \times 10^6$ and from relation 5.5 the total energy carried by the muon component of a shower of size 2×10^7 is

$$E_T = \left(1.2^{+\ 0.6}_{-\ 0.5}\right) \times 10^7 \text{ GeV}$$

Hence the mean momentum of the muons in such a shower is

$$\bar{p} = 6.7^{+\ 3.2}_{-\ 2.0} \text{ GeV/c}$$

These conclusions, which are based upon the differential momentum spectra of the muons measured in this experiment, rely upon normalization to a common size. As observed above, whilst not unfounded at low energies, this normalization of the muon densities from the smaller arrays may break down at high momenta. Shown in Figure 5.6

FIGURE 5.3

The differential momentum spectra of muons at various distances from the core of a shower of size 2×10^7.

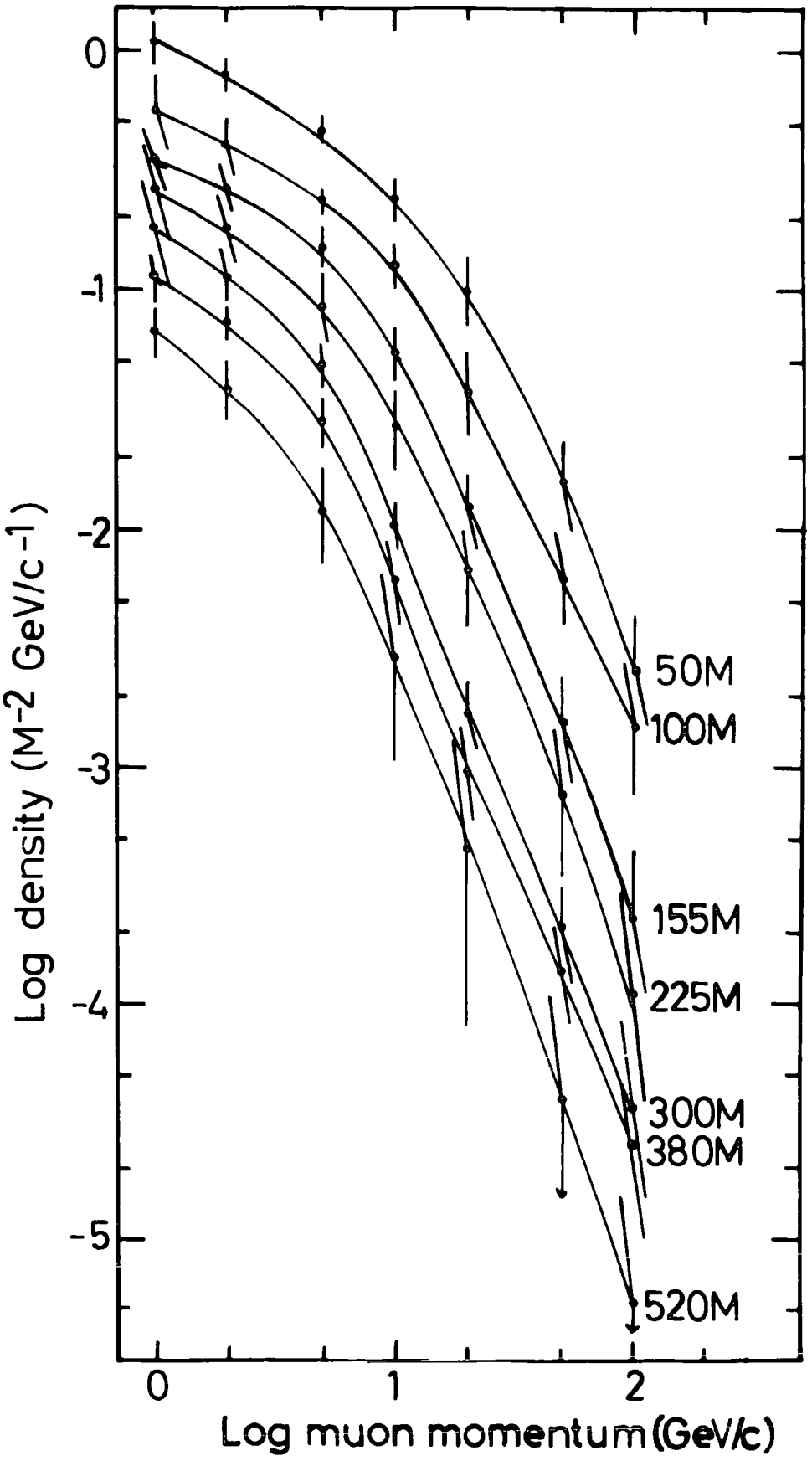
0
-1
-2
-3
-4
-5
Log density (M-2 GeV/c-1)
0
1
2
Log muon momentum (GeV/c)
50M
100M
155M
225M
300M
380M
520M

FIGURE 5.4

The integral momentum spectra of muons at various distances from the core of a shower of size 2×10^7.

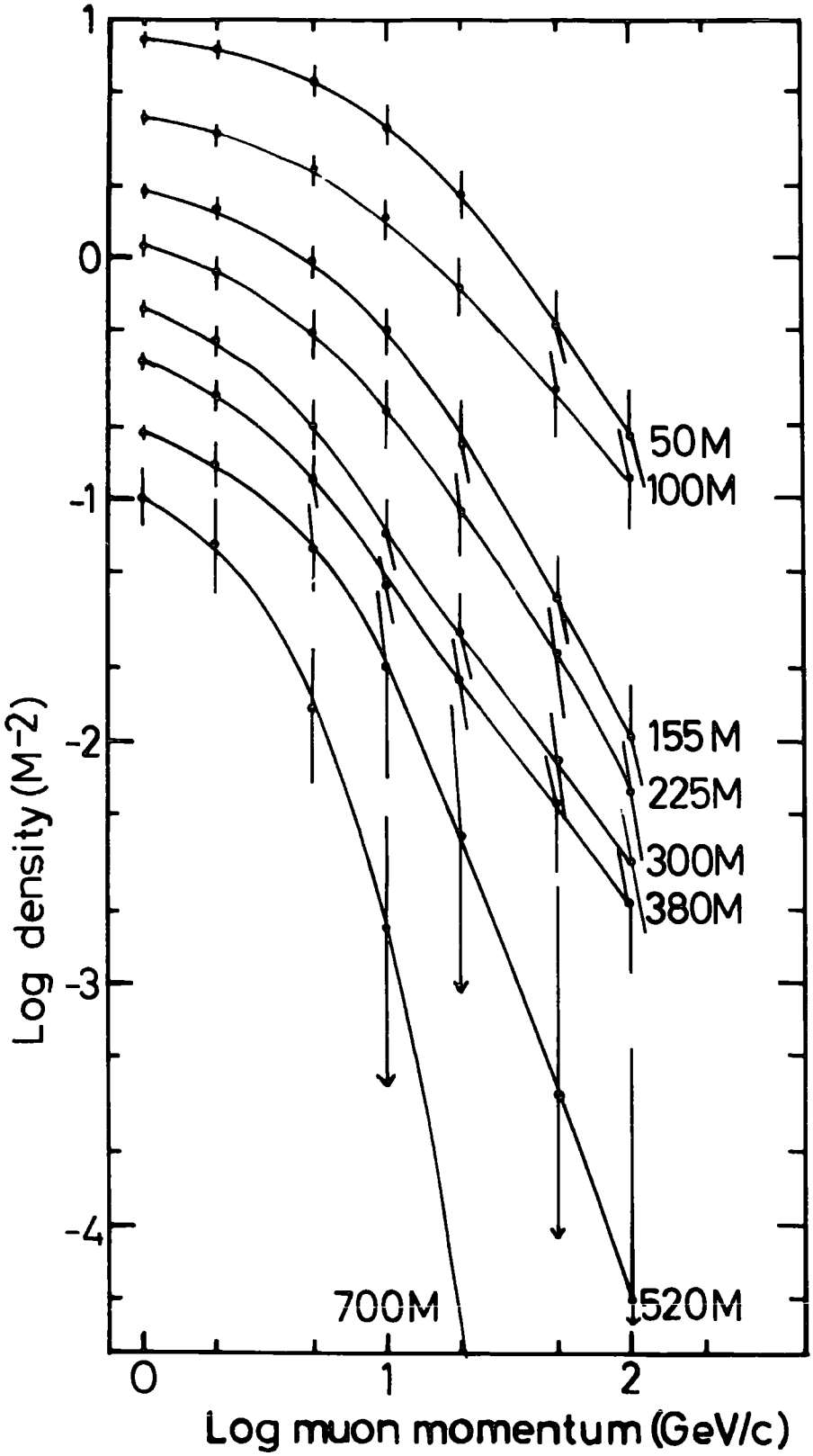
1
0
-1
-2
-3
-4
Log density (M-2)
50M
100M
155M
225M
300M
380M
700M
520M
0
1
2
Log muon momentum (GeV/c)

FIGURE 5.5

The lateral distributions of muons of momentum above various threshold values for a shower of size 2×10^7. The broken lines indicate extrapolation outside the region of measurement. The key indicates the threshold momenta.

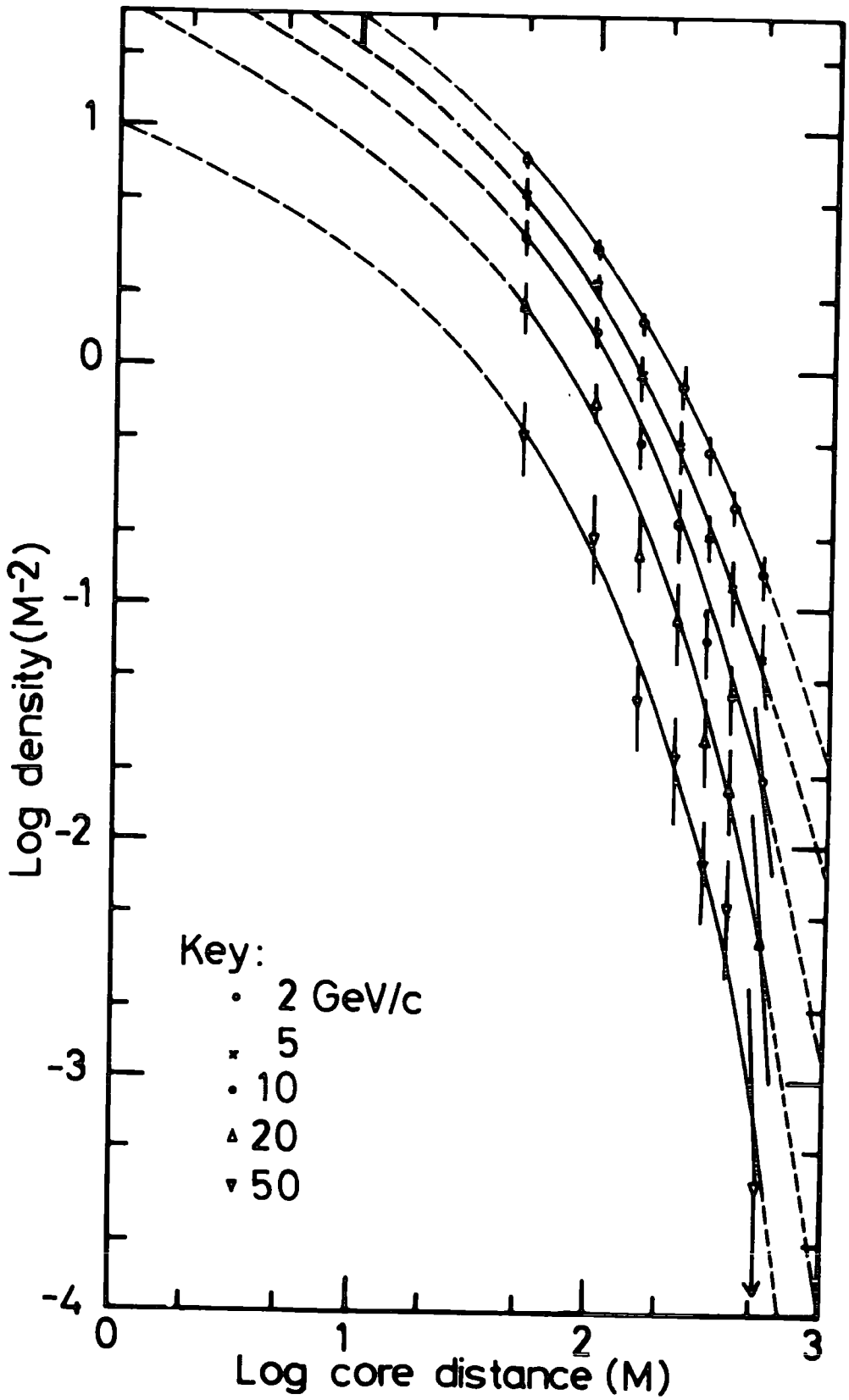
Log density (M-2)
1
0
-1
-2
-3
-4
0
1
2
3
Log core distance (M)
Key:
2 GeV/c
5
10
20
50

FIGURE 5.6

The integral momentum spectrum of all muons in a shower of size 2×10^7. The various points refer to:

(1) Present data

(2) Khrenov (1962) $p = 5$ and 10 GeV/c

(3) Barnaveli et al., (1965)

(4a) Chatterjee et al., (1966) scaled using $\alpha = 0.47$

(4b) Chatterjee et al., (1966) scaled using $\alpha = 0.78$

(5) Bennett and Greisen (1961)

(6) Greisen (1960)

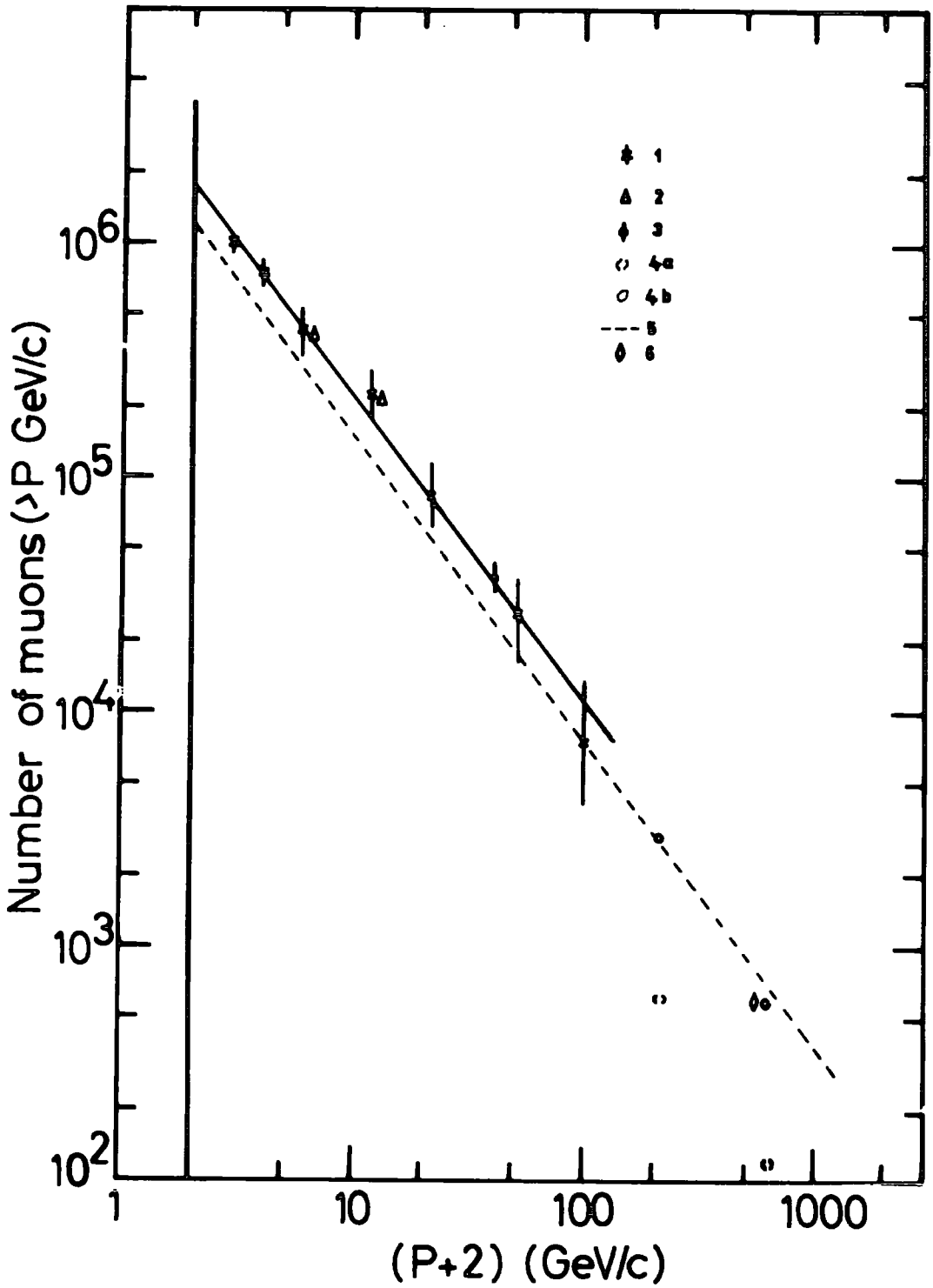
Number of muons (>P GeV/c)
10^6
10^5
10^4
10^3
10^2
1
10
100
1000
(P+2) (GeV/c)
1
2
3
4a
4b
5
6

are several points measured in other experiments and normalized to a size of 2×10^7. Attention is drawn to the numbers of muons of energy greater than 220 GeV and 640 GeV (Chatterjee et al., 1966), which clearly agree with the present data extrapolated to these energies if scaled from 10^5 particles using an exponent of 0.78 in the relation of muon number to shower size, as determined at lower energies in the present work. However, when scaled using an exponent of 0.47, as suggested by Chatterjee et al., such agreement is not found. These results, together with the agreement with the present data of muon numbers measured by other groups scaled by the exponents found by these groups which vary from 0.7 to 0.85, suggest that, from size 10^5 to 2×10^7 and for all momenta important in the present study, muon numbers may be related to shower size using

$$N_\mu (\geq p) \quad \alpha \quad N_e^{0.78}$$

5-3.3 The momentum spectrum of muons at distances greater than 600 m from the core

Showers falling at distances greater than 600 m from the spectrograph have very uncertain core locations and hence the muons detected in such showers are best treated as a single sample located at the median distance from the core of 700 m. The operation of the 2 km array should enable much more accurate analyses to be made and samples of muons at these great distances may then be subdivided. To date, however, 100 muons have been recorded by the spectrograph

in this region of the showers, of which 70 are within the imposed limits of ψ_0 and $\Delta\psi$. Half of these useful muons occur in showers which have been fully analysed by the Leeds group; the other air showers have been analysed by a more simple procedure. Due to this very small sample it was thought more useful to attempt to derive the momentum spectrum appropriate to these muons using the direct method of estimating the momentum spectrum from the individual deflections of the muons.

As an initial trial spectrum that spectrum determined for muons at 520 m from the core was used. The inappropriateness of this spectrum was evident in the difference of the spectrum derived from one iterative cycle. In all, some eighteen iterative cycles were carried out until the spectral shape became unchanging with further iteration. This final spectrum was steeper than the initial trial spectrum and its uniqueness was checked by iterating again from a trial spectrum steeper than that appropriate to the data. In this case the iterative steps moved the spectrum up towards that previously found.

The form of differential momentum spectrum most appropriate to the data was not of the simple monotonic nature observed for the rest of the distance intervals examined. If the differential densities for muons of various moments found at other distances from the core were extrapolated to predict the shape of the differential momentum spectrum at 700 m, the shape of this expected spectrum agreed well

with that observed for momentum below or equal to 2 GeV/c and above or equal to 10 GeV/c. Between these two limits the spectrum observed was far below that expected. Such an effect could be real or it could be caused by statistical fluctuation in the observed deflection spectrum.

The latter cause is thought to be more probable, the iterative procedure producing a momentum spectrum which will follow the observed deflections without smoothing the fluctuations at all. To check this hypothesis the two portions of the spectrum which agreed with extrapolation were smoothly connected and the momentum spectrum so produced was processed to derive the appropriate deflection spectrum. Within the statistical uncertainties of the data this deflection spectrum was not inconsistent with that observed. The integral spectrum derived from this differential spectrum is plotted in Figure 5.4.

The direct method of deduction of a momentum spectrum from the observed deflections has been shown to be an iterative procedure with a unique result; however, from the above it may be seen that for small samples of data the method is very liable to fluctuation. Whilst in some cases it could be the only applicable method, care must be exercised in the interpretation of the results of this procedure.

5-4 The spectrum as a function of shower size and zenith angle

The variation of the momentum spectrum of muons with distance from the shower core has been discussed above, and the evidence for any variation with the other EAS parameters will now be presented. In this study the second method described above for the derivation of a momentum spectrum must be used, as the distributions of arrival directions are not at all similar to those found for a normal sample of events. For this reason the low energy corrections to the derived spectra have not been carried out.

5-4.1 The variation with zenith angle

In section 5-3.1 it was noted that no variation of mean zenith angle with deflection was observed, suggesting that the observed deflection spectrum is not strongly dependent upon zenith angle. The distributions of deflection for the same interval of distance and narrow bands of zenith angle confirm this, but, due to the variation of the distribution of incident angle with zenith angle, the momentum spectrum may well vary with zenith angle.

The most populous spectrum, at 300 m, was divided into two bands of zenith angle at 20° and the momentum spectra derived for these bands. The spectra were very similar in shape for momenta above about 5 GeV/c, although they were somewhat affected by statistical fluctuations. Below 5 GeV/c the spectrum for the more inclined showers was considerably lower than in the vertical showers. The mean

energies of the two spectra were:-

$0^{\circ} < \theta < 20^{\circ}$ $\quad \bar{p} = 5.43$ GeV/c

$20^{\circ} < \theta < 40^{\circ}$ $\quad \bar{p} = 8.02$ GeV/c

This effect may be ascribed to an absorption of low energy muons by the extra depth of atmosphere penetrated by the more inclined showers and to a loss of low energy muons in the magnet due to an increase in the thickness of iron presented to inclined muons, requiring a 10% increase in the energy of muons to penetrate the magnet.

5-4.2 The variation with shower size

The distribution of shower size for showers falling within a restricted region of distance from the specirograph is quite narrow, ranging from about 7×10^6 to about 8×10^7. In examining a variation with shower size significance can only be retained if only two intervals of size are used. Showers falling between 200 m and 450 m from the spectrograph were used and they were divided into two bands of size at 3×10^7. The deflection spectra for the two regions of size were compared for the usual distance intervals, but the results of these comparisons were inconclusive, due to statistical fluctuations. Thus for each distance interval the numbers of particles above and below 3×10^7 were normalized to the same figure and the resultant distributions of deflection and angle of incidence summed over all the intervals. The final distributions are shown in Figure 5.7. The distributions of incident angle are slightly different

FIGURE 5.7

Distributions of deflection and incident direction for muons between 200 m and 450 m from the core of showers greater than and less than 3×10^7.

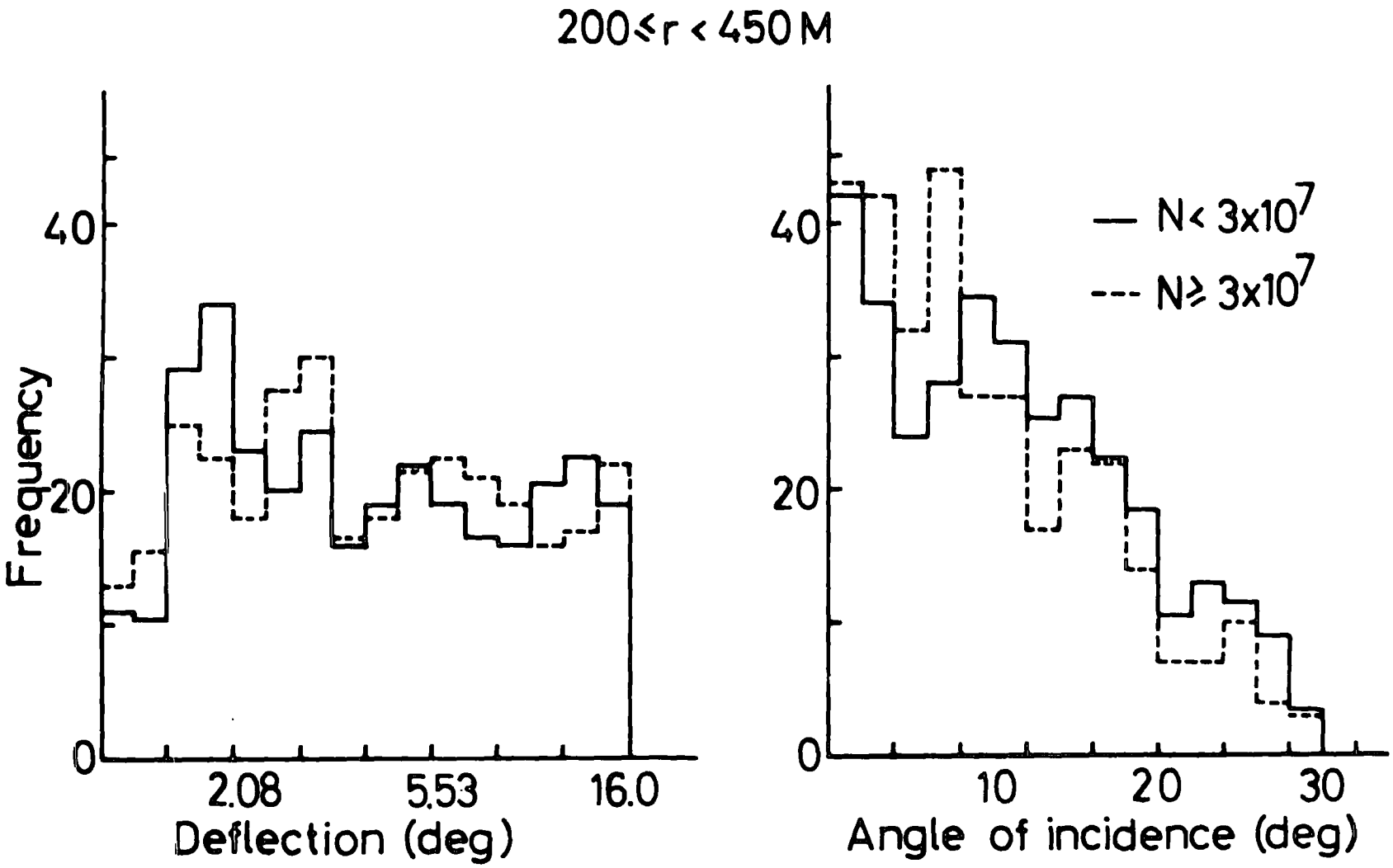
200≤r<450M
40
20
0
Frequency
2.08
5.53
16.0
Deflection (deg)
40
20
0
10
20
30
Angle of incidence (deg)
— N< 3x10^7
--- N≥ 3x10^7

but insufficiently so to affect the momentum spectra derived from the deflection spectra, which are similar within the statistical errors.

It may thus be concluded that the momentum spectrum of muons does not vary significantly with shower size, over the rather limited range examined.

5-5 Discussion of results

The determination of the momentum spectrum of muons in extensive air showers at Haverah Park has ranged further in momentum and distance from the core than any previous studies. It is useful, however, to compare the results of the present experiment with those obtained previously.

In Figure 5.8 the densities of muons of momentum greater than three threshold values at various distances from the core determined by absorption methods by Khrenov (1962) and Barnaveli et al.(1965) are compared with the lateral distributions deduced from the momentum spectra measured at Haverah Park. The points are scaled to a size of 2×10^7, using a value of α of 0.85 for the results of Khrenov, this being the value he measured, and using 0.78 in the case of Barnaveli et al., who quote no variation. In all cases the densities recorded furthest from the core are lower than is suggested by the present results. These points all refer to showers falling outside the array, where core location will be very poor, often leading to

FIGURE 5.8

Comparison of the data of Khrenov (1962) and Barnaveli et al. (1965) with the lateral distributions derived from the present experiment. All data scaled to shower size of 2×10^7 particles.

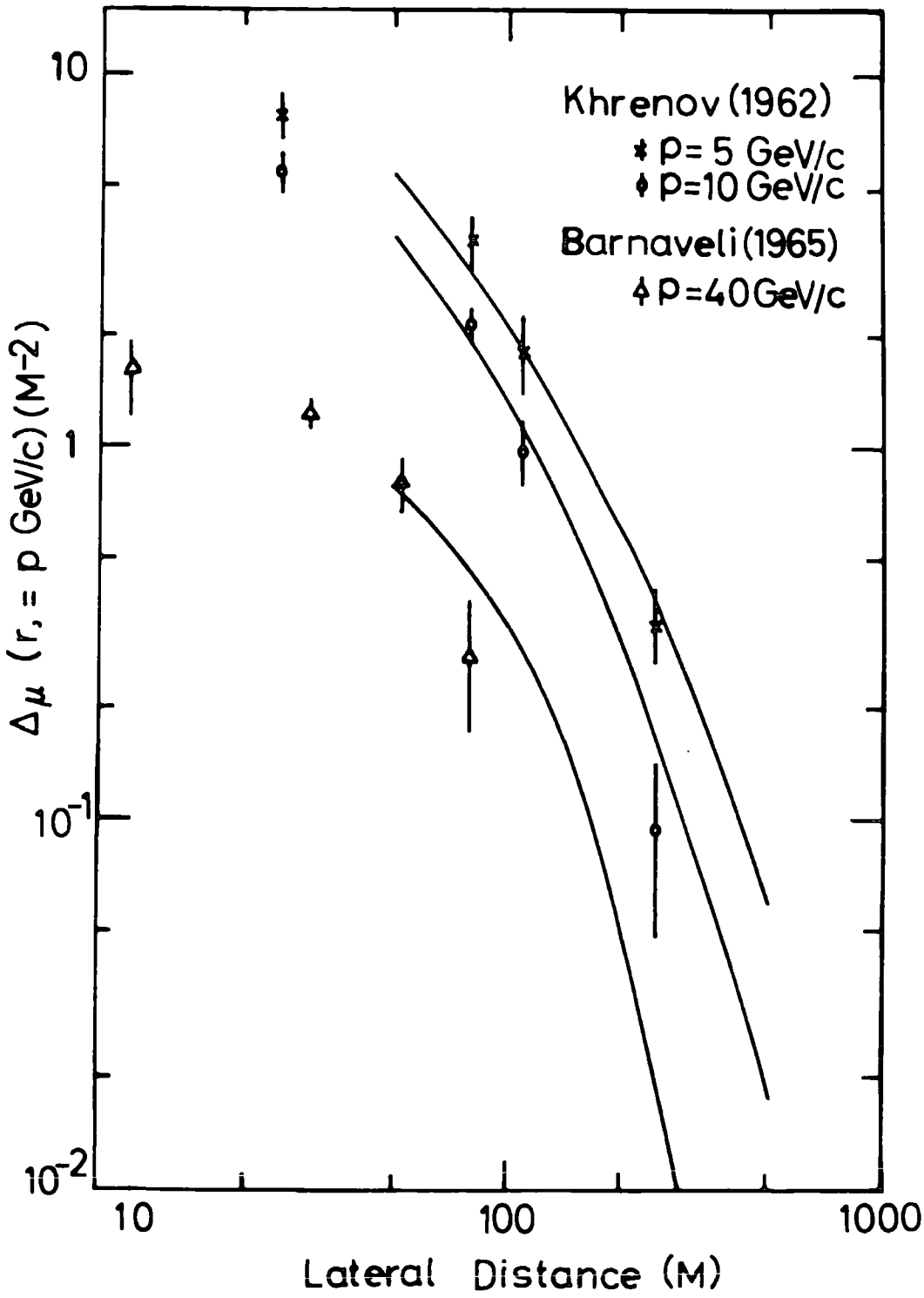
Khrenov (1962)
p= 5 GeV/c
p=10 GeV/c
Barnaveli (1965)
p=40GeV/c
10
1
10^{-1}
10^{-2}
$\Delta\mu$ (r, = p GeV/c) (M-2)
10
100
1000
Lateral Distance (M)

an overestimate of the shower size and hence an underestimate of muon density when scaled to a common size.

Crude measurements on the integral momentum spectra of muons at various distances from the core have been made using absorption techniques in the past. These measurements, which have been summarized by Rochester et al. (1966), mainly give results in fair agreement with the present spectra. They have, however, been overshadowed by the experiment of Bennett and Greisen (1961) using a magnet spectrograph of m.d.m. equal to 20 GeV/c. The results of this experiment are shown in Figure 5.9, normalized at 1 GeV/c to the present integral momentum spectra. The points at 25 m from the core are not compared with any line as an appropriate spectrum has not been determined from the Haverah Park data in this analysis. However, the spectrum is nearly unchanging with distance at these low distances from the core and a comparison may be made with the shape of the spectrum shown at 50 m.

One further experiment must be mentioned, which suggests an energy spectrum of muons much softer than any other. De Beer et al. (1962), using the scattering of muons, find an energy spectrum which is unchanging from 100 m to 300 m from the core and which is very much steeper than that found in the present work.

In Figure 5.6, in addition to the results of the present experiment, several other determinations of numbers of muons above a fixed muon energy are shown. The points due to Khrenov, Greisen

FIGURE 5.9

Comparisons of the integral momentum spectra of Bennett and Greisen (1961) with those derived from the present study. All data scaled to shower size of 2×10^7 particles.

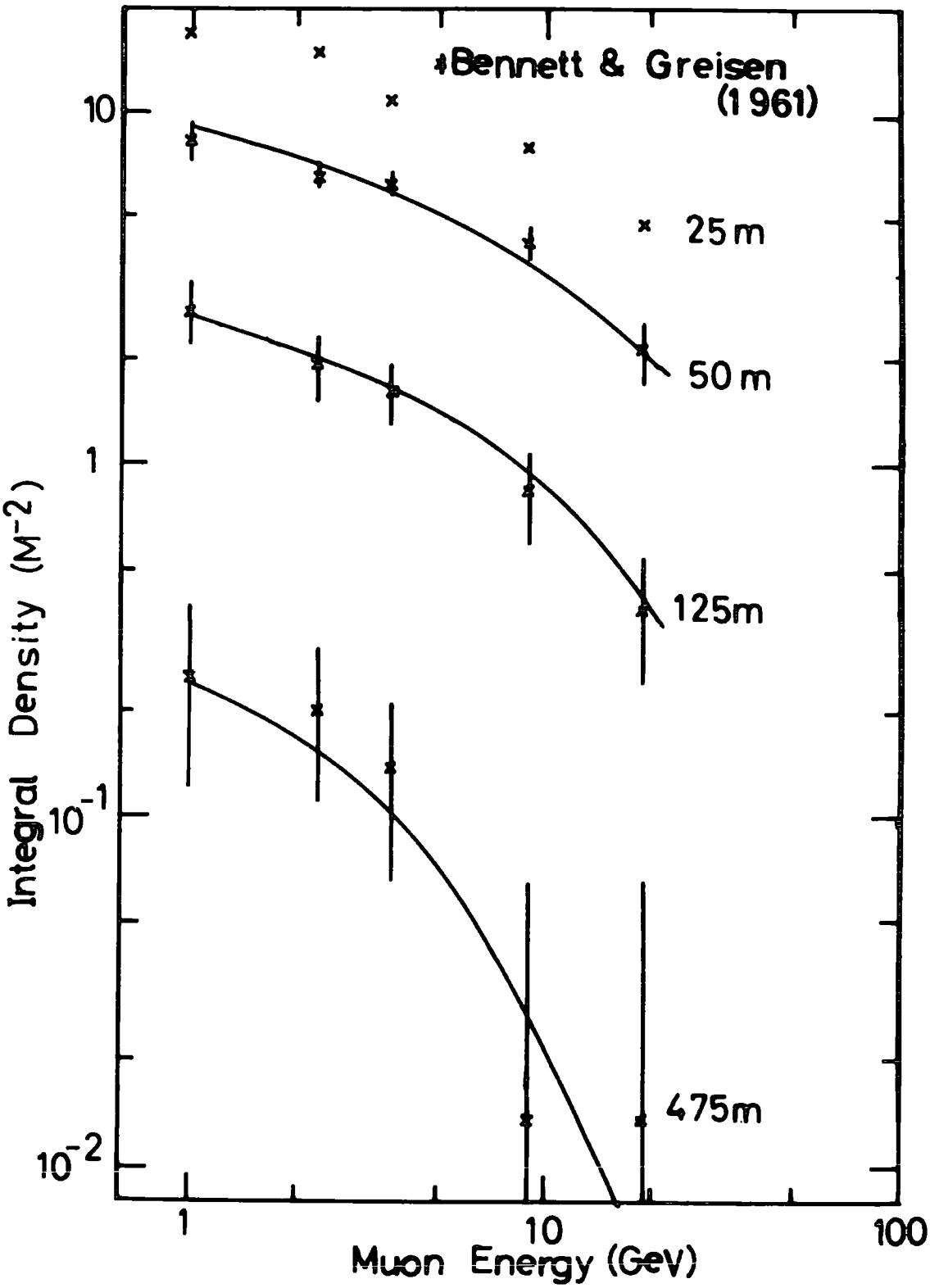
Bennett & Greisen
(1961)
25m
50m
125m
475m
10
1
10^{-1}
10^{-2}
Integral Density (M^{-2})
1
10
100
Muon Energy (GeV)

and Chatterjee et al. are scaled according to the value of α determined by these workers, respectively 0.85, 0.7 and 0.47. The results of the two former groups appear consistent with the present work, as does the point due to Barnaveli et al., scaled using the present value of α , 0.78. If the results of Chatterjee et al. are scaled as 0.78. then agreement is reached with the rest of the data. The line derived by Bennett and Greisen is normalized to a size of 2×10^7 using the value of α, 0.75, which they ascertained. It may be seen that the numbers of muons found in the present experiment is some 45% higher than is found by these authors.

It has been found that the density of muons greater than p GeV/c at a distance r metres from the core of a shower of size N determined in the present study can adequately be represented by the formula quoted by Bennett and Greisen, suitably renormalized:-

$$\Delta_\mu (N, r, \geq p) = \frac{26\ r^{-0.75}}{(1+r/320)^{2.5}} \left(\frac{N}{10^6}\right)^{0.78} \frac{51}{p+50} \left(\frac{3}{p+2}\right)^{0.14} r^{0.37}$$

CHAPTER 6

THEORETICAL PREDICTIONS OF CHARACTERISTICS OF MUONS IN AIR SHOWERS

6-1. Introduction

The present experiment has determined the lateral distribution in air showers of muons of momenta greater than 1 GeV/c over a range of distance from 10 m to 1100 m from the core and the variation with distance from the core of the momentum spectrum of muons between 1 GeV/c and 100 GeV/c. It has been shown that the present experimental results are supported by most previous experiments wherever these experiments can be compared. It is hoped by comparisons of the measured densities of muons with theoretical predictions based upon assumptions on the nature of the nuclear cascade to test the validity of these assumptions and thus derive information on the nuclear interactions at great energies and the nature of the primary particles initiating the air showers.

6-2. Theories of the muon component of air showers

Several groups have calculated the characteristics of the muon component of air showers. Some of these (Lal 1967, Cowsik 1966) have concentrated their attention upon the longitudinal development of the shower and hence predict only the total momentum spectrum of all the muons in a shower of fixed primary energy. Their results

are in substantial agreement with the more detailed calculations to be described later and thus will not be described here in detail. It is of interest to note that these workers suggest that the number of muons above several hundred GeV varies with shower size in a manner nearer to that given by the present work than that given by Chatterjee et al.(1966).

Turning to theoretical studies of the lateral distributions of muons in air showers, Hillas (1966) and de Beer et al.(1966, 1967), using models which are similar to each other, have predicted the densities of muons above fixed momenta in a shower. The detailed characteristics of these models are summarized in Table 6.1. An important feature which may be mentioned is the treatment of the first interactions of the primary particle and the interactions of the early generations of pions. Hillas fixed the height of the first interaction at an atmospheric depth of 100 gm cm^{-2}, subsequent interactions taking place at 100 gm cm^{-2} intervals. De Beer et al. selected the point of interaction of the primary particle using a Monte-Carlo method. The pion cascade was sampled, for six pion energies, at six levels in the atmosphere, spaced 180 gm cm^{-2} apart and commencing 30 gm cm^{-2} below the first interaction point. This matrix of pion energy and depth was interpolated using a 3rd order polynomial fit to find the characteristics of any interaction of a particular energy. While Hillas considered only primary nucleons, de Beer et al.considered both primary protons and nuclei of mass 20;

TABLE 6.1

CHARACTERISTICS OF AIR SHOWER MODELS

Parameter of model	de Beer et al.	Hillas	Orford & Turver (2)
Primary energy	6×10^6 GeV	10^8 GeV	10^6 - 3×10^8 GeV (2×10^8)
Primary mass	1, 20	1	1 - 56 (> 10)
Fragmentation fraction	see text	-	0.1 - 0.5 (0.22)
$K_{nucleons}$	0.5	0.5	0.3 - 0.7 (0.5)
$\lambda_{nucleons}$	80 gm cm^{-2}	100 gm cm^{-2}	70 - 90 gm cm^{-2} (80)
$\lambda_{nucleus\ (A)}$	see text	-	$205/(0.6+A^{\frac{1}{3}})^2$ gm cm^{-2}
secondaries	π^{+-0}	π^{+-0}	π^{+-0} (see text)
K_π	1.0	1.0	1.0
λ_π	120 gm cm^{-2}	100 gm cm^{-2}	120 gm cm^{-2}
n_s(1)	0.25, 0.5 (2×10^3 GeV)	0.50 (3×10^3 GeV)	0.1 - 1.0 (0.5) (3×10^3 GeV)
Distribution of energy and p_t	CKP $\bar{p}_t$ = 0.4 GeV/c	Bristol data $\bar{p}_t$ = 0.35 GeV/c	CKP $\bar{p}_t$ = 0.4-0.6 GeV/c (0.5)

(1) The values quoted under 'n_s' are the exponents of the relation $n_s \propto E^\beta$ above values of E quoted. Below these energies the exponent is 0.25.

(2) Wide ranges of many parameters have been used by Orford and Turver to investigate the effect of these variations. The values finally used as most appropriate are shown in parentheses. The wide range of primary energy used was necessary to explain the data recorded in showers of a wide range of size.

showers initiated by a nucleus of mass A and energy E being considered as a superposition of A showers, each initiated by a proton of energy E/A.

A rather different approach is represented by the careful Monte-Carlo calculations of the nuclear cascade in small air showers by Bradt and Rappaport (1967), and McCusker et al. (1968). These calculations, which yield some information on the muon component, are limited to rather low primary energies because of the vast increases in computing time for larger energies. Similar considerations restrict these studies to particles of energy above 50 GeV/c. Thus the interactions yielding the largest part of the muons studied by the present experiment are not considered and the ranges of momentum and distance covered are very restricted.

6-2.1 Predictions and comparisons with present work

Hillas presents the unnormalized integral momentum spectra at various distances from the core of a shower of 2×10^7 particles. Three of these spectra are shown in Figure 6.1, compared with the spectra measured at distances near to those for the calculated spectra. The predicted spectra have been normalized to the observed densities at a momentum of 1 GeV/c.

De Beer et al. give lateral distributions for muons of momentum greater than 1, 10 and 100 GeV/c in a shower of size 10^6 particles. These are shown in Figure 6.2, normalized to a shower of size 2×10^7

FIGURE 6.1

Comparison of integral momentum spectra at three distances from the core of a shower of size 2×10^7 with the predictions of Hillas (1966).

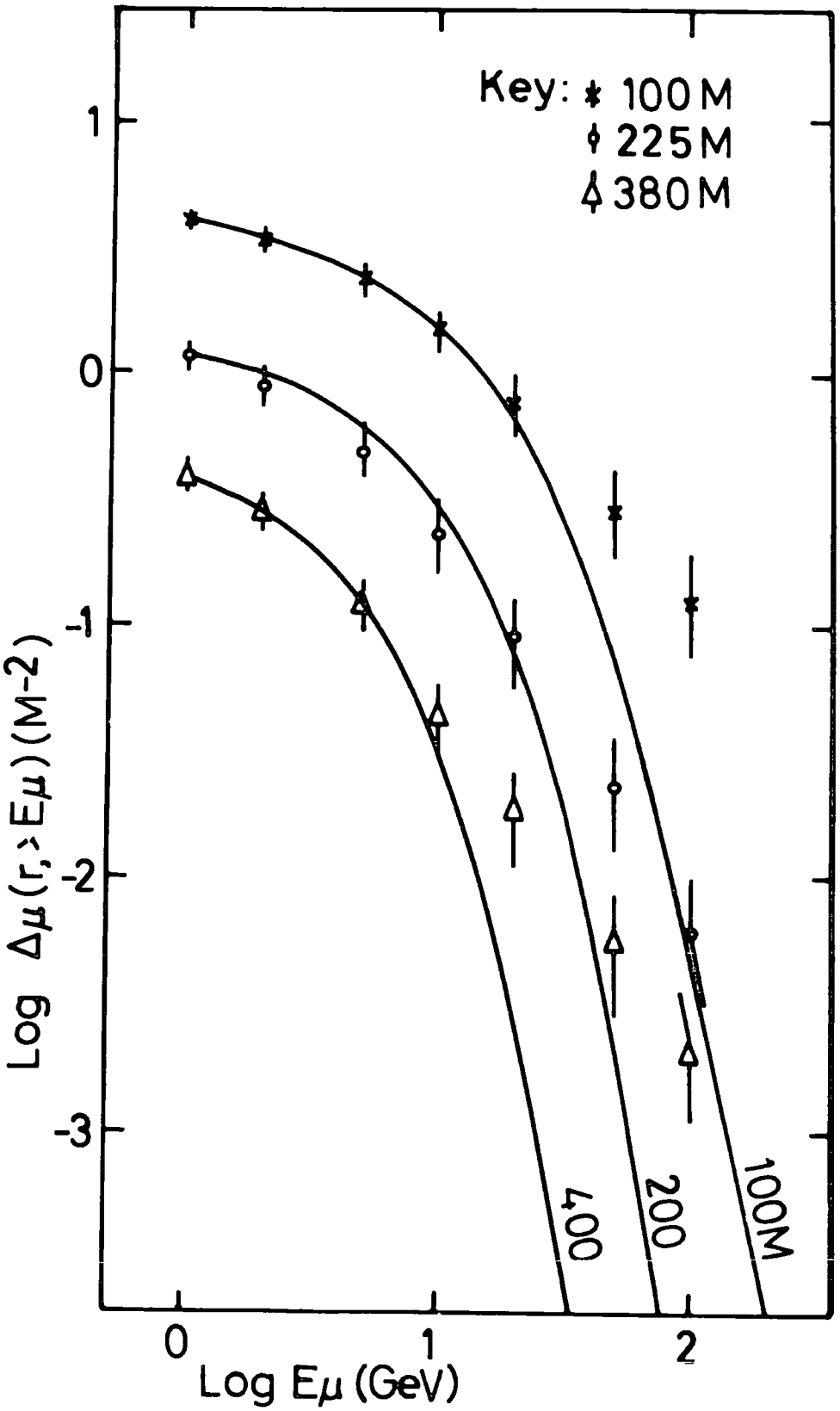
Key: * 100M
225M
380M
1
0
-1
-2
-3
Log Δμ(r,≥Eμ)(M-2)
0
1
2
Log Eμ (GeV)
400
200
100M

FIGURE 6.2

Comparison of lateral distributions of muons above three threshold momenta in a shower of size 2×10^7 with the distributions predicted by de Beer et al (1967).

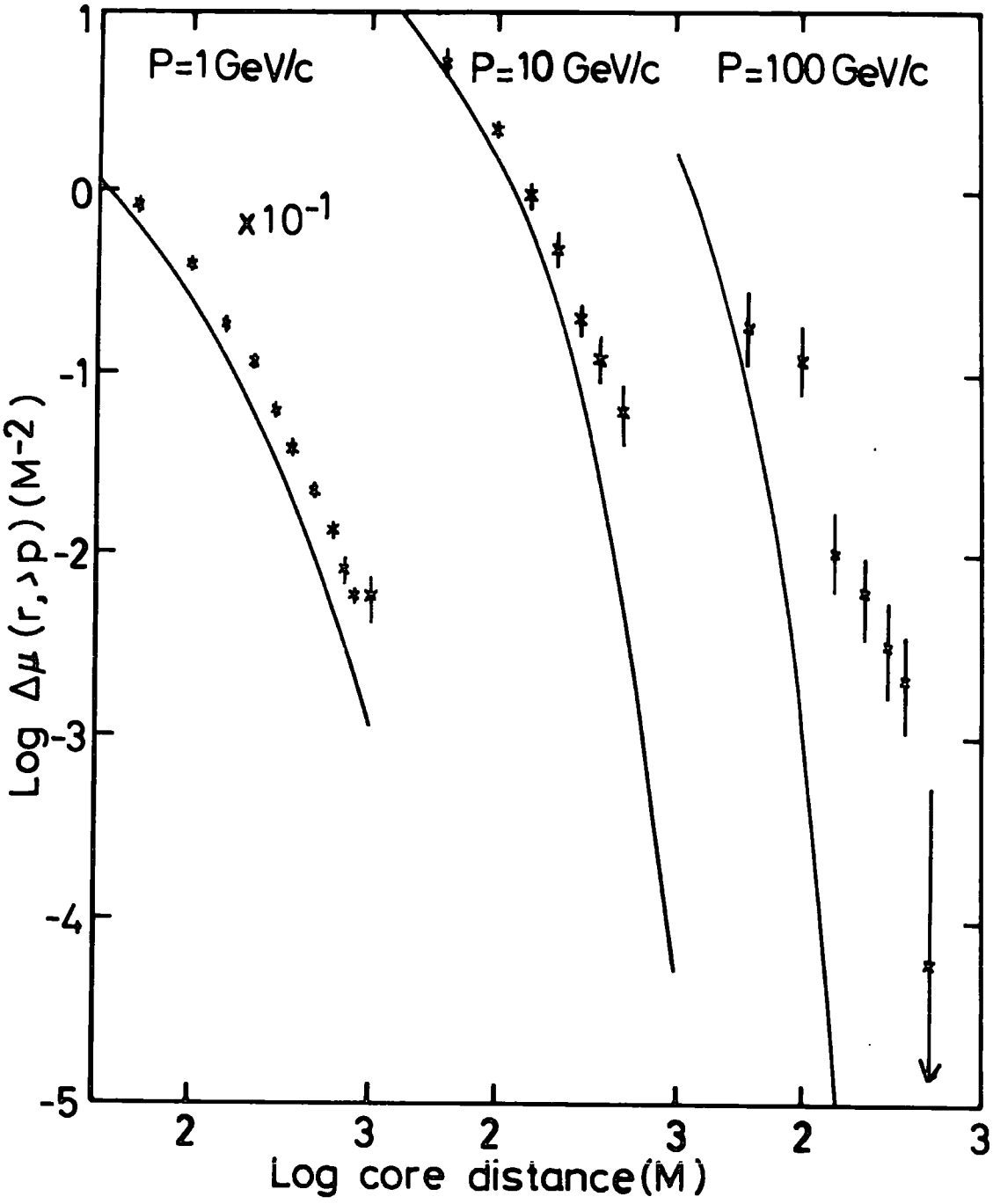
P=1 GeV/c
P=10 GeV/c
P=100 GeV/c
x10⁻¹
Log Δμ (r, >p) (M⁻²)
Log core distance (M)
1
0
-1
-2
-3
-4
-5
2
3
2
3
2
3

using $\alpha = 0.78$. The experimental points plotted are those derived from the present spectra.

From these two comparisons it can be seen that whilst at low energies and moderate distances from the core these theories predict densities quite close to the observed data, this agreement is not found at larger momenta and distances. It can be seen that, as the distance from the core increases, the momentum at which this divergence occurs decreases.

Turning to the study of the densities of muons of momenta above 1 GeV/c, the dependence on the shower size of the total number of muons may be expected to reflect any variation with energy of the composition of the primary cosmic rays, as an air shower initiated by a heavy nucleus of given energy should contain more muons of fixed energy than one initiated by a proton of similar energy. Adcock et al. (1968) have predicted the changes in the dependence of total muon number on the shower size expected on the galactic modulation model. These changes are largely consequent upon fluctuations of shower size. The fluctuations in the observed size parameter in the present experiment, E_{100}, are expected to be much less than those in the conventional shower size and so the variations predicted by Adcock et al. may not be relevant to the present data. In fact no significant variation of α has been observed over a range of shower size from 8×10^4 to 3×10^8.

6-2.2 Discussion of the comparisons of theoretical prediction with experimental data

At the International Conference on Cosmic Rays held at Calgary in 1967 Earnshaw et al. (1967c) presented momentum spectra based upon the data used in the present analysis, and noted discrepancies similar to those shown above in comparison with theoretical predictions. Since that time the most searching re-scrutiny of the data using the criteria described in Chapter 5, while bringing to light some few dubious events, has failed to reveal any sources of error sufficient to account for these anomalous densities. Despite the removal of these dubious events from the body of data, the momentum spectra presented in this thesis are very similar to those given at Calgary. For example, the 300 m spectrum presented at Calgary contained 559 particles, of which 43 had deflections less than 0.72^{o}. Seven of these low deflection muons have been removed as dubious, causing the integral density of muons of momentum greater than 100 GeV/c to be reduced by a factor of two compared with that previously derived.

The models used in the theoretical analyses have been examined to reveal any inaccuracies which may be inherent in these treatments. The anomalously high muon densities observed could be caused by either a change in the distribution of transverse momentum used, giving an increased mean p_t, or an increase in the effective height of origin of the muons falling in the relevant regions of momentum and distance. An analysis of the angular deviations of muons from the core led to

an explanation of these anomalous muon intensities involving large transverse momentum (Earnshaw et al.1967b). The calculation of the distributions of the angular deviations used in this preliminary analysis was rather simple, the directions of motion of all the muons in a shower being considered. A recent theoretical treatment of the angular deviations of muons observed at a fixed distance from the core suggests that the observed directions of motion can be accounted for without the necessity of invoking large transverse momentum. A full account of these new calculations will be presented in Chapter 7.

6-3. A new model of the muon component

A new model of the muon component of air showers has been evolved by Orford and Turver (1968). This calculation was initiated to account for the muon densities at a momentum of 100 GeV/c and at distances from the core greater than 100 m. Preliminary calculations showed that muons in this region of momentum and distance originate in the first few interactions, and, in particular, that it is necessary to examine the cascade above an altitude of 10 km accurately. To check that the model parameters necessary to give the observed muon densities at a momentum of 100 GeV/c do not distort the rest of the shower, the calculations must be continued to sea level approximately. This approximate treatment must mean that at distances less than 100 m and momenta less than 100 GeV/c the predicted muon densities are not expected to be as accurate as the range of momentum and distance

covered by the first part of the calculations. An altitude of 10 km is equivalent to a depth of 260 gm cm^{-2} for a vertical shower and hence the detailed calculations must cover the first three nuclear interaction lengths.

The method used in this upper portion of the atmosphere is that of successive collisions. It is found, taking the cascade to the third secondary interaction, that practically the total muon densities at a momentum of 100 GeV/c can be accounted for. The numerical values of the various parameters used are shown in Table 6.1. Below 10 km fixed interaction levels are used, the nuclear interaction mean free paths for the various types of particle being shown in Table 6.1. Throughout, full account has been taken of the decay of pions and the energy loss and decay of muons.

Both pion and kaon secondaries have been considered, the muon intensities being somewhat larger for the latter case. The K/π ratio has been taken as 0% in most of the calculations, yielding underestimates of the muon densities; some work has been done for a value of 25% to investigate the charge ratio.

6-3.1 Comparisons of the predictions of the model with experimental data

As indicated above, wide ranges of many parameters have been used in the theoretical approach. It has been found that the momentum spectra of muons at large distances from the core depend very strongly

FIGURE 6.3

Comparison of the differential momentum spectra of muons at three distances from the core of a shower of size 2×10^7 with the predictions for a shower initiated by a primary nucleus (energy 2×10^8 GeV) having mass 20 when the multiplicity varies as $E^{0.5}$ for energies above 3×10^3 GeV.

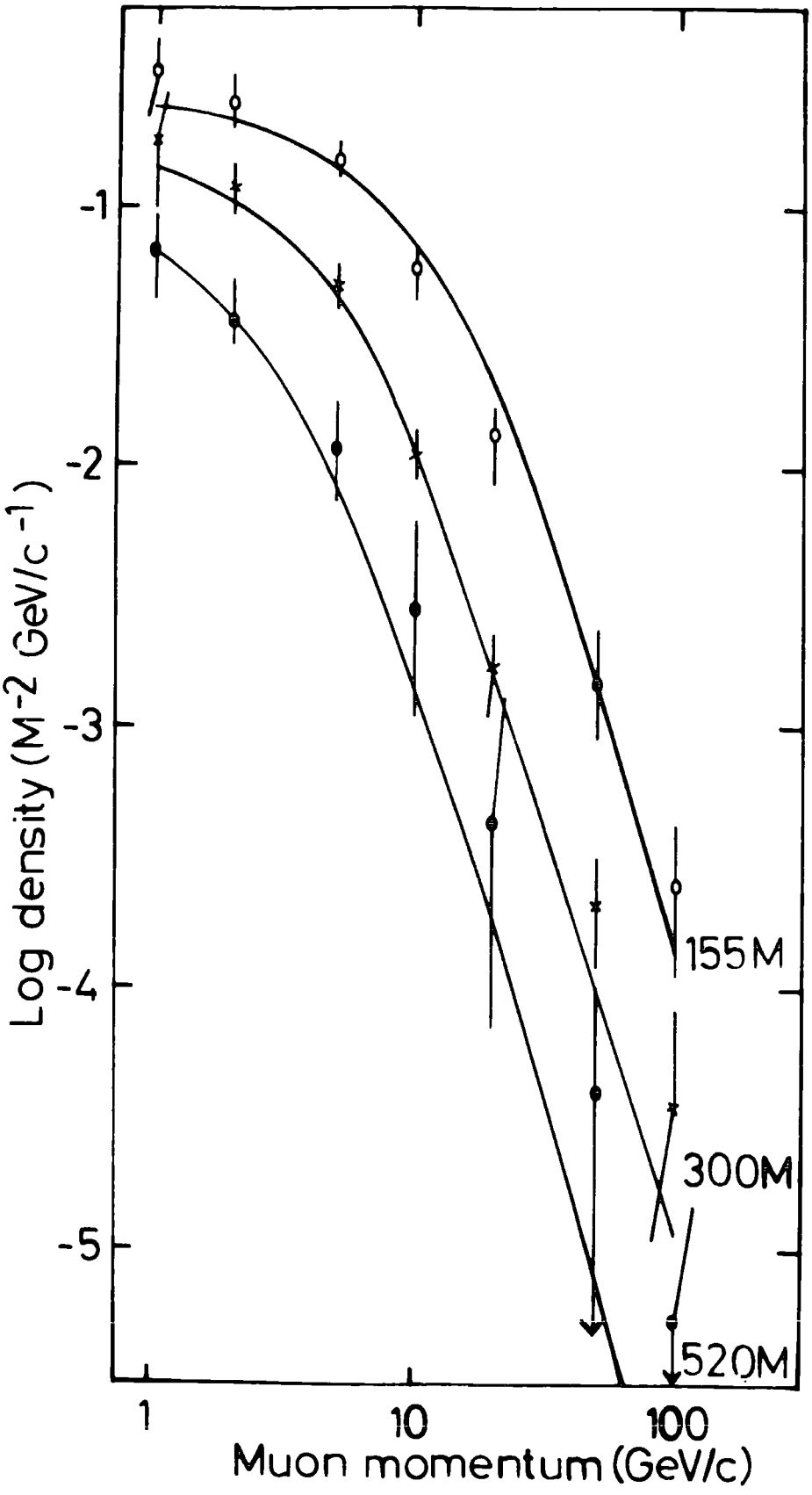
-1
-2
-3
-4
-5
Log density (M-2 GeV/c-1)
155M
300M
520M
1
10
100
Muon momentum (GeV/c)

FIGURE 6.4

A comparison of the lateral distribution of muons of momentum greater than 1 GeV/c with the distributions predicted for primary nuclei of masses 20 and 1.

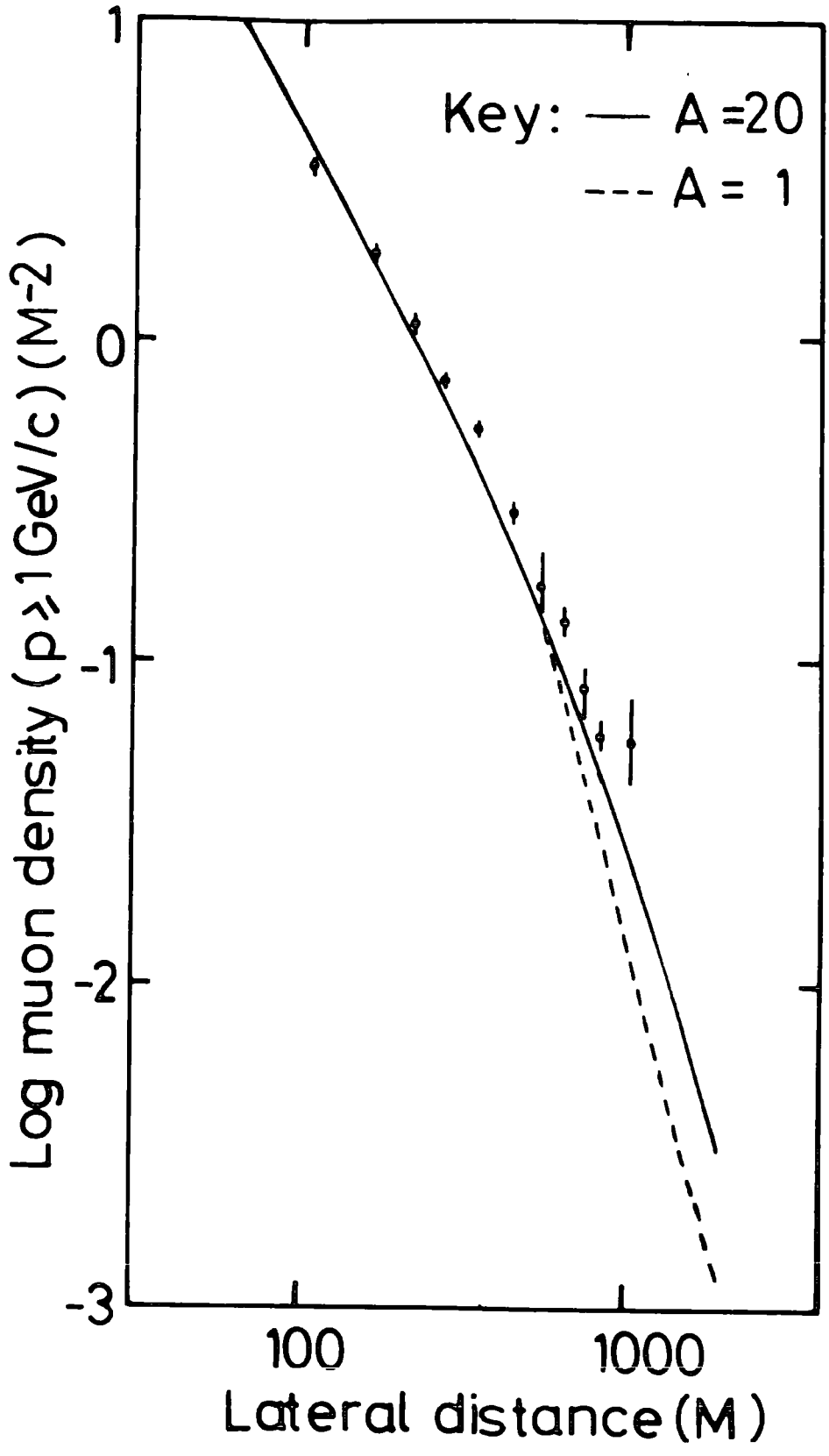
Key: — A =20
--- A = 1
Log muon density (p≥1GeV/c) (M-2)
1
0
-1
-2
-3
100
1000
Lateral distance (M)

upon the rate of degradation of the energy of the particles of the nuclear cascade in the atmosphere. This rate is related closely to both the mass of the primary particle (A) and the multiplicity of pions formed in the nuclear interactions (n_s).

After a consideration of a wide range of possibilities, it is concluded by Orford and Turver (1968) that the most likely values of the two parameters are a mass greater than 10 (taken as 20) and a multiplicity which varies as $(E)^{0.25}$ for energy (E) less than 3×10^3 GeV and as $(E)^{0.5}$ for greater energies. With a primary nucleus of total energy 2×10^8 GeV, these values give an adequate representation of the spectra determined experimentally (Figure 6.3).

The variation of the muon momentum spectrum with zenith angle has been examined experimentally at 300 m from the core. The changing spectra have mean moments which can be compared with the predictions of this model:

	$0 < \theta < 20^\circ$	$20 < \theta < 40^\circ$
experiment	5.43 GeV/c	8.02 GeV/c
theory	5.41 GeV/c	7.39 GeV/c

This agreement suggests that the calculated shower behaves realistically as the zenith angle varies.

Integration of the differential spectra at different distances from the core yields the lateral distribution of muons of momentum above 1 GeV/c. In Figure 6.4 the experimental densities are compared with those expected in a shower initiated by a primary particle of mass

20 having energy 2 x 10^8 GeV. Also shown are the densities for a proton initiated shower of similar energy normalized at distances about 300 m. In both cases the multiplicity varied as $E^{0.5}$ for large energies. The densities predicted for distances less than about 100 m are much higher than those observed, as the model used cannot adequately describe this region. At a distance of about 1 km, the difference between the two predicted distributions becomes appreciable, the observed densities lying closer to the densities predicted for the case of the heavy primary particle.

The lack of agreement between the predicted variation of dependence of muon number on the shower size and the observed dependence has been ascribed to an absence of fluctuation in E_{100}. Thus it was thought useful to predict the expected muon densities at 300 m from the core of showers of sizes equal to the means of the bands of size used in the analysis of the muon densities (Chapter 4) to examine the possibility of checking the variation of primary mass with energy. For each band of shower size the mean size (N) and the distance (r) characteristic of the recorded showers were determined. By a consideration of the variation of the mass composition of the primary particles with shower size (Bray et al.1966) an effective mass (A) can be ascribed to the shower size. The energy (E) of a nucleon giving a shower at sea level containing N/A particles was found from the calculations of de Beer et al. (1966) for the model (model III) closest to that used in the present theoretical work, primary energy being correlated to shower

FIGURE 6.5

A comparison of the densities of muons of momentum greater than 1 GeV/c at 300 m from the cores of showers of various sizes with the values predicted for a modulated primary mass composition.
The points without error bars are the predicted values.

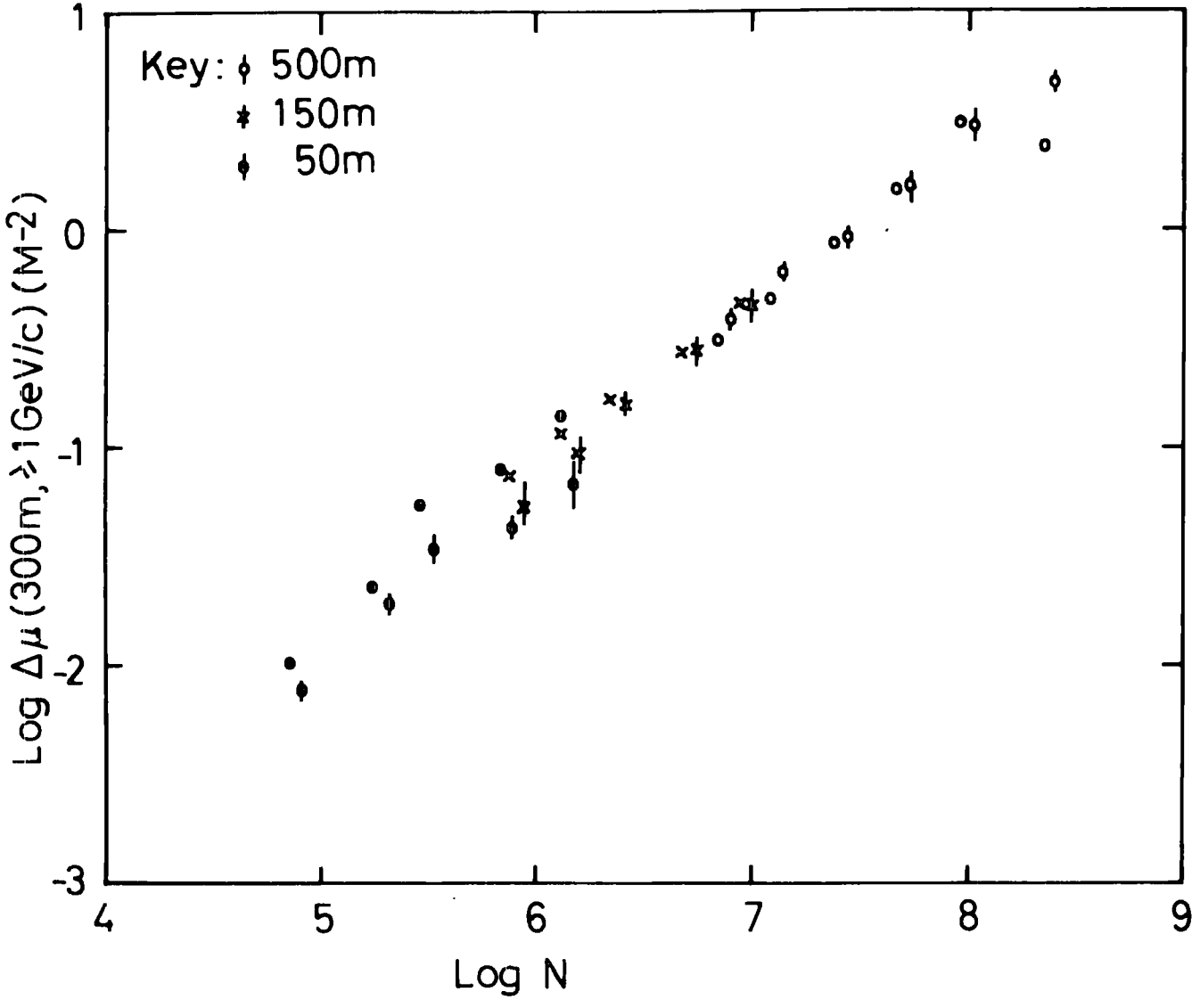
Key: 500m
150m
50m
Log Δμ (300m, ≥1GeV/c) (M⁻²)
Log N
1
0
-1
-2
-3
4
5
6
7
8
9

size for primary protons of fixed energy. Muon densities at a distance r from the core of a shower initiated by a primary particle of mass A and energy E x A were calculated and then scaled to 300 m from the core using the shape of Greisen's (1960) lateral distribution. The densities so determined were larger by a factor of about two than those observed for 500 m showers. This is attributed to the conversion of shower size to primary energy for particles of fixed energy; whilst the arrays at Haverah Park measure a quantity, E_{100}, thought to be closely connected to primary energy, a conversion of E_{100} to shower size by a comparison of rates (Chapter 2) must necessarily result in the shower size attributed to a shower being the size equivalent to the primary energy for showers of fixed size. Although de Beer et al. do not plot a relation between energy and (fixed) shower size for model III, they do give the two cases of fixed energy and fixed size for a rather different model. Assuming that the two cases are similarly related for the two models, the difference between these two cases is sufficient to explain the discrepancy between the densities predicted and those observed. The predicted densities have been normalized to fit the observations in the region of size covered by the 500 m array. In Figure 6.5 the predictions are shown compared with the observed densities. For shower sizes above 2×10^6 particles the agreement is very good, but below this size the predicted densities are larger than those observed. These latter cases are those for which the distance r was less than 100 m. A full investigation of the variation of the muon numbers with shower size must await refinement of the model to treat

muons falling within 100 m of the axis of the shower.

6.3.2 The heights of production of muons

The model calculations give the densities of muons of given momentum at a given distance from the core originating at various levels in the atmosphere. Thus the distributions of height of origin of these muons can be found. In general the contributions from the two regions of the atmosphere - above and below 10 km - do not fit exactly on to each other and the two contributions have been connected by a linear interpolation (Figure 6.6). The effect of the exact form of interpolation used has been shown to be trivial and will be discussed later.

The variation of the distributions of height of origin (a) with distance for a given momentum, and (b) with momentum for a given distance are shown in Figure 6.6, for muons in a shower of primary energy 2×10^8 GeV, using the 'best' parameters, being those chosen on the basis of the density information. Hillas has given the distributions in height of origin for muons of various momenta at three distances from the core (25 m, 200 m and 600 m) of a proton-initiated shower. At 200 m and 600 m, for muon momentum about 3 GeV/c the distributions are shown in Figure 6.6 compared with the distributions predicted by the present model, for the 'best' parameters, at 155 m and 520 m. The sensitivity of the distributions of height to primary mass and multiplicity is illustrated in Figure 6.7. Here, for momentum of 6.61 GeV/c and a distance of 300 m, the distributions of height are

FIGURE 6.6

Distributions of height of origin of muons, predicted using the 'best' values of primary mass and multiplicity.

(a) Variation in the distribution with muon momentum for a fixed distance. The dotted lines indicate the contributions to the distributions from the upper portion of the calculated cascade.

(b) Variation in the distribution with distance for a fixed muon momentum. The dotted lines represent the distributions suggested by Hillas (1966) for muons, of about 3 GeV/c momentum, 200 m and 600 m from the core. These distributions have been normalized at heights about 700 gm cm^{-2}.

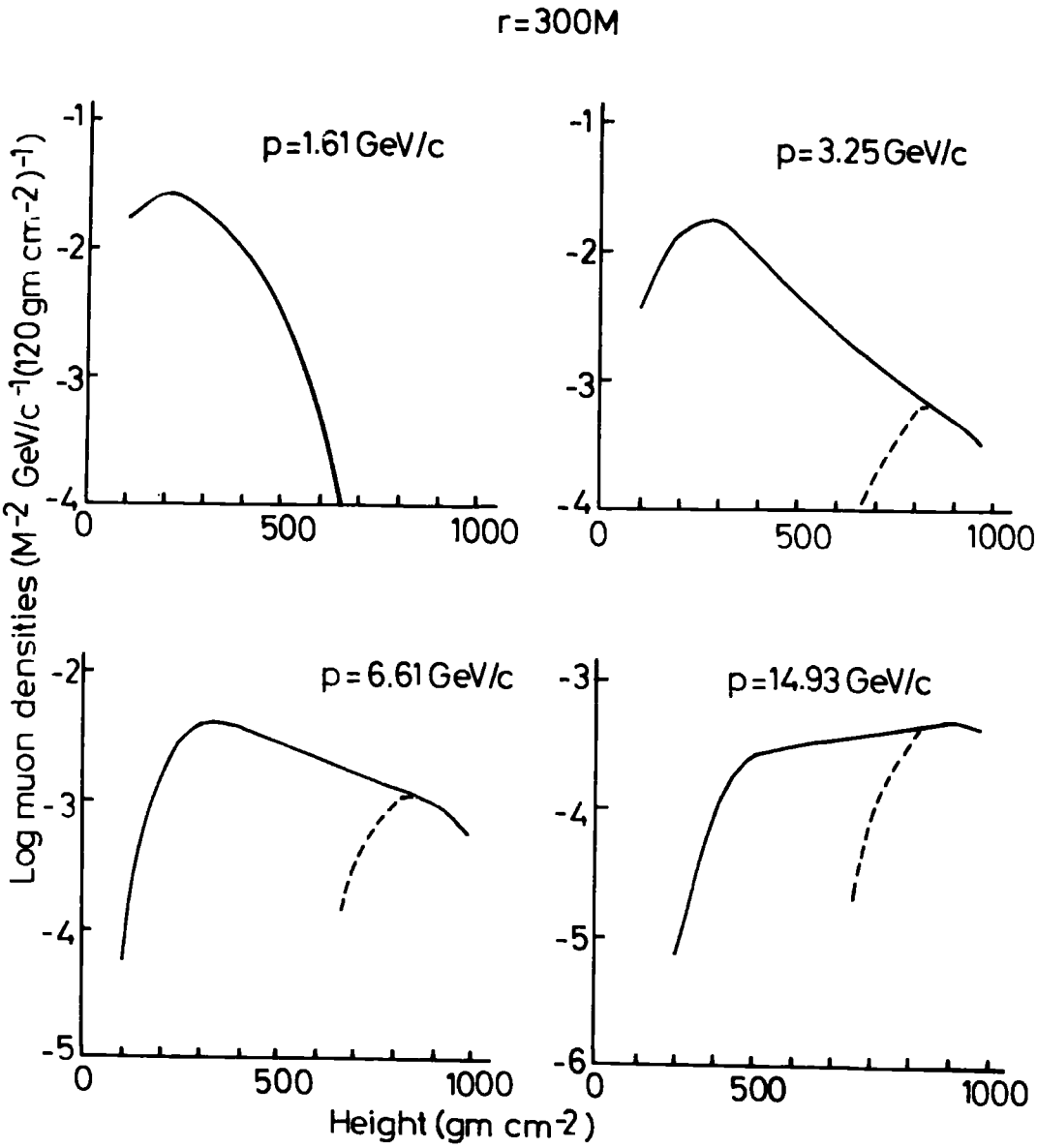
r=300M
p=1.61 GeV/c
p=3.25 GeV/c
p=6.61 GeV/c
p=14.93 GeV/c
Log muon densities (M-2 GeV/c -1(120 gm cm-2)-1)
Height (gm cm-2)
0
500
1000
-1
-2
-3
-4
-5
-6

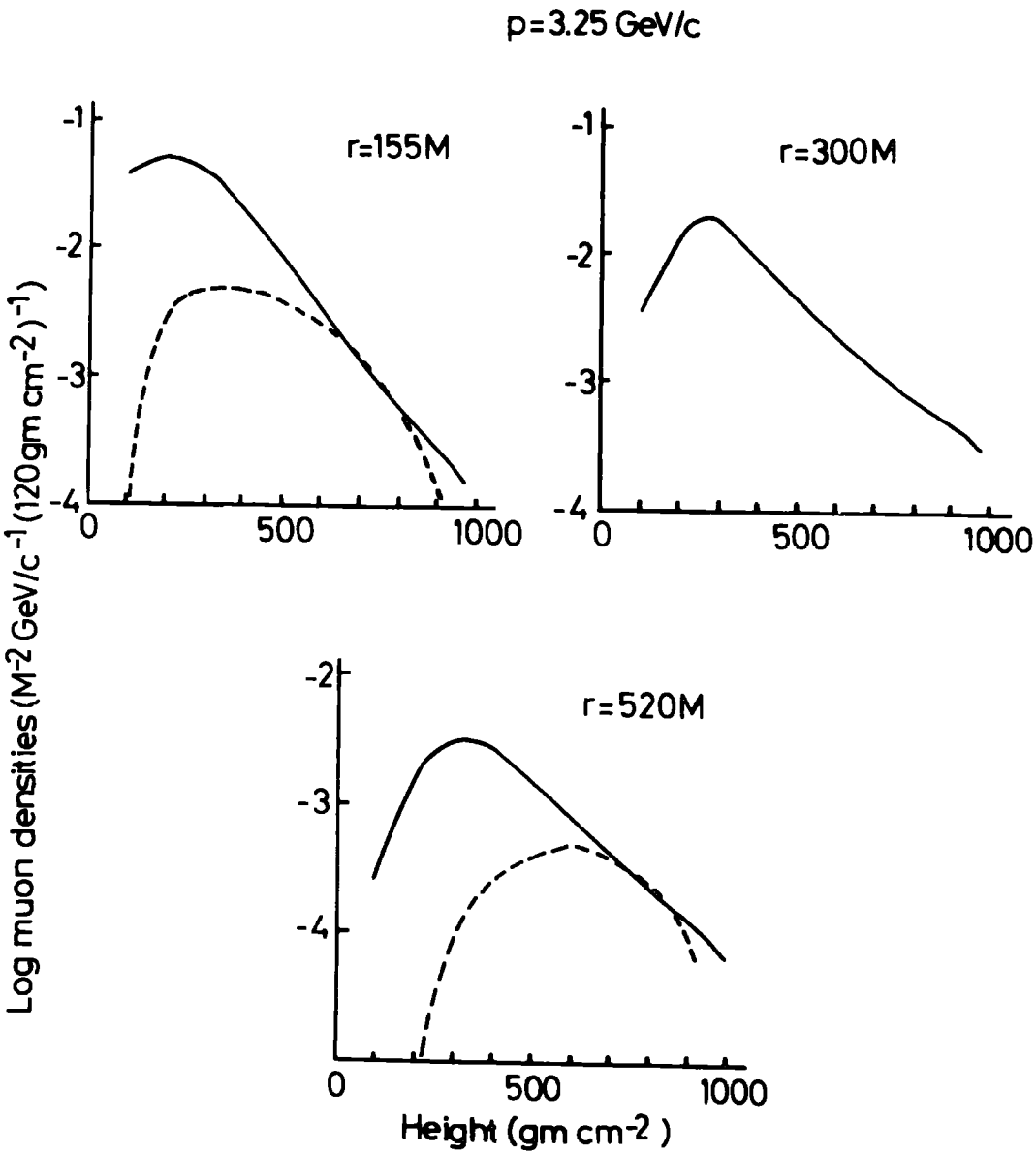
p=3.25 GeV/c
r=155M
r=300M
r=520M
Log muon densities (M-2 GeV/c-1 (120gm cm-2)-1)
Height (gm cm-2)
-1
-2
-3
-4
0
500
1000

FIGURE 6.7

The dependence of the height distribution for fixed muon momentum and distance on the values of primary mass and multiplicity (A, n_s). The contributions from the first three interactions are dotted in.

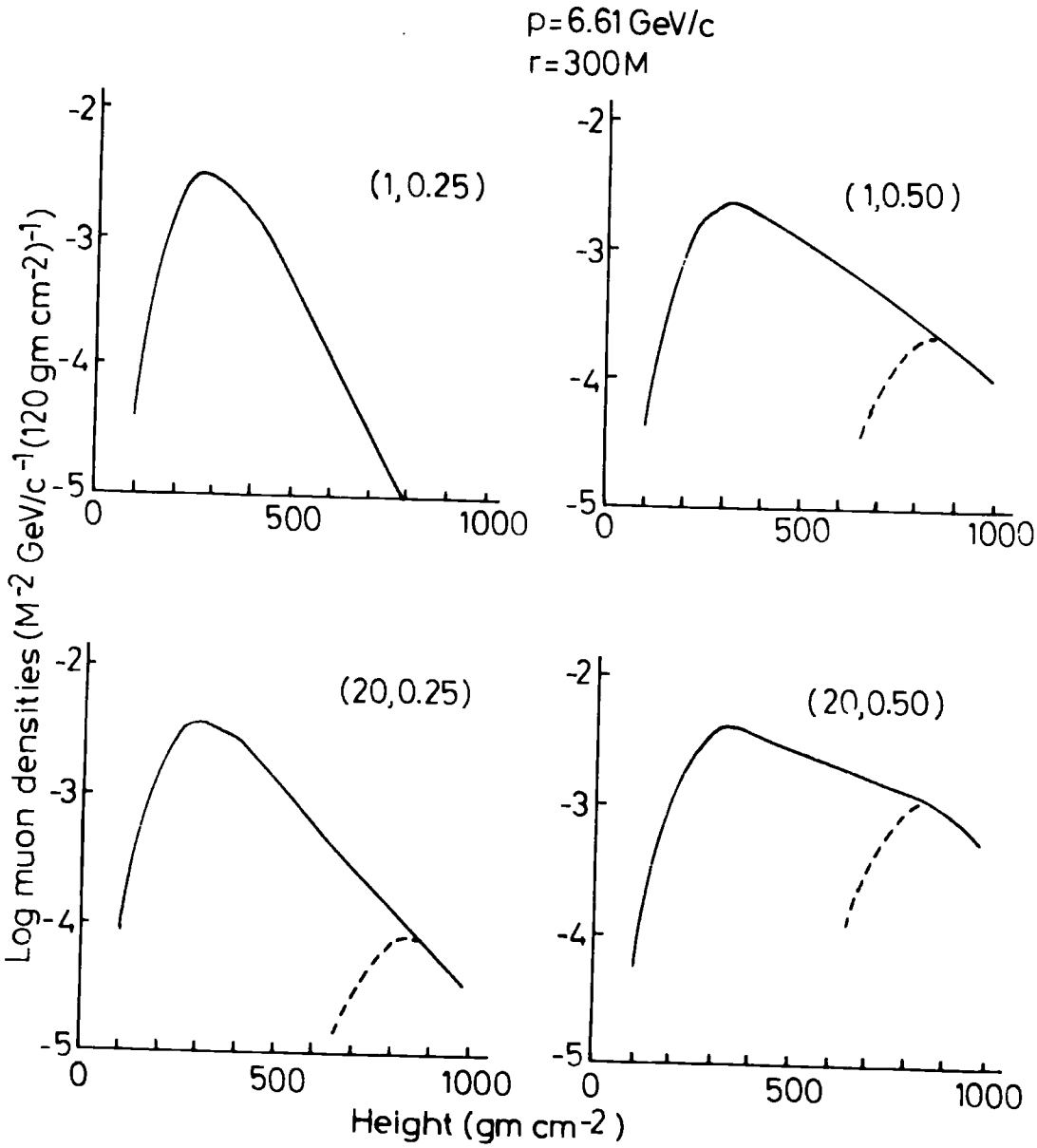
p=6.61 GeV/c
r=300M
(1,0.25)
(1,0.50)
(20,0.25)
(20,0.50)
-2
-3
-4
-5
0
500
1000
Log muon densities (M^{-2} GeV/c^{-1}(120 gm cm^{-2})$^{-1}$)
Height (gm cm^{-2})

plotted for A of 1 and 20, and n_s proportional to $E^{0.25}$ and $E^{0.5}$ for energies greater than 3×10^3 GeV. Some considerable variation in the distributions is evident; the possibility of experimentally distinguishing between them will be discussed in the following chapter.

6-4. Conclusions

The measured densities of muons above various threshold energies are seen to be incompatible with the simple theories of the muon component. They can, however, be adequately accounted for by the predictions of a more rigorous treatment of the upper portion of the cascade together with an approximate treatment of the lower part, if the mass of the primary particles initiating the air showers is greater than 10 and if the multiplicity of pions varies with energy as $E^{0.5}$ above an energy of 3×10^3 GeV. These assumptions have been shown not to distort the other characteristics of the shower from those observed. This model, together with various other combinations of the primary mass and multiplicity, has been used to predict distributions of heights of origin of muons of various momenta at various distances from the core.

CHAPTER 7

THE HEIGHTS OF ORIGIN OF MUONS IN EAS

7-1. Introduction

The heights of origin of the muons present in air showers are of great interest in that these heights reflect the development of the nuclear cascade. If the particle initiating the shower is of large mass, the particle will interact higher in the atmosphere than is the case for a proton primary of similar energy, due to a reduction in the nuclear interaction length. Thus the muons, especially those of high energy, in such a shower should originate higher in the atmosphere. Further it is hoped that a knowledge of the production height distribution of muons of a given energy will enable an estimation of the characteristics of the nuclear cascade to be made from a different standpoint to that taken in the study of the lateral distributions of the muons.

While some estimates of the average height of production of all the muons in a shower or of muons at a given distance from the core have been made previously, a defect common to all these measurements is a lack of knowledge of the energy of the muons. From the above considerations such a knowledge would greatly enhance the value of any determination of the heights of origin.

Two quite different methods of estimation of the heights of origin of muons have been used for the 500 m data in the present experiment namely,

(1) the geomagnetic distortion of the lateral distributions of muons (following a suggestion by Somogyi (1966)),

(2) the directions of motion of muons within a shower, due to the transverse momentum imparted to the parent particles on production. Each of these approaches has been used to determine the average height of production for muons of given momentum and to test various assumed distributions of heights of production predicted using the model of Orford and Turver (1968).

7-2. The geomagnetic deflection of muons

As an air shower develops the geomagnetic field displaces particles of opposite electric charge in opposed directions, depending on the angle of the shower with respect to the field. The muons, having a long undisturbed path length in the field, display large deflections. The electromagnetic component, on the other hand, spends half the time as uncharged photons and the other half equally as positive and negative electrons, and thus shows a much smaller effect when observed at sea level, the main contribution coming from the last radiation length of the atmosphere, where the energy of the particles is lowest (Oren 1959, Cocconi 1961).

In showers incident from the north and falling to the west of the spectrograph the observed density of positive muons will be enhanced as they are displaced towards the spectrograph. The geomagnetic displacements and the resultant expected charge ratios may be calculated

for muons of various momenta originating at fixed heights in showers incident from various directions. These calculated charge ratios may then be compared with those observed. This method relies upon a knowledge of the undistorted charge ratio of the muons in air showers, which has been established by Orford et al. (1967) as indistinguishable from unity in the range of momentum and distance considered here. The charge ratios observed for showers falling between 100 m and 600 m of the spectrograph for the bands of momentum used are shown in Table 7.2; they do not vary much for smaller bands of distance within this large band.

Preliminary results on the deduction of heights of origin using the geomagnetic effect were presented by Orford et al. (1967).

7-2.1 The derivation of mean heights of production

The deflection (dr) of a muon originating at a fixed level in the atmosphere in a shower arriving from a given direction may be found by the method outlined in Appendix B and the mean distance (r) of the spectrograph from the axis of the shower determined from the observed events for the bands of momentum considered (Appendix A). The deflections were computed for momenta corresponding to the means of these bands.

Using the observed lateral distribution of muons of momenta within these bands as a sufficient approximation to that which would be observed in the absence of any geomagnetic field, the densities of muons at $(r \pm dr)$ may be found, corresponding to the densities at the

spectrograph of muons of opposite electric charge in a shower falling at a distance r. This leads directly to an estimate of the expected charge ratio of muons originating at a prescribed height in a shower incident from the fixed direction. As an illustration, the charge ratios expected for muons of various momenta originating at various heights are shown in Table 7.1 for showers falling to the west of the spectrograph and incident with the observed distribution of azimuth and zenith angles up to 40°, the charge ratios of showers with zenith angles greater than 20° incident from the southern hemisphere being reversed and added to the total effect. A comparison of the observed charge ratios with those predicted for various heights enables a value of the height of origin of the muons to be deduced. This average height of origin corresponds to the mean altitude of production rather than the mean atmospheric depth.

For the bands with mean momentum less than 10 GeV/c, the use of the mean momentum of the bands has been shown to entail a slight underestimation of the expected charge ratio for a given height of origin compared with that computed using the distributions of momentum. An exact figure for this effect is not easy to arrive at, but it may be said that the effect increases with increasing height, being less than a 2% increase in the ratios computed for heights of origin of 400 gm cm^{-2} and less than a 5% increase for 700 gm cm^{-2}. This error in the analysis has been neglected in the present work.

TABLE 7.1

EXPECTED CHARGE RATIOS (see text)

p GeV/c	height gm cm^{-2}				
	250	400	550	700	900
1.61	1.06	1.22	1.44	1.96	-
3.25	1.04	1.10	1.19	1.42	-
6.61	1.02	1.04	1.10	1.21	1.88
14.93	1.00	1.03	1.06	1.12	1.40
45.0	1.00	1.00	1.01	1.03	1.16

7-2.2 The mean heights of origin

From the fourfold nature of the array all but the largest showers will be detected preferentially in three areas, each lying between two of the outer huts (Suri 1966). A consideration of the directions of the coordinate system used at Haverah Park (Figure 2.1) shows that one such lobe may be characterized by $X^{-}Y^{\pm}$ and the other two may be defined as $X^{+}Y^{+}$ and $X^{+}Y^{-}$ respectively. For each of these areas there are incident directions which lead to a distortion of the charge ratio of muons at the spectrograph, and thus regions of a space $G(X,Y,\theta,\phi)$ may be defined in which marked charge ratios are expected. Intervals of X and Y are as specified above, zenith angle being broken down into two cells above and below 20° (the angle of dip at Haverah Park being 21.5°), and azimuth being subdivided by 45° intervals centred about the eight principal points of the compass. The statistical

weight of each cell of G is rather low and thus it is useful to group the observations together whenever possible.

For showers falling in the X^- region from all directions (region 1 of G), the y component of dr (dy) cancels and only the x component (dx) need be considered. Positive muons in showers falling from all directions are deflected in the same sense, except those falling with zenith angles greater than the angle of dip and arriving from the southern hemisphere. The expected charge ratios for these showers are opposed to those for the rest and thus may be inverted in both observation and prediction and added to the other cells of zenith angle and azimuth to enhance the statistical weight. The mean dx is determined for all the cells of G falling in region 1 and the densities of positive and negative muons at the spectrograph in the average shower determined. The radius vector from the spectrograph to the average point of impact of these showers is directed along the x axis. The expected charge ratios are found for the various heights of origin and compared with the experimentally observed value.

For the regions X^+Y^+ and X^+Y^-, showers incident from the east and west suffer dy only, positive muons from the two directions being deflected in opposite directions. The region $X^\pm Y^+$ shows a charge distortion for showers incident from the east in the same sense as the region X^+Y^- for showers from the west, and vice versa. Suitably combined predictions for these regions may be compared with experimental data suitably combined to derive the heights of origin (region 2 of G).

In the case of these two lobes, however, the radius vector from the spectrograph to the average point of impact of the core is oriented at 60° to the y axis, and thus the predicted deflections must be projected onto this direction to find the expected densities of muons.

Muons in showers incident in these two lobes from the north-east and north-west have effective both dx and dy, giving dr oriented along or normal to the radius vector of the average point of impact of the showers from the spectrograph. Only those regions of G which give dr along r have been used to estimate the heights of origin (region 3 of G). Other incident directions or combinations of directions have less clear-cut effects or less significant numbers of particles and thus have not been considered.

Thus for each momentum band three estimates of the average height of origin have been found, each carrying a weight dependent upon the number of particles observed. These heights of origin are shown in Table 7.2 for the individual regions of G and in Figure 7.1 they are plotted as the weighted mean values with the standard errors of these means indicated. The horizontal error bars give an indication of the spread in the bands of momentum used.

For muons of mean momentum 45 GeV/c, the two significant observed charge ratios are very large indeed, and the calculated deflections for heights of origin as high as 900 gm cm^{-2} are insufficient to explain them. The third ratio, of unity, is of much smaller weight than the other two. It is thought from this interpretation of the data

TABLE 7.2

AVERAGE HEIGHTS OF ORIGIN FOR MUONS OF VARIOUS MOMENTA

$\bar{p}$ GeV/c	$\bar{r}$ m	Charge ratio undistorted by earth's field	Region of G	N^+ observed	N^- observed	$\bar{h}$ gm cm^{-2}	Charge distortion by earth's field
1.61	320	1.02 ± 0.08	1	122	108	275	1.333 ± 0.105
			2	65	43	520	
			3	8	25	600	
3.25	280	1.03 ± 0.07	1	188	155	500	1.200 ± 0.085
			2	94	78	420	
			3	22	24	300	
6.61	270	1.06 ± 0.11	1	74	61	600	1.293 ± 0.139
			2	31	21	720	
			3	10	14	570	
14.93	240	1.10 ± 0.16	1	35	30	710	1.205 ± 0.204
			2	14	11	750	
			3	3	4	680	
45.0	225	0.96 ± 0.16	1	33	22	~ 1000	1.750 ± 0.222
			2	20	7	~ 1000	
			3	3	3	< 250	

that muons of these energies at the distances involved originate very high indeed in the atmosphere, but, as no firm estimate of height can be made, only a lower limit of the mean height is plotted in Figure 7.1 for this momentum. The theoretical considerations of the previous chapter suggest that muons of this momentum falling at 300 m from the core originate above about 930 gm cm^{-2}. The average height of origin would be rather lower than this for muons at 225 m from the core.

FIGURE 7.1

Weighted mean heights of origin of muons of various momenta derived using the geomagnetic deflection of muons (×). Mean heights of origin derived from the angular deviations of muons from the shower directions (o). The lower limit plotted at a mean muon momentum of 45 GeV/c is derived using the geomagnetic effect. The solid line shown represents the mean heights of origin of muons at 300 m from the core.

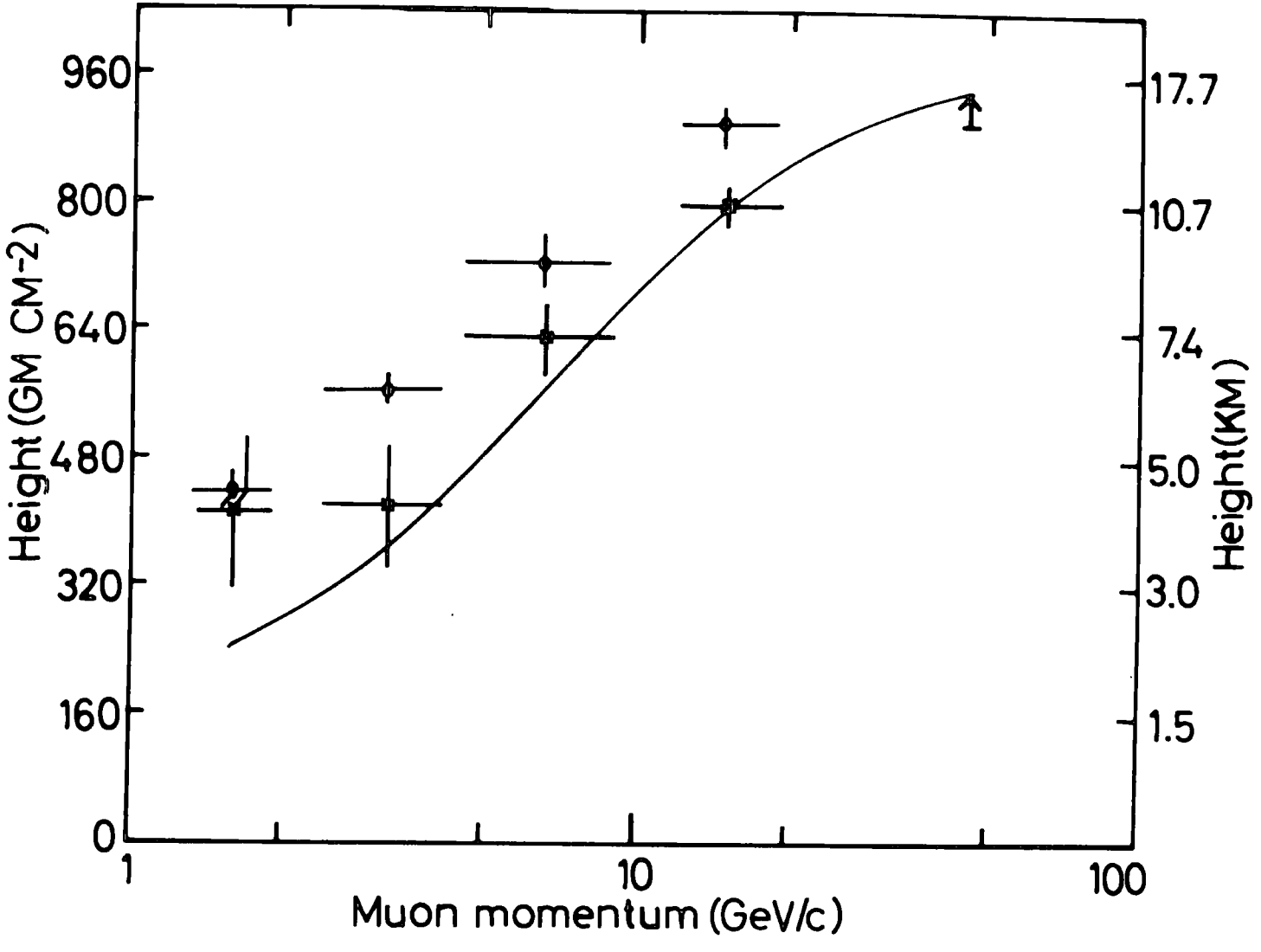
960
800
640
480
320
160
0
Height (GM CM-2)
17.7
10.7
7.4
5.0
3.0
1.5
Height(KM)
1
10
100
Muon momentum (GeV/c)

The weighted mean height of origin of all the muons observed is 547 ± 51 gm cm^{-2}, for muons falling at an average distance of 270 m from the core of a shower of average size 2×10^7.

The above mean values of height of origin may be compared with those expected on theoretical grounds; it is also possible to calculate the mean charge distortion over the regions of G used above for a given height distribution and to compare this with the total observed charge ratio, as more meaningful errors can be attached to this latter quantity. Section 7-5 contains an account of this work. The mean heights of origin (in km) predicted using the Orford and Turver (1968) model, for a shower initiated by a primary particle of mass 20 when the multiplicity of pions varies as $E^{0.5}$, are shown in Figure 7.1 compared with the measured values. At large momenta the agreement with observation is satisfactory, but for lower values the predicted heights are rather lower than those observed. The differences between the predicted and observed heights of origin will be discussed later.

7-3 Angular deviations of muons from the core direction

A muon observed in an air shower is the product of the decay of an unstable particle produced in a nuclear interaction in the core, and thus originates from a height (h) with some value of transverse momentum (p_t). For a muon whose parent had longitudinal momentum p in the lab system, this transverse momentum gives rise to an angular deviation from the core (Ω) where

$$\tan \Omega \approx p_t/p \qquad (7.1)$$

FIGURE 7.2

Typical angular deviations from the core caused by the several factors, as a function of momentum for two heights of origin. See text for key.

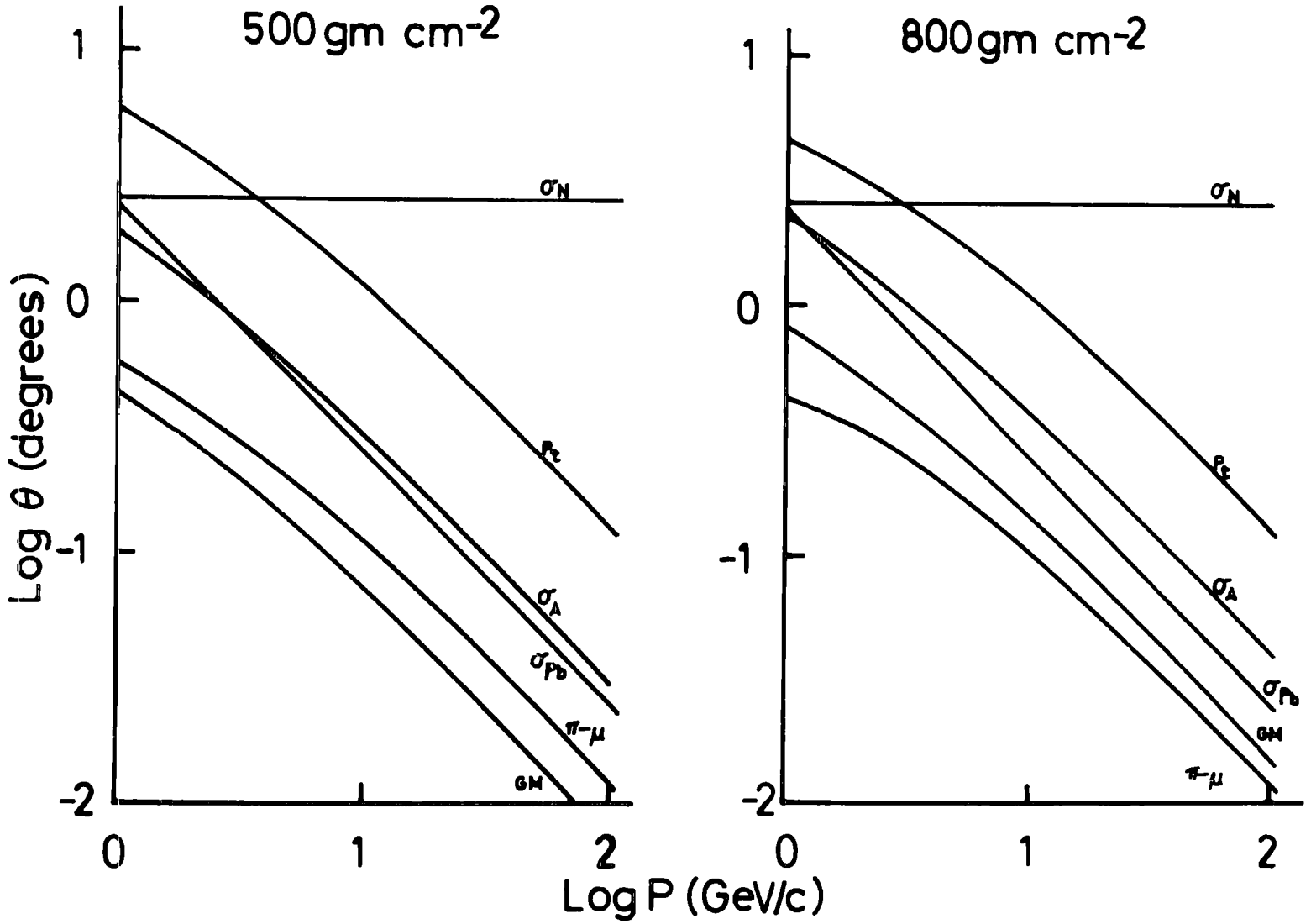
500 gm cm-2
800 gm cm-2
σN
σA
σPb
π-μ
GM
Log θ (degrees)
Log P (GeV/c)
1
0
-1
-2
0
1
2

and due to this angular deviation the muon will be displaced laterally from the core by a distance r given by

$$\tan \Omega = r/h \qquad (7.2)$$

Hillas (1966) has confirmed theoretically the experimental demonstration by Earl (1959) that the value of r determined by the opening angle of production is not on average very different from that actually observed, as effects such as geomagnetic deflection and Coulomb scattering are relatively small. Thus, in the absence of any complicating factors, observations of Ω and r are sufficient to determine h. From the measured direction of the muon in the measuring plane of the spectrograph and the incident direction of the shower axis projected into this plane, a value of Ω, the angular deviation of the muon from the core, similarly projected, can be determined. Any subsequent references to angles will imply such projection unless otherwise stated. Using the appropriately projected value of distance from the core, r, the height of origin of the muon may be estimated (Appendix C).

However, there are several effects which alter the direction of motion of the muon after production, including the decay of the parent particle, Coulomb scattering both in the air and in the lead shielding of the spectrograph, and the geomagnetic deflection of the muon. A further factor which affects the measured angular deviation of muons from the core direction is the error in determining this deviation. The magnitudes of these effects, relative to the opening angle of production, as a function of momentum are shown for two different heights of origin

in Figure 7.2. The Coulomb scattering in the air (σ_A) and lead (σ_{Pb}) are shown as the r.m.s. angles of the multiple scattering process (Rossi 1952), the decay angle ($\pi - \mu$) is plotted as the median angle of emission of muons from pion decay (Salmeron 1963), the geomagnetic effect (G - M) is estimated for a vertical shower and the opening angle of production (p_t) corresponds to the mean of the distribution of transverse momentum suggested by Cocconi et al. (1961), hereafter referred to as the CKP distribution:-

$$\text{Prob } (p_t) = \frac{p_t}{p_o^2} \exp (- p_t/p_o) d p_t$$

The mean of this distribution is 0.4 GeV/c, equal to 2 p_o. The errors in measurement (σ_N) are estimated below (section 7-3.2) and may be seen to contribute most of the angular spread for muon momenta above about 5 GeV/c.

These errors can be shown to be too small to mask altogether the expected angular deviations due to opening angles. Comparisons of the distributions of observed values of deviation for events with r (projected) of opposite sign and for mean muon momentum 6.61 GeV/c show that the two distributions are indeed displaced as expected (Figure 7.3). Similar distributions for all other bands of momentum show the same effect.

Due to the errors in measurement of angles, the height h derived by this approach is not the true height of origin (h^o) but is scattered about it. Errors in core distance have been shown to produce

FIGURE 7.3

Distribution of angular deviation for muons of momentum 6.6 GeV/c for showers falling with negative values of r(A) and positive values of r(B).

FIGURE 7.4

Distribution of reciprocal of the height derived from the events in the distributions of Figure 7.3.

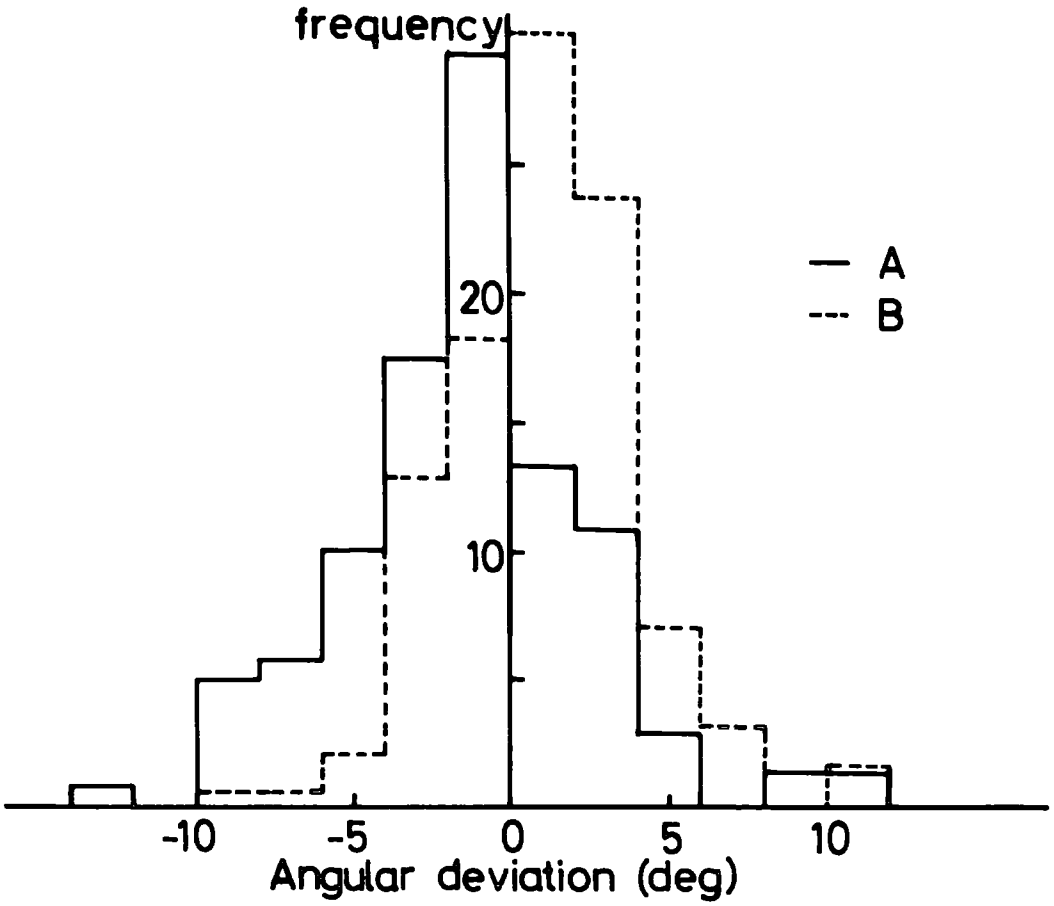
frequency
20
10
A
B
-10
-5
0
5
10
Angular deviation (deg)

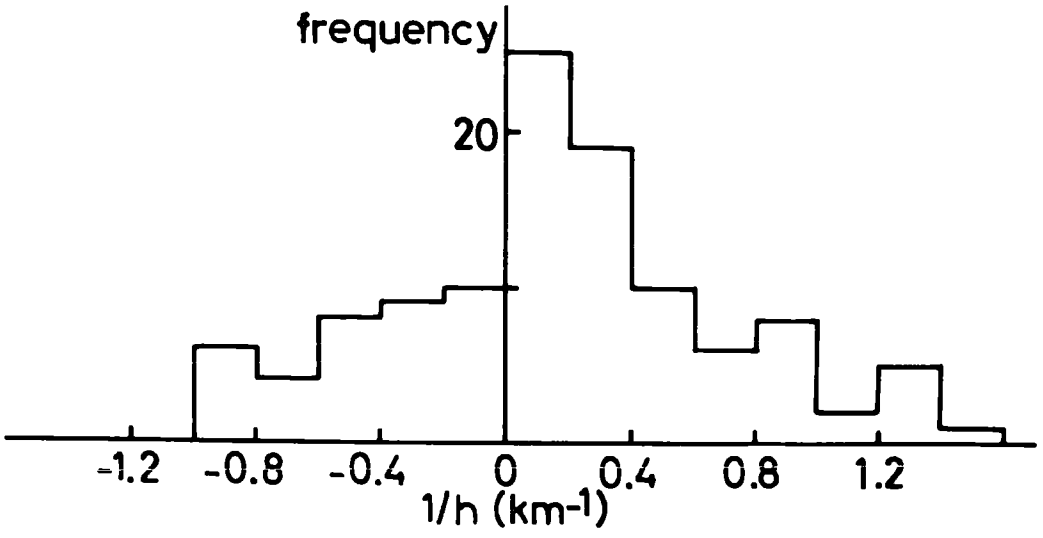
frequency
20
-1.2
-0.8
-0.4
0
0.4
0.8
1.2
1/h (km-1)

a much smaller effect (section 7-3.4). As h is inversely related to Ω, a distribution of 1/h is expected to reflect the errors in Ω. This effect may be seen in Figure 7.4, where such a distribution is shown for the same muons as those shown in the distributions of Figure 7.3. Values of 1/h greater than 1.5 km^{-1} have been omitted from this graph for simplicity. Whilst such histograms can be drawn for all bands of momentum subdivided by air shower parameters, the estimates of the average height derived from the median values of 1/h must be overestimates of the true values. This approach, although attractive because of its simplicity, is thus only of limited usefulness.

7-3.1 The derivation of heights of origin from the angular deviations

With a knowledge of the standard deviation of the distribution of measuring errors and the Coulomb scattering in the air and lead, and ignoring the other secondary effects, the probability G(h,h") that, for a given event with known r, any height h" will be scattered to give the observed value of h can be determined using relation 7.2 to determine the relevant angles. This probability assumes that any height of origin is equally probable a priori and thus a distribution of height , F(h) dh, must be assumed to weight the probabilities, as

$$P(h'')\, d\, h'' = G(h, h'')\, F(h'')\, d\, h''$$

where P(h") d h" is the unnormalized probability of this event originating at height h" and being observed at an angle corresponding to h. It is known that the parent particle must have left the core of the shower

at a positive height and thus the normalized probability is

$$Pr\ (h")\ d\ h" = \frac{P\ (h")\ d\ h"}{\int_0^H P(h")\ d\ h"}$$

where H is a height greater than the maximum height expected to contribute to the meson cascade, 60 km being used in the present analysis. Pr(h") d h" has been evaluated for heights between 0.5 km and 60 km and by summing this distribution over several observed particles, a probability distribution in height of origin appropriate to these particles is found. The procedure is iterative in nature, the length of the iteration process being dictated by the closeness of the initially assumed distribution of heights to that appropriate to the data. It has been found that by taking

$$F(h")\ d\ h" = 1$$

for all h", 20 iterative cycles are sufficient to ensure that the final form Pr(h") d h" has reached a stable form. The uniqueness of the procedure has been tested by using other forms of F(h") d h", which yield similar forms of Pr(h") d h" after rather more iterations.

Due to the large angular errors involved, the form of Pr(h") d h" is not expected to reflect accurately the distribution of heights of origin of particles in the showers, especially at large heights. However, using Pr(h") d h" it is possible to estimate the mean height of production (h') somewhat more accurately than is possible from the distributions of 1/h considered above. The value obtained can only be

regarded as an upper limit to the actual mean height of origin. The mean height will be subject to wide errors due to any fluctuations in $Pr(h'')\, d\, h''$, especially at extreme values of h'', and to reduce the effect of these fluctuations, $Pr(h'')\, d\, h''$ was integrated over 100 gm cm^{-2} bands of the atmosphere starting at the top. Each of the intensities so derived was ascribed to the mid-point of the corresponding band and from these spot heights the mean height was found. As this mean height is along the projected core direction it must be corrected for the average inclination of the core (Appendix C).

7-3.2 The determination of the errors in the angular deviations

To carry out the analysis outlined above, the measuring errors must be well accounted for. These errors are independent of the muon momentum, in contrast to all other effects contributing to the angular deviations, which vary inversely as the momentum (Figure 7.2). An examination of the distribution of deviations for muons of mean momentum 45 GeV/c suggests that the standard deviation of the distribution of projected measuring errors (σ_N) may be about 2.7°. From Figure 7.2 even the opening angle of production is seen to be small compared to this for muons of this energy. The distributions of angular deviations expected for various values of σ_N have been calculated and the value appropriate to the observed data determined using a χ^2 fitting procedure. This calculation is of the general form presented in Appendix D, but here only the result is of importance:-

$$\sigma_N = (2.65 \pm 0.30)^\circ$$

This value is independent of the height of origin assumed in the calculation and is compatible with that expected on the basis of the errors in measuring the direction of the shower (section 2-3.3) and muon direction. Using Baxter's figures (Baxter 1967) for the uncertainty in shower direction we find for a zenith angle of 20° that σ_N is 2.59°, in excellent agreement with the above figure.

7-3.3 Checks of the experimental data

Simple theoretical considerations of the directions of motion of all the muons present in a shower indicated that the experimentally observed deviations for muons of momenta below 5 GeV/c could be accounted for by the factors discussed in section 7-3 (Earnshaw et al. 1967b). All such comparisons of prediction with observation are restricted to projected angular differences from the core of less than 16°, to avoid possible biases due to the selection criteria imposed upon the data recorded by the spectrograph (section 5-1.4). However, similar comparisons for higher momenta did not reveal the same agreement, the relative numbers of observed events occurring at large angles from the core being greatly in excess of the predicted figures.

Such an anomalous population could wholly or in part be due to non-Gaussian errors in determining the direction of the axes of the showers containing the relevant muons. The events constituting this apparent anomaly and a control sample of an equal number of events drawn from the more normal portions of the distribution were checked by the Haverah Park group from Leeds University. The control events and

anomalous events were randomly ordered and no indication was given of the difference between the two types of event.

Of 69 control events, only one showed a marked change in angular deviation. In this case the azimuthal angle was most unfavourably placed, a change of 10° in this angle about a value of 270° leading to a very considerably altered angular deviation. However, in a sample of 68 anomalous events, 16 showed changes of several degrees in angular deviation, sufficient to move the events to the normal body of the distribution. Thus the anomalous events appear to be a different class of events from the control sample. The remaining events may be ascribed to five possible causes:

(1) Wrongly classified muons, which in fact are chance correlations of flash tubes,

(2) Unassociated events falling within the memory of the flash tubes,

(3) Fluctuations in shower detection giving rise to errors in direction of core (but see Baxter 1967),

(4) A possible further population of errors in shower analysis.

(5) Genuine events.

It is thought that events due to the first two causes have been reduced to a minimum by the checks described in section 5-1.4. When these checks were initiated it was thought that any events not attributable to non-Gaussian errors in measurement would be indicative of the presence of particles with transverse momentum higher than predicted by the CKP distribution used in the calculations (Earnshaw et al. 1967b). Thus

further and more detailed calculations were undertaken and it will be shown later (section 7-5) that these calculations indicate that the majority of the events surviving the air shower checks are probably in the fifth category.

7-3.4 The mean heights of origin

The data were subdivided by momentum and the three lowest bands of momentum further subdivided by distance from the core, as shown in Table 7.3. The band of mean momentum 14.9 GeV/c was not subdivided by distance, being insufficiently populous. The highest momentum region was not used, as the data on the angular deviations for these events had already been used to determine σ_N.

For each of these intervals of momentum and distance, the mean height of origin was estimated by the method given above. The errors involved in this determination of the mean heights were estimated by computing the mean heights appropriate to the upper and lower limits of the errors on the value of σ_N used. The mean heights and the associated errors of determination are shown in Table 7.3. As stated above, these mean heights can only be regarded as upper limits to the true values, diverging from these values due to the lack of resolution within the errors of measurement of the angular deviations. As these errors have a standard deviation of 2.65°, the lower boundary of this region of poor resolution may be estimated, depending on the value of projected distance from the core used. For a typical distance of 200 m, this lower bound will be about 4.3 km, and hence any mean heights found to be greatly in excess of such a value are definitely upper limits.

TABLE 7.3

MEAN HEIGHTS OF ORIGIN (km)

p(GeV/c)	r (m)				
	150	225	300	380	520
1.61	$5.3^{+0.4}_{-0.2}$	2.6 ± 0.2	4.8 ± 0.2	$5.0^{+0.1}_{-0.2}$	$6.4^{+0.1}_{-0.4}$
3.25	$7.2^{+0.6}_{-0.5}$	6.0 ± 0.4	$6.1^{+0.3}_{-0.2}$	$6.1^{+0.3}_{-0.2}$	5.7 ± 0.2
6.61	$10.7^{+0.9}_{-1.0}$			$8.2^{+0.6}_{-0.5}$	
14.93	15.0 ± 1.2				
1 - 10	$5.6^{+0.6}_{-0.4}$			$5.8^{+0.3}_{-0.2}$	

The variation of mean height with distance has been examined for all the muons in the three lowest bands of momentum and for distances from the core greater than and less than 250 m, for comparison with the results of other experiments. These mean heights are shown in the bottom row of Table 7.3, and it can be seen that no great variation is observable. However, the mean heights are in good agreement with that determined over the whole range of distance and momentum using the geomagnetic method.

To compare the mean heights of origin for muons of various momenta with the results obtained using the geomagnetic effect, the results

for those intervals of momentum which have been subdivided by distance have been recombined, giving the variation of mean height of production as a function of muon momentum shown in Figure 7.1 in comparison with the geomagnetic results. For small heights the two methods are in satisfactory agreement, but they do not agree so well for greater heights, the angular deviations suggesting a greater height than is derived from the geomagnetic distortion of the lateral distributions of muons.

A possible source of error in the derivation of these mean heights lies in the errors in the distance of the core from the spectrograph projected into the measuring plane (r). These errors will clearly be of the same order as the errors in core location (section 2-3.2), and allowing for projection may be estimated at ± 30 m. When r is of the order of 200 m, such an error will be of no consequence compared with the error involved in the angular deviations. However, when r is of such a value that it is markedly altered by such errors, the value of height obtained will be affected by the errors in r. To test the effect of the inclusion of events with such values of r, the sample of events with mean momentum 14.9 GeV/c has been reprocessed with those events for which r is less than 100 m removed. This sample, with this source of error effectively removed, has a $Pr(h'')\, d\, h''$ identical in shape with that for all the data. The mean height is quite unaffected. Thus it is concluded that the errors in r are negligible in their effect.

7-4. Discussion

The average heights of origin of muons of various momenta falling at distances between 100m and 600 m from the core of showers of about 2×10^7 particles have been determined by two independent methods. Despite some shortcomings in one of these methods, the results of the two are in fair agreement; in particular, the mean heights of production derived for muons of momentum greater than 1 GeV/c are closely similar.

Previous workers have measured the mean height of origin of muons above some fixed energy, using several different techniques. The results are shown in Table 7.4. A method frequently employed has been the use of timing measurements to establish a value of the radius of curvature of the shower front. This radius of curvature has been taken to be an estimate of the height of production of the muons in the shower. A distribution of the reciprocal of this radius extends to negative values, due to measuring errors (e.g. Suri 1966), and it is suggested that the results obtained using this method may be upper limits to the true values, for reasons similar to those outlined in section 7-3.1. Whilst Bassi et al. (1953) have shown that close to the core of an air shower the electrons precede the muons, this situation is reversed at greater distances (Baxter et al. 1966), and thus measurements on the first detectable signal at these distances probably refer to muons.

At Haverah Park such measurements have been carried out by Suri (1966), giving results in broad agreement with the present experiment. Linsley and Scarsi (1962c), while timing the arrival of muons, found some

variation in height of production with core distance, but concluded that the data was all consistent with a mean depth of production of 320 ± 70 gm cm^{-2}, a value confirmed by their measurements on the first detectable signal. This value is rather higher than is found in the present work, but Linsley and Scarsi at Volcano Ranch were at an altitude of 1800 m, compared to 220 m at Haverah Park. Also, they were on average further from the core than in the present case. Bennett et al. (1962) found an average radius of curvature of 3.3 km, timing on the first detectable signal and making some allowance for errors of measurement.

Baxter (1967) working at Haverah Park has studied the time delays of muons relative to the first detectable signal, giving results in fair agreement with the other measurements at Haverah Park, especially in view of the lack of positive identification of the particles as muons and the inclusion of muons of energy below 1 GeV.

Rather nearer the core of somewhat smaller showers, an analysis by Firkowski (1967, 1968 private communication) of the barometric attenuation of muons in air showers suggests a rather large height of origin for muons of energy above 1 GeV. De Beer et al (1962) find a very high mean height of production for muons above about 3 GeV/c at distances greater than about 400 m from the core.

The average heights of origin of muons measured by several different methods at Haverah Park are seen to be in reasonable agreement. Measurements at other arrays seem to be scattered rather widely about the present values.

TABLE 7.4

COMPARISON OF HEIGHTS OF ORIGIN

Author	Distance (m)	Mean Heights
Suri (1966)	150 - 200 200 - 600 600 - 800	4.2 km 5.8 km 8.5 km
Baxter (1967)	400 600	$4.0\ ^{+\ 0.9}_{-\ 0.7}$ km $4.7\ ^{+\ 2.5}_{-\ 1.6}$ km
Linsley & Scarsi (1962c)	200 - 1100	320 ± 70 gm cm^{-2} (depth)
Bennett et al. (1962)	~ 500	3.3 km
de Beer et al. (1962)	> 400	220 gm cm^{-2} (depth)
Firkowski (1968)	80	$8.5\ ^{+\ 2.5}_{-\ 1.5}$ km
Present	100 - 600	547 ± 51 gm cm^{-2} 5.7 ± 1.0 km

7-5. Distributions of heights of origin

In the previous chapter a theoretical approach to the muon component was outlined and the variation of the characteristics of this component, in particular the heights of origin, with various parameters of the cascade was discussed. To establish whether the different distributions can be experimentally distinguished it is necessary to calculate the observable effects, including the angular deviations of muons from the core and the distortion of the lateral distributions of muons by the geomagnetic field, and compare these predictions with experimental observations.

7-5.1 The use of height distributions to predict distributions of angular deviation

In an interaction at a given height, only secondaries produced in a restricted band of opening angle will give muons falling within a given band of distance from the axis of the shower. Effects acting upon the muon after production are quite limited in their effect upon the distance from the core at which the muon is detected. Thus for a given distance interval and for muons of various momenta it is possible to predict the distributions of angular deviation from fixed heights. These can then be weighted by the height distribution to be tested. The combined distribution can be compared with that observed.

The factors contributing to the angular deviations have been examined above, and the method of calculating the expected distributions of angular deviation is given in Appendix D. Here it is sufficient

to note that the opening angles, Coulomb scattering and the measuring errors are allowed for fully and that small corrections are made for the secondary effects of decay and geomagnetic deflection. An important point is that the predicted distributions depend only weakly on the mean transverse momentum assumed, as the angles of production of the muons are fixed by observing muons in a fixed band of distance.

The distributions of angular deviation have been computed for the height distributions for muons of the usual mean momenta falling at three distances (155, 300 and 520 m) from the core. The height distributions calculated for four sets of assumptions (section 6-3.2) have been used. The distributions of angular deviation are normalized to the number of particles observed in the relevant region of momentum and distance.

To examine the possibility of distinguishing these distributions experimentally, the predicted numbers of particles in each cell of angular deviation for the various assumptions about A and n_s are shown in Figure 7.5 for the various distances and momenta. The ratios of these numbers to the numbers for A = 20 and $n_s \propto E^{0.5}$ above energies of 3×10^3 GeV are plotted. From these comparisons it can be seen that the muons falling at 155 m cannot be expected to yield a great deal of information about the cascade. This is also the case for muons in the lowest band of momentum at all distances. This insensitivity must largely derive from the remoteness of these muons from the very high energy interactions, and in the latter case, to large Coulomb scattering of the particles. Muons of 3.25 GeV/c or 6.61 GeV/c falling at 300 m

FIGURE 7.5

The angular deviations from the core of muons in certain regions of momentum and distance for three different models. The number of muons in each cell of angular deviation for a given model (A, n_s) is plotted as the ratio of this number to the number for (20, 0.50).

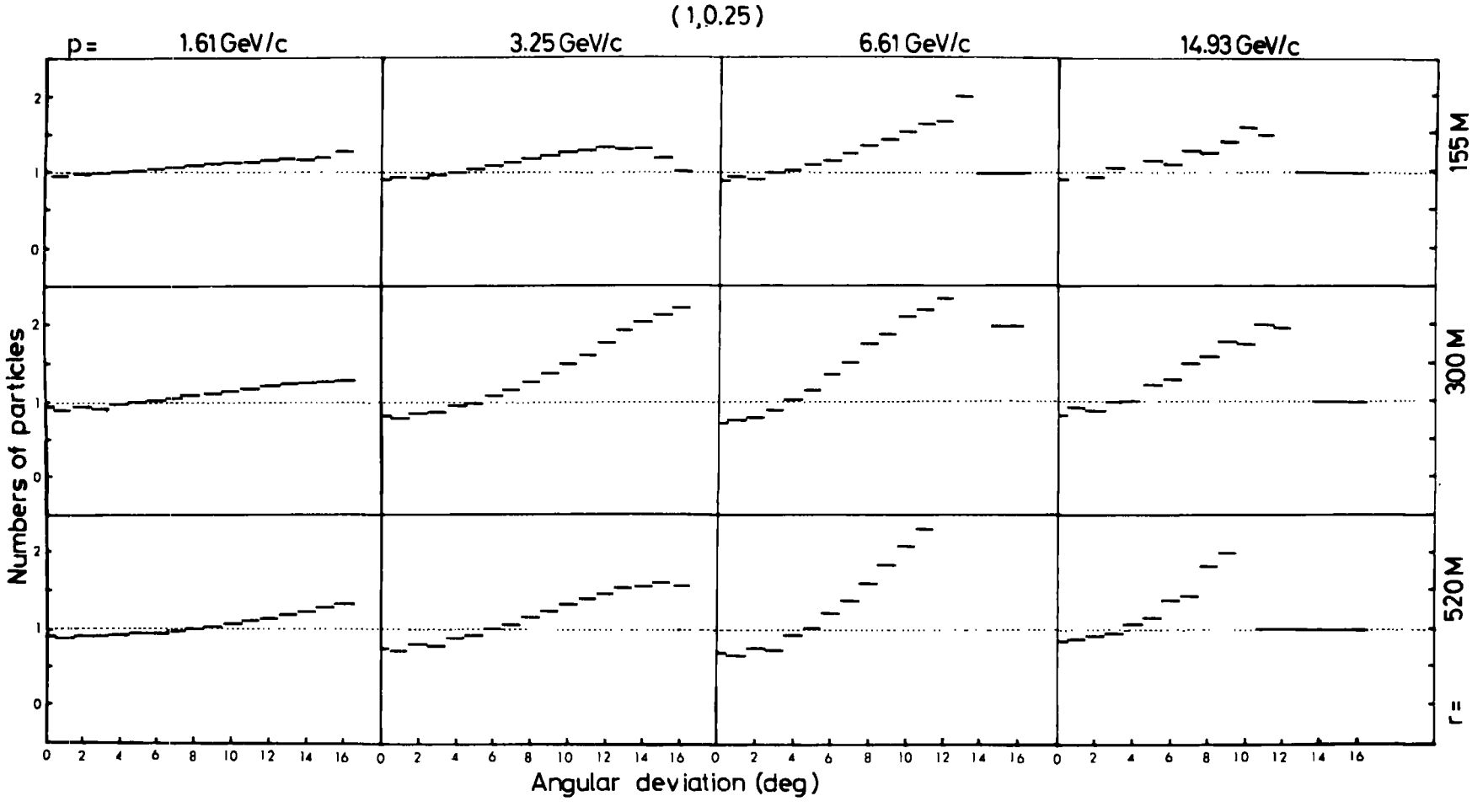
(1,0.25)
p = 1.61 GeV/c
3.25 GeV/c
6.61 GeV/c
14.93 GeV/c
155 M
300 M
520 M
r =
Numbers of particles
Angular deviation (deg)

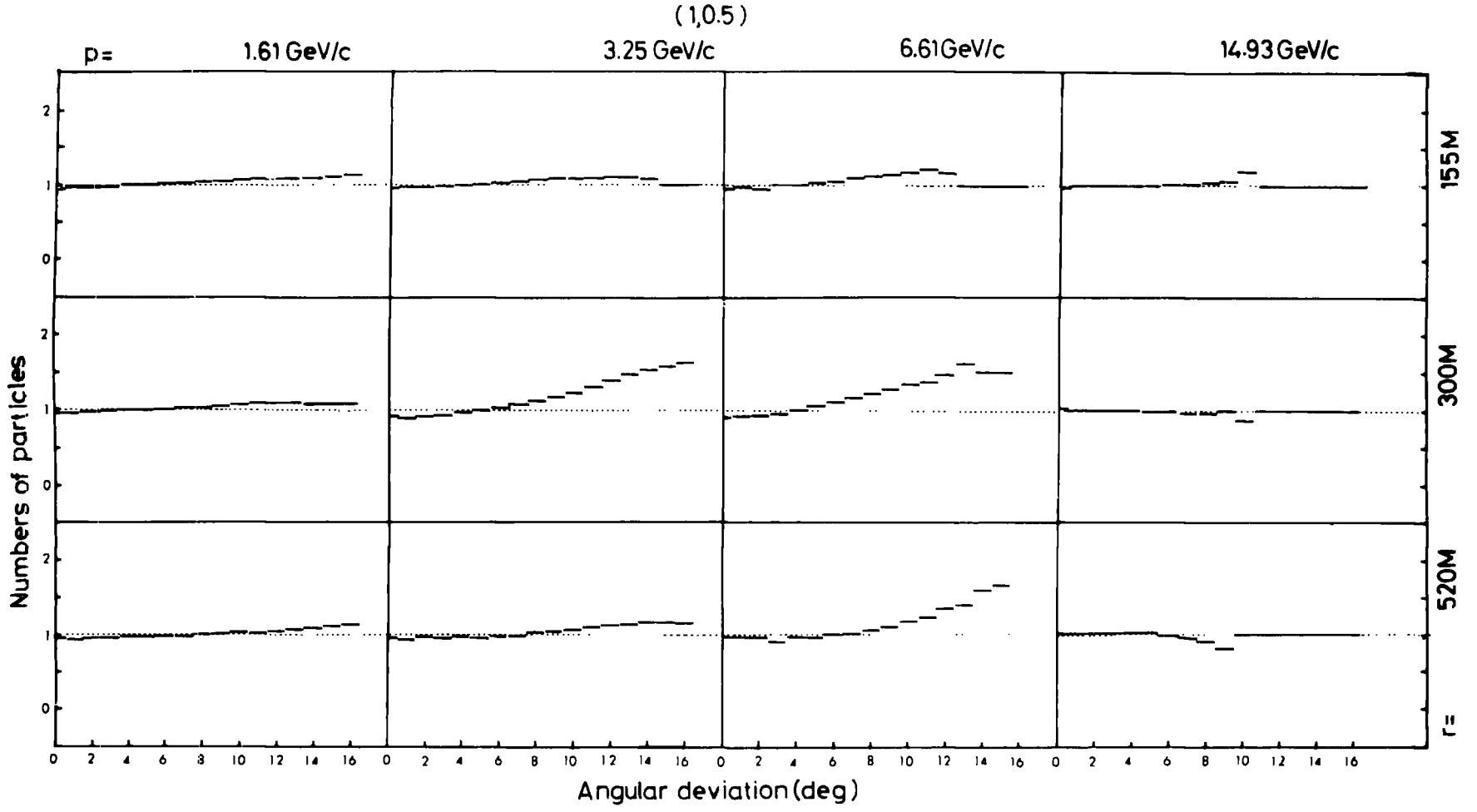
(1,0.5)
p=
1.61 GeV/c
3.25 GeV/c
6.61GeV/c
14.93GeV/c
155M
300M
520M
r=
Numbers of particles
Angular deviation (deg)

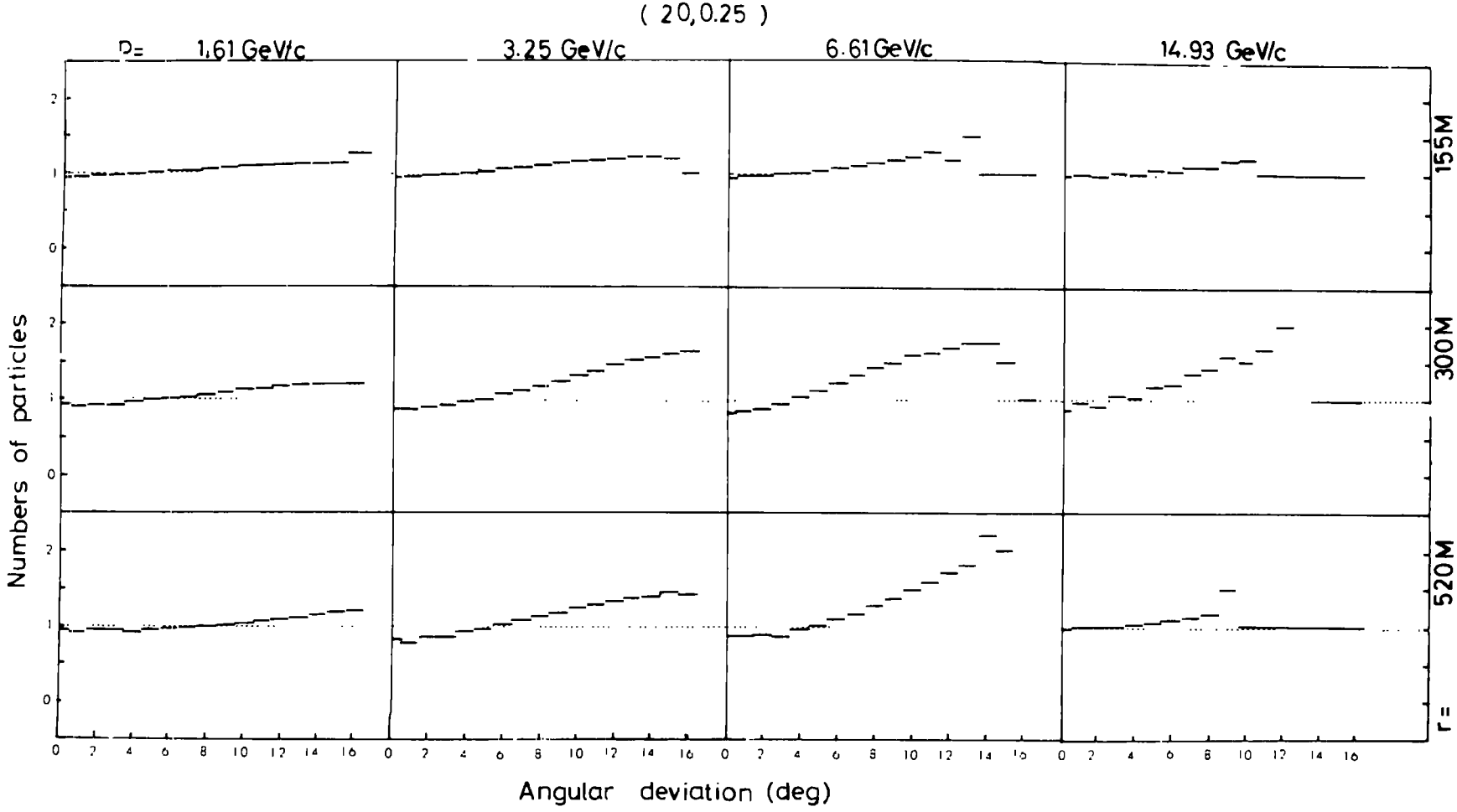
(20,0.25)
P= 1.61 GeV/c
3.25 GeV/c
6.61 GeV/c
14.93 GeV/c
155M
300M
520M
r=
Numbers of particles
Angular deviation (deg)

TABLE 7.4

NUMBERS OF MUONS IN MOMENTUM AND DISTANCE REGIONS

r(m)	p (GeV/c)			
	1.61	3.25	6.61	14.93
155	188	231	109	62
300	229	255	82	36
520	97	72	27	10

from the core appear rather sensitive to the assumed nature of the cascade. A consideration of the numbers of muons observed in these regions of momentum and distance (Table 7.4) shows that the only sensitive region with an adequate population is that with momentum of 3.25 GeV/c at a distance equal to 300 m.

The predictions for this region appropriate to the four various assumptions are plotted in Figure 7.6 as the ratio of the number of particles predicted to those observed experimentally. The fit of prediction to observation can be seen to be improved slightly by increasing the mass of the primary particle and similarly by a more rapid variation of multiplicity with primary energy. As a consequence, the model which comes nearest to fitting the muon intensities is also, of those tested, that which most nearly fits the angular deviations. A consideration of the value of χ^2 for each of these predictions (Figure 7.7) shows that, whilst this trend can be measured, there is

FIGURE 7.6

Comparisons of the observed distribution of angular deviation for muons of momentum 3.25 GeV/c at 300 m from the core with the distributions predicted for various cases. The ratio of the predicted numbers of particles to those observed is plotted against angular deviation.

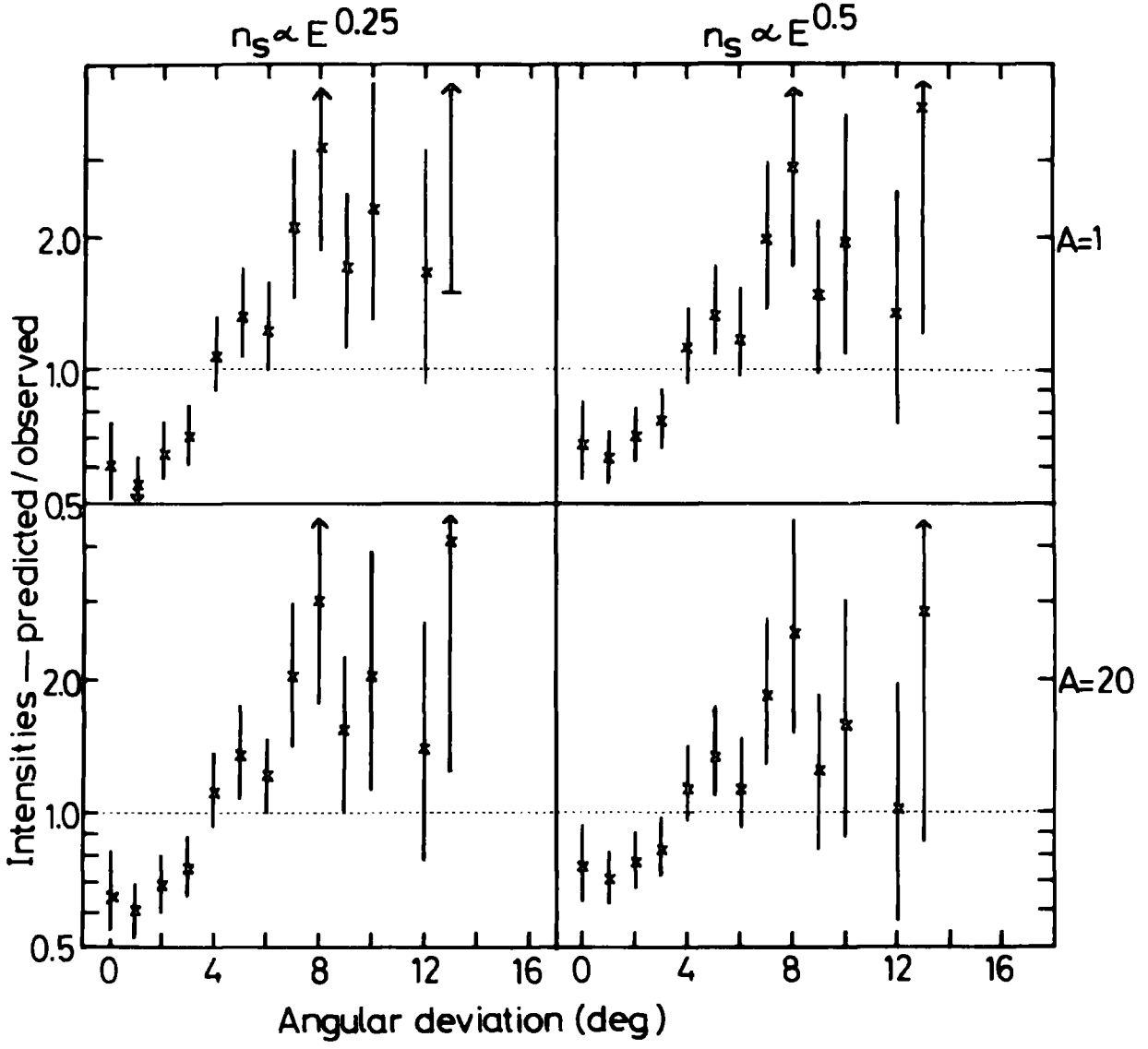
$n_s \propto E^{0.25}$
$n_s \propto E^{0.5}$
A=1
A=20
Intensities — predicted / observed
2.0
1.0
0.5
0
4
8
12
16
Angular deviation (deg)

not a very large probability that the distribution of angular deviations for A of 20 and $n_s \propto E^{0.5}$ is identical to that observed (Probability $\simeq$ 0.01). The number of degrees of freedom was kept constant for each comparison at a given momentum and distance, so that the χ^2 value is a direct indication of the probability.

To check both the selection of this region of momentum and distance as the most sensitive and the conclusions of the above paragraph, the variation of χ^2 for all the regions of momentum and distance with the various assumptions has been investigated, and is shown in Figure 7.7. For all momenta at 155 m from the core, no separation of the assumptions is possible experimentally, whereas at 300 m there is some difference observable, especially at a momentum of 3.25 GeV/c. At a distance of 520 m from the core differences are again observed. The distributions for muons of mean momentum 14.9 GeV/c are well fitted by the predictions, the fit improving as the distance from the core increases.

To improve the statistical significance of these predictions, the data from the three bands of distance considered have been added together in both prediction and observation. The variation of χ^2 with momentum for each of the four sets of assumptions is shown in Figure 7.7. The distributions calculated for the 'best' model are the best fits to the data, but the only momentum displaying significant differences is 3.25 GeV/c. It may be noted that, for the muons of mean momentum 14.9 GeV/c, the multiplicity law dominates the variation of χ^2 with model.

FIGURE 7.7

The variation of χ^2 (the goodness of fit of predicted to observed distributions of angular deviation) with momentum for four different cases. The points for 'all r' refer to a summation of the data at the three distances displayed individually.

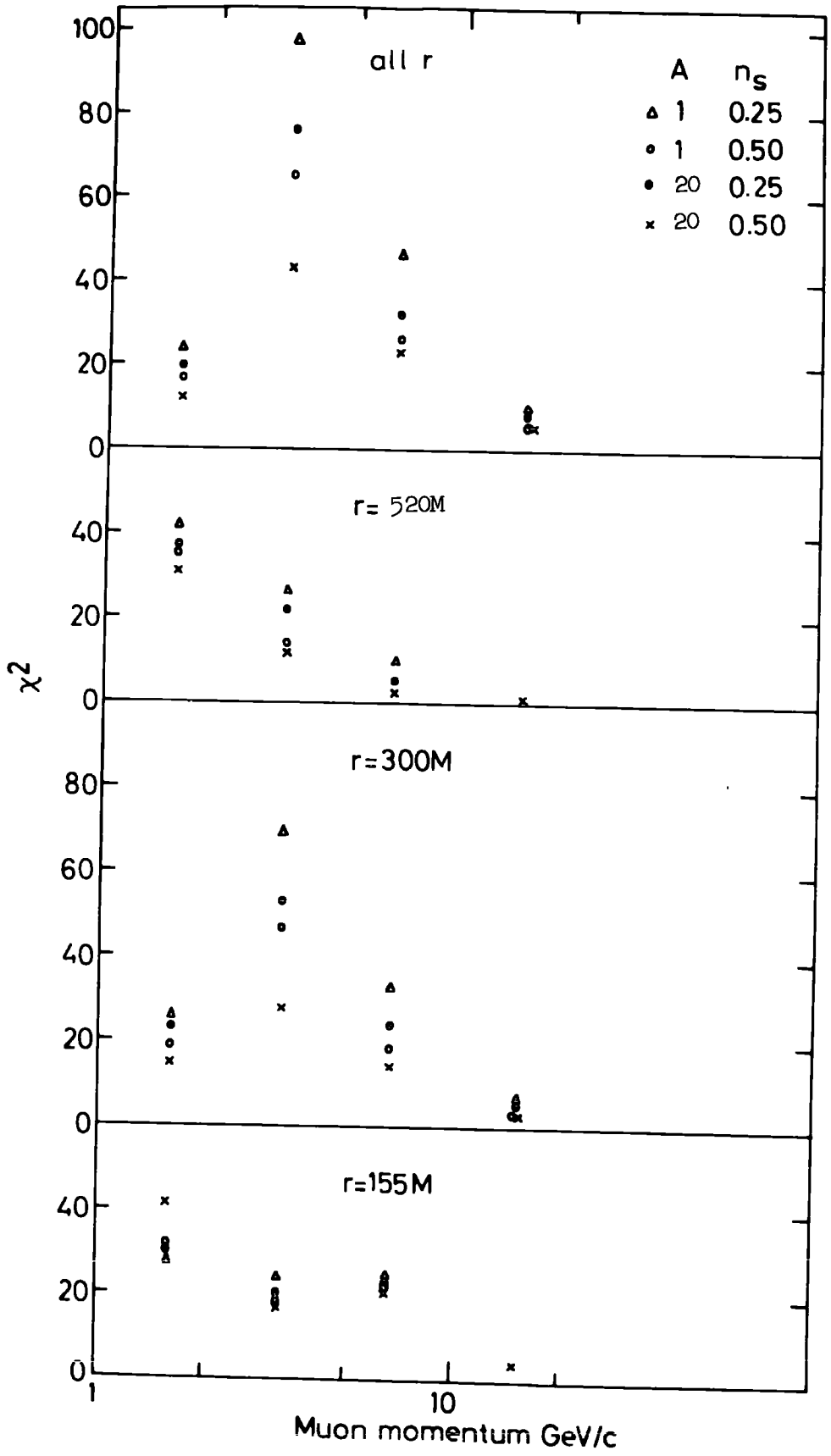
all r
A
n_s
1 0.25
1 0.50
20 0.25
20 0.50
r= 520M
r=300M
r=155M
χ^2
Muon momentum GeV/c

To investigate the cause of the comparatively poor fit of the prediction based on the preferred set of assumptions noted above, the effect of the linear interpolation used to bridge the gap between the height distributions given by the calculations for the regions of atmosphere above and below 10 km must be considered. This linear interpolation is expected to be most nearly correct when one of the contributions from the two regions is much smaller than the other, but if they are similar this assumption could be in error. For muons of momentum 6.61 GeV/c and distance 300 m from the core the contributions to the muon density from above and below 10 km are, for the 'best' model, of the same order of magnitude. There are sufficient muons present in the sample of data to test any variations in height distribution. In addition to the linear interpolation, two different cases, which appear to limit the range of realistic interpolation, have been tested. The upper limit gives a distribution of angular deviation which is somewhat closer to that observed ($\chi^2 = 10.9$) than that given by the linear interpolation ($\chi^2 = 14.5$). However, the probability corresponding to this value of χ^2 is still not very high.

Thus some of the discrepancy between the observed distributions and those predicted for A of 20 and $n_s \propto E^{0.5}$ may be removed by a careful treatment of the region between the two parts of the atmosphere considered. However, the total difference will not be removed in this fashion. It will be recalled that the calculations based upon these parameters did not predict muon intensities exactly similar to those observed, but rather gave under-estimates. The predicted

densities, for muons of large momentum, could be raised by an increase in the numbers of muons originating high in the atmosphere. This effect would be produced by an increase in the mass of the primary particle leading to an early degradation of the energy of the nuclear cascade, or an increase in the transverse momentum of the pions at large energies, or a contribution to the muon flux from the production and decay of kaons. The effects of the mass are concentrated in the first interaction of the primary particle, whereas the other factors would continue to affect the cascade deeper in the atmosphere. The multiplicity of pions is limited for dynamical reasons to a variation which is not much faster than $E^{0.5}$. It appears from the study of the angular deviations from the core that at lower momenta the muons must again originate higher in the atmosphere than is presently predicted (see also Figure 7.1), due probably to a combination of the factors cited above.

It is of interest to note that all the muons of large deviation which survived the checks detailed in section 7-3.3 have been accounted for by this theoretical treatment.

7-5.2 The use of height distributions to predict the charge distortion of muons

The distributions of height of origin predicted for muons of various momenta falling at 300 m from the core have been tested further by using them to predict the charge distortion expected due to the geomagnetic field (section 7-2).

FIGURE 7.8

Ratio of observed charge ratio to that predicted on the basis of theoretical distributions of heights of origin. Four cases are shown.

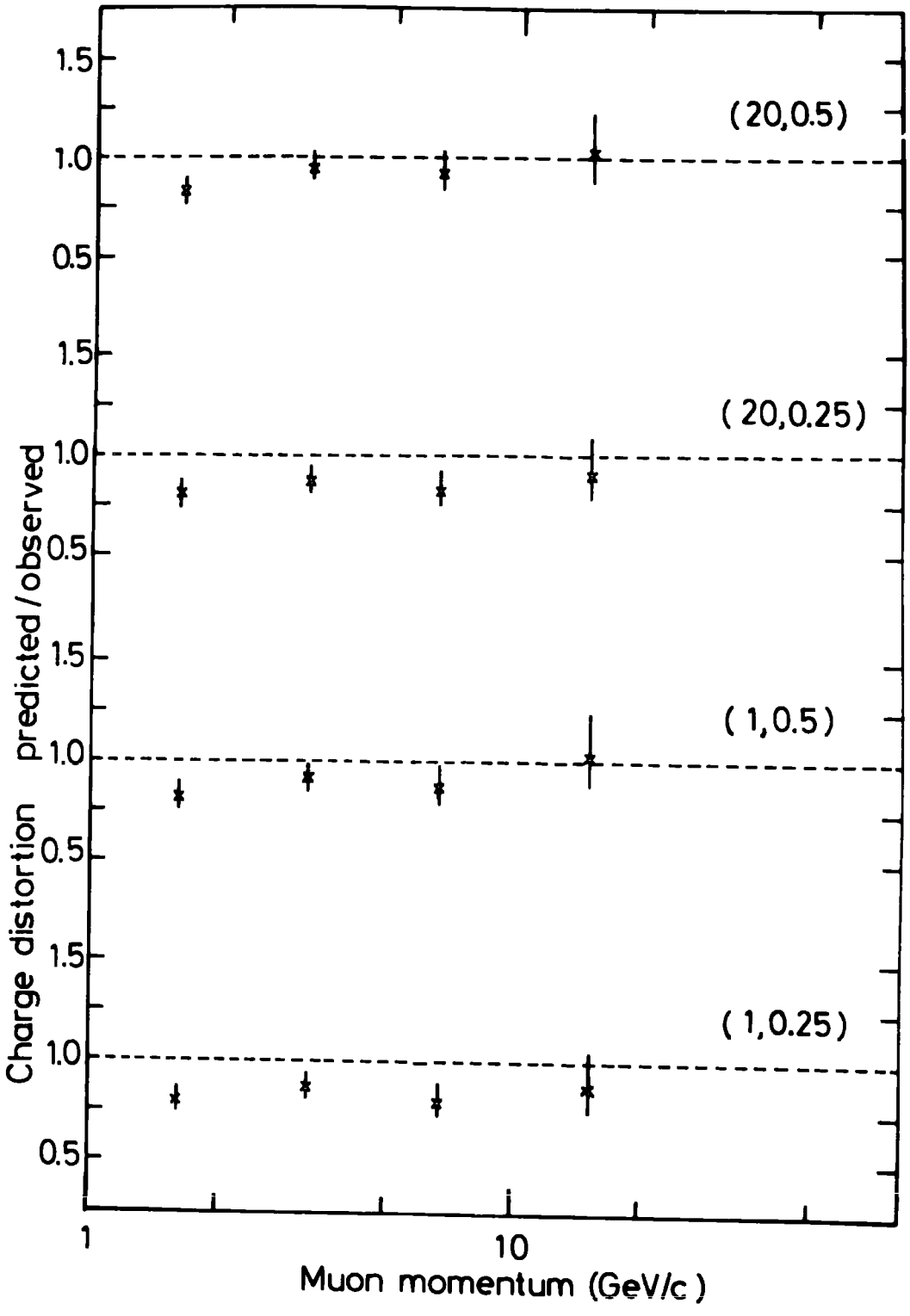
1.5
1.0
0.5
(20,0.5)
1.5
1.0
0.5
(20,0.25)
1.5
1.0
0.5
(1,0.5)
1.5
1.0
0.5
(1,0.25)
Charge distortion predicted/observed
1
10
Muon momentum (GeV/c)

For each of the three regions of the space G discussed in that section the distorted charge ratios for muons of fixed momentum were determined for heights spaced 100 gm cm^{-2} apart, commencing from 100 gm cm^{-2}. The charge ratios were weighted in accordance with the height distribution to be tested and the average charge ratio determined for each region. Using these charge ratios the expected numbers of muons of each sign were found from the numbers of muons observed in each region, and hence the overall charge distortion (with negative excesses reversed)of muons falling in these regions of G was determined. This predicted charge ratio was then compared with that found experimentally, these values being shown in the last column of Table 7.2.

For the height distributions in question the ratios of predicted to observed charge distortion are shown in Figure 7.8 as a function of momentum. Here, too, the mass of the primary particle appears only to affect the predictions in second order compared with the variation of multiplicity with energy. With the present numbers of muons, the effects predicted for particles of mass 1 or 20 with $n_s \propto E^{0.5}$ are adequate representations of the data, without being exact fits. The departures of the predictions from observation are such that an increase in the mean heights of origin would improve the agreement (see also Figure 7.1).

7-5.3 Conclusions

The distributions of heights of origin of muons have been examined using two effects. The sensitivity of the angular deviations of muons from the core direction to the assumed nature of the nuclear cascade

has been established, and the data recorded in the present experiment have been seen to be adequate to distinguish between the different possibilities with some degree of reliability in a rather restricted region of momentum and distance.

From these studies it is possible to select the variation of multiplicity with energy as the most important factor considered governing the height distributions for muons of rather low energy, the mass of the primary particle being of lesser importance. The height distributions of muons in a shower initiated by a primary particle of mass 20 when the multiplicity varies as $E^{0.5}$ for energy greater than 3×10^3 GeV are nearest to those appropriate to the observed data. However, these predicted distributions are not in exact agreement with observation. These conclusions are supported by the tests of the height distributions using the distortion of the charge ratios of muons by the geomagnetic field.

It must be remembered that parameters of the model, such as multiplicity, have not been permitted to fluctuate. Such fluctuations must exist and could lead to an increase in the effective height of production of muons, depending upon the variation of height with these parameters.

CHAPTER 8

CONCLUSIONS AND FUTURE WORK

At great energies the only source of information upon the nature of nuclear interactions is the observation of various characteristics of air showers. The muon component especially seems likely to yield significant information upon these interactions and also upon the nature of the primary particles initiating the showers. Previous experiments have determined the broad features of the muons and the present experiment has measured the momentum spectrum of muons as a function of distance from the shower core and the height of origin of muons of various momenta. The directions of motion of muons within a shower have also been investigated.

By comparisons of these measured data with theoretical predictions, based upon various assumptions of the nature of the primary particles and of the nuclear interactions, information about the first few interactions in these very energetic events has been derived.

8-1. The lateral distributions of muons

In Chapter 6 of this thesis the lateral density distributions of muons above various threshold momenta were seen to be in disagreement with the predictions of rather simplified models of the nuclear cascade, wherever the muons originated in the early portions of the cascade. A rigorous treatment of the cascade in the atmosphere above 10 km, combined with a treatment similar to the simple models below this height, predicts muon densities comparable with those measured

experimentally in the regions of energy and distance which previously gave rise to discrepancy (Orford and Turver 1968).

Using this treatment, the effects of various values of the mass of the primary particles and other parameters upon the muon densities have been investigated. It has been concluded that the typical 500 m showers are initiated by particles of energy 2×10^{17} eV, having effective mass greater than 10 (taken as 20) whilst the multiplicity of pions in nuclear interactions rises as $E^{0.25}$ for energies below 3×10^{3} GeV, but thereafter varies as $E^{0.5}$. Neither of these conclusions is exact, in that some variation of the parameters is possible within the errors of the measured data. The values given are, however, lower limits of the mass and multiplicity.

All the measured features of the momentum spectra of muons are shown to be in satisfactory agreement with the predictions of this model. In particular the predicted densities of muons of momentum greater than 1 GeV/c at great distances from the core were shown to be sensitive to the mass of the primary particle. The measured densities are closer to those predicted for a heavy primary than for the case of a proton primary.

8-2. The heights of origin of muons

The average heights of origin of muons of various momenta have been ascertained by two independent methods, the results of which are in good agreement. The muons of very high energy, present in showers with densities which are much higher than those predicted on simple

theories (such as Hillas 1966), have been shown to originate considerably higher in the atmosphere than these theories would allow. This fact reduces the requirement for the large transverse momentum attributed to particles decaying to give these muons by de Beer et al. (1967).

The population of muons with large angular deviations from the core which led Earnshaw et al. (1967b) to assume the presence of particles of high transverse momentum has been reduced considerably by a careful check of air shower arrival directions. The deviations have been shown to depend on the assumed height distribution much more strongly than upon transverse momentum. The surviving large deviations have been accounted for by a more careful treatment using normal values of transverse momentum.

The distributions of angular deviations for certain regions of momentum and distance have been shown to be sensitive to the nature of the nuclear cascade assumed in predicting distributions of heights of origin. For the numbers of muons presently accumulated with the spectrograph, there is only one such region of energy and distance for which the data are sufficiently significant to differentiate between the different assumptions used. The effect on the predicted distributions of height (and hence of angular deviation) of the mass of the primary particle is less than the effect of the variation of multiplicity with energy. The values of mass and multiplicity to give densities comparable with those observed experimentally are insufficient to give height distributions exactly compatible with the distributions in the observed showers. The predicted distributions give a mean height which

is too low. This mean height is affected by various parameters of the nuclear cascade, and it seems possible that values of these parameters which give muon densities equal to those observed at high momenta may also give height distributions close to those observed.

The geomagnetic charge distortion has also been used as a basis for checking the distributions of heights of origin predicted by the theoretical approach. The results are somewhat less sensitive to the nature of the nuclear cascade assumed, but the observed results are closest to those predicted for a primary particle of mass 20 and pion multiplicity varying as $E^{0.5}$. Changes in the height distribution as suggested above would increase the agreement between prediction and observation.

The changes in the parameters of the model suggested by this study of the distributions of heights of origin will result in an increase in the effective height of production of the muons of mean momentum 45 GeV/c, giving closer agreement with the height of origin deduced from the measured charge distortion for these muons.

8-3. Conclusions

The present experimental work has been shown to be in agreement with the predictions of a theoretical model using conventional values for parameters such as the transverse momentum of particles produced in nuclear interactions. The multiplicity of pions produced in nuclear interactions must vary as $E^{0.5}$ for energies greater than 3×10^3 GeV, and the mass of the particles (of energy 2×10^{17} eV)

initiating the showers must be greater than 10.

Thus the mass spectrum of primary cosmic rays at an energy about 2×10^{17} eV is rather narrow compared to that observed in nuclear emulsions at energies about 10^{13} eV (Table 1.1). Linsley and Scarsi (1962a), studying the fluctuations of the muon numbers in showers of primary energy greater than 10^{17} eV, concluded that the mass spectrum of the particles initiating the showers was rather narrow, being probably a pure beam of protons. However, in a later report Linsley (1964) said 'The evidence (for proton primaries) comes from the shower-size distribution for events with fixed total number of muons. The distribution we presented at Kyoto for primaries $\geqslant 10^{17}$ eV is rather narrow and is inconsistent with a primary composition similar to the one at lower energies. This requires that the mass spectrum of primaries with total energy $\geqslant 10^{17}$ eV must be relatively narrow. This means that either protons predominate, or that most of the primaries are nuclei in the iron group. Another test, based on the distribution at another depth, below the shower maximum, favours the first alternative although the second is not excluded.' Thus the present conclusion is not thought to confict with the work at Volcano Ranch.

The contrast of the rather narrow mass spectrum of the primary particles at an energy of 2×10^{17} eV with that observed up to primary energies of 2×10^{15} eV suggests some change must take place in the acceleration or transportation mechanisms affecting the cosmic rays between these energies. It is not possible on the present evidence to

differentiate between the several possibilities, which include (a) a failure of the galactic magnetic containment at a magnetic rigidity of 2×10^{15} eV, (b) a break in the spectrum of cosmic ray sources, and (c) the interaction of the universal black-body microwaves with cosmic rays in an evolving universe (Hillas 1967a,b). It may become possible to differentiate between these possibilities with a knowledge of the effective mass of primary cosmic rays of energy both above and below the present energy of 2×10^{17} eV. Experiments at Haverah Park described in the next section should enable these masses to be determined.

8-4. Future work

The present report is based upon the data gathered over two years of operation, up to May 1967. Since that time much data has accumulated on 500 m triggers and the addition of this to the present data will be of some use in the study of muon densities.

Future developments will include a considerable refinement of the analysis of very distant or very large showers as a consequence of the operation of the 2 km array. Preliminary results from this array (Earnshaw R.A., et al. 1967, Andrews et al. 1968) indicate that large showers, initiated by particles of great energy, give a large response in all the detectors, corresponding to a constant structure function exponent from 300 m to 3 km from the core. In Chapter 6 it was seen that for vertical 500 m showers at distances from the core greater than about 1 km it is practicable to distinguish experimentally between

FIGURE 8.1

The lateral distributions of muons of momentum greater than 1 GeV/c for primary particles of energy 5×10^{18} eV and mass 1 and 20. Also shown as a function of distance is the ratio of the density for a heavy primary to that for a proton.

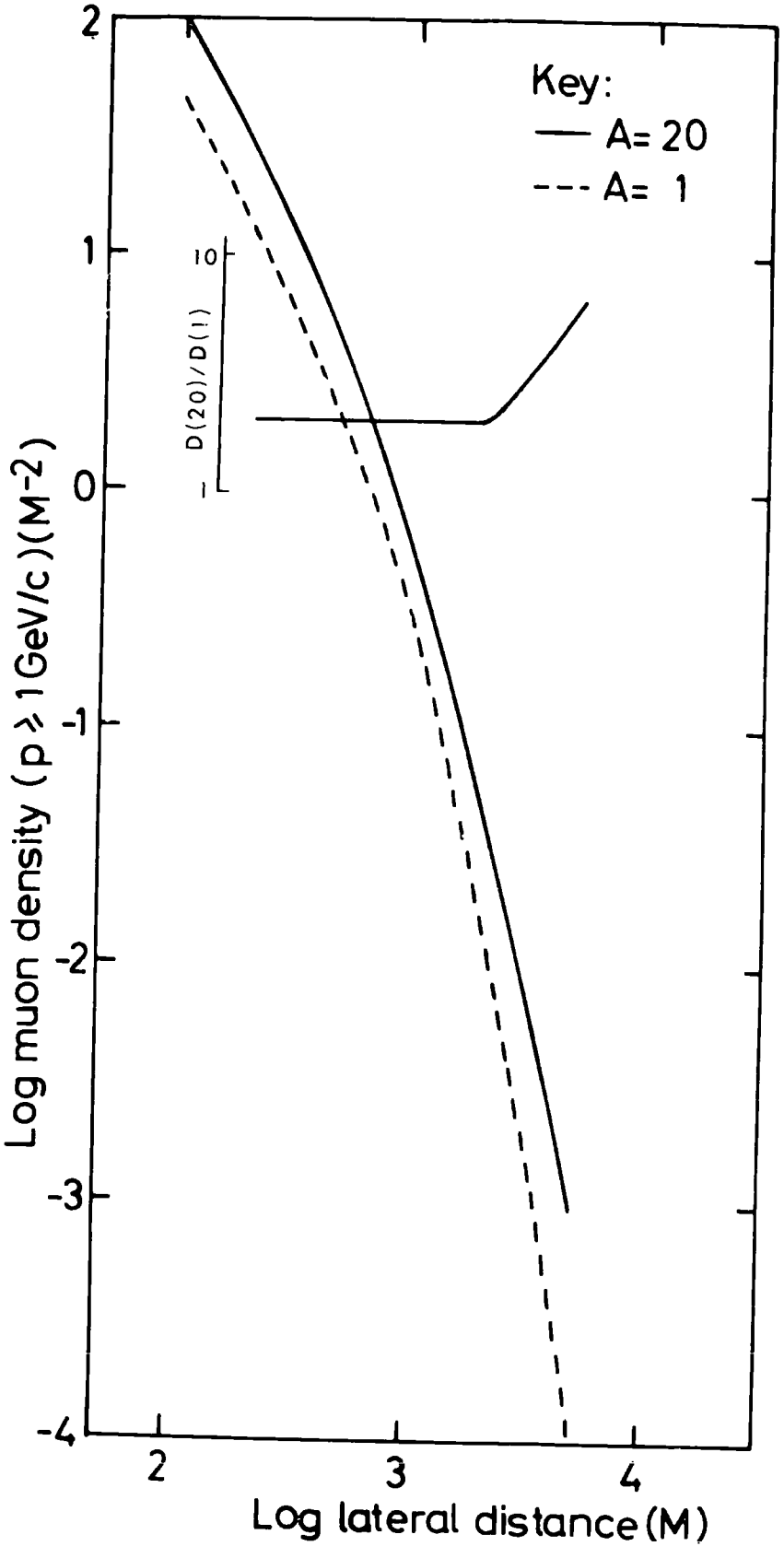
Key:
A= 20
A= 1
D(20)/D(1)
10
1
Log muon density (p ≥ 1GeV/c)(M⁻²)
2
1
0
-1
-2
-3
-4
2
3
4
Log lateral distance (M)

heavy primary particles and protons using the density of muons of momenta above 1 GeV/c. A similar comparison is shown in Figure 8.1 for showers incident at a zenith angle of 20^{o}, initiated by protons and particles of mass 20 of energy 5×10^{18} eV per nucleus. An investigation of the lateral distribution of muons in large showers at distances greater than 2 km from the axis may lead to the determination of the mass composition of the particles initiating the showers. To distinguish between the two cases at these great distances it would be necessary to employ large areas of muon detectors. One possibility would be to use very large area flash tube trays, shielded by about 20 cm of lead to give a sufficiently large muon threshold energy for the flux of muons to be easily calculable. However, at these very large distances from the core, nearly all the particles present are muons and any electrons or photons are of very low energy. Thus the response of the Cherenkov detectors of the air shower arrays must be principally due to the muon component, and it may be possible to use the lateral distribution of this response in place of the lateral distribution of muons. The validity of this use of the Cherenkov detectors far from the core may be checked by a comparison, at these distances, of the density of 'equivalent muons' recorded in the central 500 m Cherenkov detector and the density of muons observed in the large area shielded liquid scintillator which is adjacent to this detector.

Another development is an increase in the areas at each of the outer 150 m array detectors. This array will be run in parallel with the 500 m

array, seven pulse heights being recorded whenever either array is triggered. This should lead to the analysis of 500 m showers which now fall too close to the central detector for accurate analysis and also to a great improvement in the core location for showers detected by both the 500 m and the 150 m arrays. This should enable the momentum spectrum of muons in 150 m showers to be subdivided by distance to quite large distances, enabling a more accurate examination of the dependence of the spectrumon size to be carried out. At distances characteristic of the 150 m array, a substantial increase in the m.d.m. of the spectrograph would enable the expected dependence on the early interactions of the nuclear cascade of the very high energy muon densities at these distances to be established. The primary energies of the particles initiating the 150 m showers will be rather below 2×10^{17} eV, and thus an estimate of the effective mass of these particles will be of great interest.

The conclusions reached about the distributions of height of origin were limited by the amount of data available. The anticipated two-fold increase in the number of muons should serve to increase the precision of the results and will enable further comparisons of angular deviations to be made, giving increased weight to the conclusions. It has been seen that the present calculated distributions of height of origin apparently underestimate the contributions to the muon densities from great heights; various factors which would reduce this discrepancy were cited above. If the predictions of the amended calculations are not in

agreement with the statistically improved data, a close inspection of the data for any sources of bias must precede any further modifications of the theoretical approach.

These increases in the data should enable the variation of the mean height of origin with distance from the core to be ascertained, using the geomagnetic distortion of the lateral distributions of muons. The same effect, used with the data from the modified 150 m array, will enable the variation of heights of origin with shower size to be investigated.

Occasionally in the spectrograph records a particle making a very large angle with the general shower direction is observed. Some of the particles constitute the expected flux of unassociated muons and the remainder have been shown to come from the direction of the core (Earnshaw et al. 1967b). They have been searched for, and tentatively identified as delayed penetrating particles (Blake et al. 1967). From the results on the angular deviations of muons, it can be seen that muons originating very low in the shower with transverse momentum of the same order as their longitudinal momentum in the lab system should be observed at great angles to the rest of the shower particles. Bjornboe et al. (1968) have concluded that such delayed particles are not heavy (e.g. quarks), nor can they be muons of energy greater than 2 GeV. Further observations on this phenomenon could be of great interest.

APPENDIX A

SUBDIVISION OF THE DATA BY MOMENTUM

When dealing with effects which are functions of momentum and examining the dependence upon other parameters or evaluating the variation with momentum it is convenient to treat limited bands of momentum. Because of the scattering of muons by the magnet iron it is not possible to correlate directly deflection with momentum. However a momentum may be ascribed to each particle to which the deflection would correspond in the absence of any scattering (pure magnetic momentum), and subdivision on the basis of this estimate is possible.

The data have been subdivided for all purposes into five bands with limits shown in column one of Table A.1. The data within each band have been analysed to derive a momentum spectrum corresponding to these deflections (section 5.2.2), yielding the true momentum spread corresponding to these bands of pure magnetic momentum. From these spectra the mean true momentum for each band has been found using

$$\bar{p} = \frac{\int_1^{1000} p\, S(p)\, dp}{\int_1^{1000} S(p)\, dp}$$

TABLE A.1

Limits of pure magnetic momentum (GeV/c)	$\bar{p}$ (GeV/c)
1 - 3	$1.61^{+0.28}_{-0.26}$
3 - 8	$3.25^{+0.80}_{-0.85}$
8 - 15	$6.61^{+2.3}_{-2.2}$
15 - 30	$14.93^{+4.6}_{-3.0}$
> 30	$45.0^{+22.8}_{-19.3}$

and upper and lower limits placed on this mean momentum corresponding to momenta including 40% of the areas above and below the mean value, with the results shown in Table A.1.

The trial spectrum was closely similar to that appropriate to the total data recorded by the 500 m array, but it is expected that as the distance from the core varies and the momentum spectrum varies, so the mean momentum for a given band will vary. This variation of $\bar{p}$ has been examined and found to be within the errors quoted on $\bar{p}$ for the total 500 m case. Thus the stated values of mean momentum have been used.

APPENDIX B

THE DEFLECTION OF MUONS BY THE GEOMAGNETIC FIELD

The geomagnetic deflection of muons observed with momentum p_o GeV/c produced at an altitude Z Km above sea level in an air shower of zenith angle θ and azimuth ϕ can be derived as follows.

The mean momentum of the muons between production and observation is

$$p = p_o + \frac{2.23}{2} \left\{1 - \exp(-Z/7.5)\right\} / \cos\theta \text{ GeV/c}$$

Let a be the angle between the shower axis (and assumed muon direction) and the magnetic field (angle of dip = i), given by

$$\cos a = \cos i \cos\theta - \sin i \sin\theta \cos\phi$$

Writing p in eV/c, these muons will have radii of curvature (R) in the earth's magnetic field (H gauss) of

$$R = p/300\ H \sin a \qquad \text{cm}$$

Thus the angle (Ω) through which the muon is bent is

$$\Omega = \frac{Z \times 10^5}{\cos\theta} \times \frac{1}{R}$$

and hence the linear deflection of the muon normal to the lines of force is

$$dr = R \sin a \, (\sec\Omega - 1)$$

with x and y components

$$\begin{cases} dx = X\,(dr \cos\phi) \\ dy = Y\,(dr \sin\phi)/\cos i \end{cases}$$

where X = + 1 for a positive muon if shower does not arrive 'under' the lines of force

Y = + 1 for a positive muon.

In this calculation it is assumed that the increasing deflection of a muon as it loses energy may be successfully averaged by using the mean momentum of the muon. This has been checked by dividing the atmosphere into 100 gm cm^{-2} bands and treating each of these as described above and summating these bands over the path length in question. The distances through which the muons are deflected are slightly smaller in this case than those calculated by the above formulation, leading to a reduction in the charge ratios predicted. This has not been allowed for in this thesis as it will be offset to some extent by the effect discussed in section 7-2.1.

APPENDIX C

THE DERIVATION OF THE HEIGHT OF PRODUCTION OF A MUON FROM ITS ANGULAR DEVIATION FROM THE CORE

The projected incident angle of the shower core (ψ_p) is found from θ, ϕ by

$$\tan \psi_p = \tan \theta \cos(\phi + 34.5)$$

and by rotation of the axes used, the distance along the ground from the core of the shower to the spectrograph is projected into the measuring plane (AC in Figure C.1).

Referring to Figure C.1 the height of production may be found as follows:-

Let $AC = x$

$GC = r$

$OC = h$

$$AG = \sqrt{(r^2 - x^2)}$$

Using the sine rule:

$$GF = \frac{AG \sin \psi_o}{\sin(90 - \Omega)} \qquad \text{where } \Omega = \psi_p - \psi_o$$

$$\therefore \quad CF = r + \frac{Y\sqrt{(r^2 - x^2)} \sin \psi_o}{\sin (90 - \Omega)}$$

$Y = +1$ if ψ_p and ψ_o are of opposite signs

$Y = -1$ if ψ_p and ψ_o are of the same sign

$$h = CF/\tan (\Omega)$$

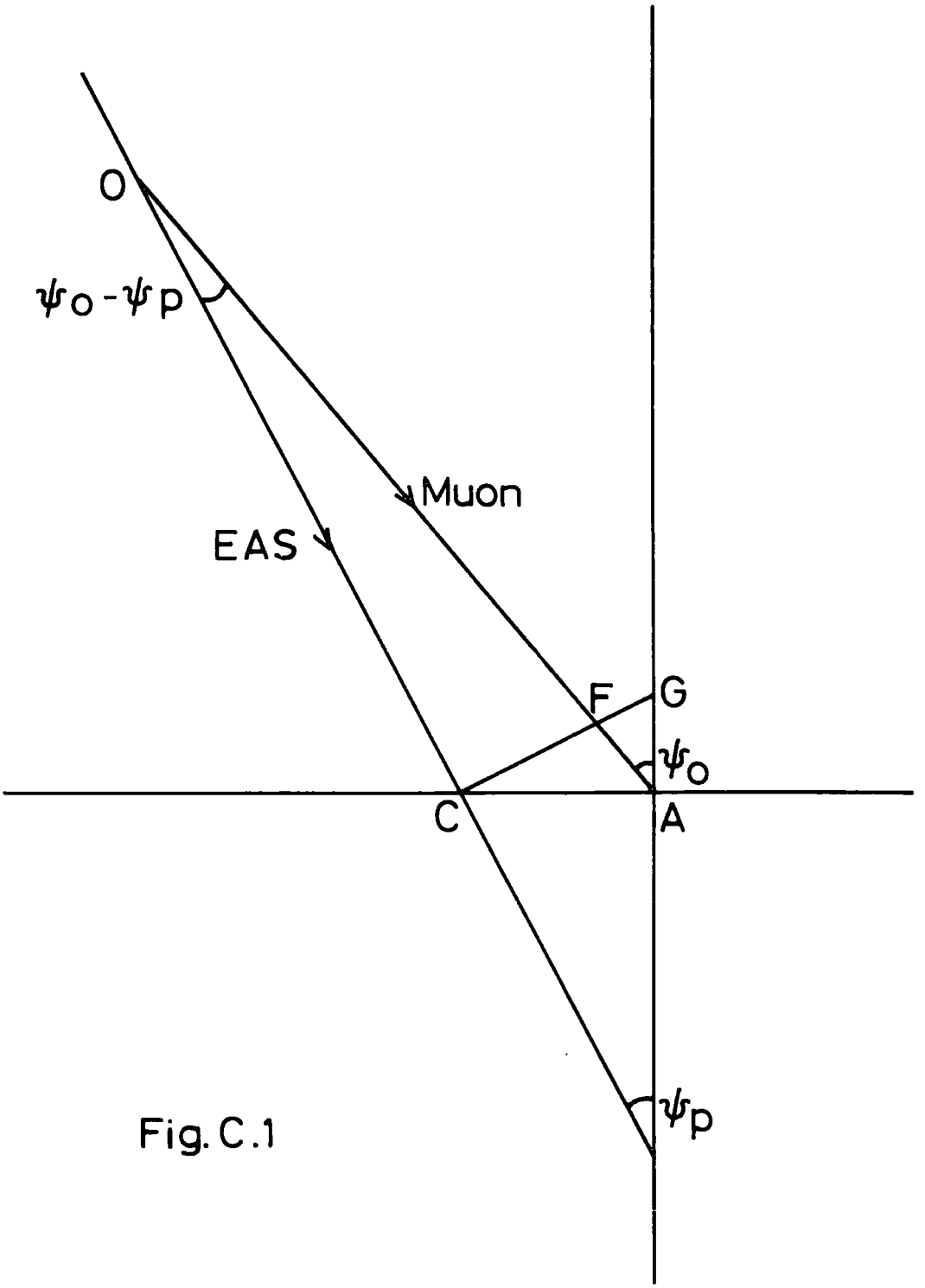

Fig. C.1

Now this value of h must be corrected for core inclination:-

$$h' = h \cos(\psi_p)$$

APPENDIX D

THE PREDICTION OF THE DISTRIBUTION OF ANGULAR DEVIATIONS OF MUONS FROM THE CORE DIRECTION

A muon is assumed to lose energy at a constant rate of 2.23 MeV $gm^{-1} cm^{-2}$ and thus at a height ℓ gm cm^{-2} a muon observed with momentum p has momentum

$$p' = p + 0.1 + \ell \times 0.00223 \quad \text{GeV/c} .$$

It is assumed that this muon is the decay product of a pion which decayed promptly on formation and thus has an average momentum

$$p_\pi = 1.32\, p' \quad \text{GeV/c}$$

the median angle of the decay process being

$$\theta = 2.17/(\sqrt{2} \times p_\pi) \quad \text{degrees} .$$

The muon trajectory is bent by the geomagnetic field (H) and an average value (ϕ) is used for this, evaluated for the case of a vertically incident shower

$$\phi = \frac{300 \times H \times \sin 25^\circ}{(p + p')/2} \times 57.29 \quad \text{degrees.}$$

The decay and geomagnetic angles of deviation are taken as delta functions and thus the projected angular deviations of the muon from the core can be changed by an amount ψ where

$$\psi = \theta \pm \phi$$

The total width (σ) of the Gaussian scattering distribution is

composed of measuring errors (σ_N) and Coulomb scattering in the air (σ_A) and lead shielding (σ_{pb}) as

$$\sigma = \sqrt{(\sigma_N^2 + \sigma_A^2 + \sigma_{pb}^2)}$$

Because of this scattering, muons may be scattered to within the 16° limit imposed on the data. Thus spatial opening angles of production between - 50° and 50° are considered. For a fixed height and a band of distance those values of opening angle (Ω) which will not fall within the band are rejected and for those which are accepted

$$p_t = p_\pi \sin \Omega \qquad \text{GeV/c}$$

and the probability of this p_t occurring is evaluated using the CKP distribution -

$$g(\Omega) = f(p_t) = \frac{p_t}{p_o^2} \exp(- p_t/p_o)\, dp_t$$

where $p_o = 0.2$ GeV/c.

This is now projected into the measuring plane of the spectrograph, allowance made for ψ, and the probability distribution of projected angular deviation is scattered by a Gaussian distribution of standard deviation σ. This scattered distribution is normalized to unit area between - 16° and 16° and folded about zero to give the final distribution of the absolute values of the angular deviation from the core. Due to the method of calculation the first cell of angular deviation is only half as wide as the other cells, and thus

in any comparisons it is only given half the weight of the others.

REFERENCES

The following short forms of reference have been used:-

'Kyoto Conference' - Proc. 7th Int. Conf. on Cosmic Rays, Kyoto, 1961 (J. Phys. Soc. Japan (Suppl. AI-III), 17)

'Jaipur Conference' - Proc. 8th Int. Conf. on Cosmic Rays, Jaipur, 1963, (Bombay: Commercial Printing Press)

'London Conference' - Proc. 9th Int. Conf. on Cosmic Rays, London, 1965, (London: Institute of Physics and Physical Society)

'Calgary Conference' - Proc. 10th Int. Conf. on Cosmic Rays, Calgary, 1967, (Ottawa: National Research Council of Canada)

ABROSIMOV, A.T., BAZILEVSKAYA, G.A., SOLOV'EVA, V.I., and KHRISTIANSEN, G.B., 1960, Soviet Physics - JETP, 11, 74-79.

ADCOCK, C., DE BEER, J.F., ODA, H., WDOWCZYK, J., and WOLFENDALE, A.W., 1968, J. Phys. A (Proc. Phys. Soc.), [2], 1,82-88.

AKASHI, M., et al., (Japanese and Brazilian Emulsion Groups), 1966, London Conference, 2, 744-750.

ALLAN, H.R., BEAMISH, R. F., BRYANT, D.A., KASHA, H., and WILLS, R.D., 1960, Proc. Phys. Soc., 76, 1-16.

ALLAN, H.R., BLAKE, P.R., and PIDCOCK, J.K., 1966, London Conference, 2, 772-773.

ALLAN, H.R., BLAKE, P.R., NEAT, K.P., and PIDCOCK, J.K., 1967, Calgary Conference (in the press).

ANDREWS, D., EVANS, A.C., REID, R.J.O., TENNENT, R.M., WATSON, A.A., and WILSON, J.G., 1968, Nature, 219, 343-346.

ASHTON, F., and WOLFENDALE, A.W., 1963, Proc. Phys. Soc., 81, 593-603.

BARNAVELI, T.T., BIBILASHVILI, M.F., GRUBELASHVILI, G.A., DZHAVRISHVIL, A.K., KAZAROV, R.E., KURIDZE, R.V. and KHALDEEVA, I.V., 1965, Bull.Acad.Sci., USSR., Phys. Ser., 28, 1782-3.

BARRETT, P.H., BOLLINGER, L.M., COCCONI, G., EISENBERG, Y., and GREISEN, K., 1952, Rev. Mod. Phys., 24, 133-178.

BASSI, P., CLARK, G., and ROSSI, B., 1953, Phys. Rev., 92, 441-451.

BAXTER, A.J., WATSON, A.A., and WILSON, J.G., 1966, London Conference, 2, 724-726.

BAXTER, A.J., 1967, Ph.D. Thesis, University of Leeds.

BAXTER, A.J., 1968, University of Leeds Preprint.

BENNETT, S., and GREISEN, K., 1961, Phys. Rev., 124, 1982-1987.

BENNETT, S., DELVAILLE, J., GREISEN, K., and KENDZIORSKI, F., 1962, Kyoto Conference, AIII, 196-202.

BJORNBOE, J., DAMGARD, G., HANSEN, K., CHATTERJEE, B.K., GREIDER, P., KLOVNING, N., LILLETHUN, E., and PETERS, B., 1968, Nuovo Cimento, 53B, 241-263.

BLAKE, P.R., ALLAN, H.R., and NEAT, K.P., 1967, Calgary Conference (in the press).

BRADT, H.V., CLARK, G., LA POINTE, M., DOMINGO, V., ESCOBAR, I., KAMATA,K., MURAKAMI, K., SUGA, K., and TOYODA, Y., 1966, London Conference, 2, 715-717.

BRADT, H.V., and RAPPAPORT, S.A., 1967, Phys. Rev., 164, 1567-1583.

BRAY, A.D., CRAWFORD, D.F., JAUNCEY, D.L., McCUSKER, C.B.A., MELLEY, D., NELSON, D., POOLE, P.C., RATHGEBER, M.H., SEET, S.H., ULRICHS, J., WAND, R.H., and WINN, M.M., 1966, London Conference, 2, 668-671.

BULL, R.M., NASH, W.F., and RASTIN, B.C., 1965a, Nuovo Cimento, 40, 348-364.

BULL, R.M., NASH, W.F., and RASTIN, B.C., 1965b, Nuovo Cimento, 40, 365-384.

CHATTERJEE, B.K., MURTHY, G.T., NARANAN, S., SREEKANTAN, B.V., SRINIVASA RAO, M.V., and TONWAR, S.C., 1966, London Conference, 2, 627-631.

CLARK, G., EARL, J., KRAUSHAAR, W., LINSLEY, J., ROSSI, B., and SCHERB, F., 1958, Suppl. to Nuovo Cimento, 8, 623-652.

COCCONI, G., 1961, Handbuch der Physik, 46/1, 215-271.

COCCONI, G., KOESTER, L.G., and PERKINS, D.H., 1961, Lawrence Radiation Laboratory, High Energy Physics Study Seminars No. 28, part 2, UCID-1444, 1-36.

COLGATE, S.A., 1966, London Conference, 1, 112-115.

COWSIK, R., 1966, London Conference, 2, 656-659.

COXELL, H., 1961, Ph.D. Thesis, University of Durham.

COXELL, H., MEYER, M.A., SCULL, P.S., and WOLFENDALE, A.W., 1961, Suppl. to Nuovo Cimento, 21, 7-20.

DE BEER, J.F., CRANSHAW, T.E., and PARHAM, A.G., 1962, Phil. Mag., 7, 499-514.

DE BEER, J.F., HOLYOAK, B., WDOWCZYK, J., and WOLFENDALE, A.W., 1966, Proc. Phys. Soc., 89, 567-585.

DE BEER, J.F., HOLYOAK, B., ODA, H., WDOWCZYK, J., and WOLFENDALE, A.W., 1967, Calgary Conference (in the press).

DELVAILLE, J., KENDZIORSKI, F., and GREISEN, K., 1962, Kyoto Conference, AIII, 76-83.

EARL, J., 1959, M.I.T. Technical Report No. 70.

EARNSHAW, J.C., ORFORD, K.J., ROCHESTER, G.D., SOMOGYI, A.J., TURVER, K.E., and WALTON, A.B., 1967a, Proc. Phys. Soc., 90, 91-108.

EARNSHAW, J.C., MASLIN, G.C., and TURVER, K.E., 1967b, Calgary Conference (in the press).

EARNSHAW, J.C., ORFORD, K.J., ROCHESTER, G.D., TURVER, K.E., and WALTON, A.B., 1967c, Calgary Conference (in the press).

EARNSHAW, R.A., EVANS, A.C., HUGHES, R.R., REID, R.J.O., TENNENT, R.M., WATSON, A.A., and WILSON, J.G., 1967, Calgary Conference (in the press).

FIRKOWSKI, R., WDOWCZYK, J., and ZAWADZKI, A., 1967, Institute of Nuclear Research, Lodz, Report 'P' No. 803/VI PH.

FOWLER, P.H., ADAMS, R.A., COWEN, V.G., and KIDD, J.M., 1967, Proc. Roy. Soc., A, 301, 39-45.

GINZBURG, V.L., and SYROVATSKII, S.I., 1964, 'The Origin of Cosmic Rays', Oxford : Pergamon Press.

GREISEN, K., 1960, Ann. Rev. Nucl. Sci., 10, 63-108.

GREISEN, K., 1966a, London Conference, 2, 609-615.

GREISEN, K., 1966b, Phys. Rev. Letters, 16, 748-50.

HASEGAWA, H., MATANO, T., MIURA, I., ODA, M., SHIBATA, S., TANAHASHI, G., and TANAKA, Y., 1962, Kyoto Conference, AIII, 86-88.

HASEGAWA, H., NOMA, M., SUGA, K., and TOYODA, Y., 1966, London Conference, 2, 642-645.

HILLAS, A.M., 1966, London Conference, 2, 758-761.

HILLAS, A.M., 1967a, Physics Letters, 24A, 677-678.

HILLAS, A.M., 1967b, Calgary Conference (in the press).

IMAEDA, K., 1967, Nuovo Cimento, 48, 482-505.

KHRENOV, B.A., 1962, Soviety Physics - JETP, 14, 1001-1007.

LAL, S., 1967, Nuovo Cimento, 48A, 466-480.

LILLICRAP, S.C., 1963, Ph.D. Thesis, University of London.

LINSLEY, J., and SCARSI, L., 1962a, Phys. Rev. Letters, 9, 123-125.

LINSLEY, J., SCARSI, L., and ROSSI, B., 1962b, Kyoto Conference, AIII, 91-102.

LINSLEY, J., and SCARSI, L., 1962c, Phys. Rev., 128, 2384-2392.

LINSLEY, J., 1964, Jaipur Conference, 4, 77-99.

McCUSKER, C.B.A., PEAK, L.S., and RATHGEBER, M.H., 1968, University of Sydney Preprint.

MATANO, T., MIURA, I., NAGANO, M., ODA, M., SHIBATA, S., TANAKA, Y., TANAHASHI, G., and HASEGAWA, H., 1964, Jaipur Conference, 4, 129-142.

MATANO, T., NAGANO, M., SHIBATA, S., SUGA, K., TANAHASHI, G., and HASEGAWA, H., 1967, Calgary Conference (in the press).

NIKOLSKII, S.I., 1967, Soviet Physics - JETP, 24, 535-545.

NORMAN, R.J., 1956, Proc. Phys. Soc., A, 69, 804-820.

OREN, Y., 1959, Bull. Res. Coun. Israel, 8F, 103-112.

ORFORD, K.J., TURVER, K.E., and WALTON, A.B., 1967, Calgary Conference (in the press).

ORFORD, K.J., and TURVER, K.E., 1968, Nature (in the press).

REGENER, M.V., 1951, Phys. Rev., 84, 161-162.

ROCHESTER, G.D., SOMOGYI, A.J., TURVER, K.E., and WALTON, A.B., 1966, London Conference, 2, 765-768.

ROLL, P.G., and WILKINSON, D.T., 1967, Annals of Physics, 44, 289-321.

ROSSI, B., 1952, 'High Energy Particles', Prentice Hall Inc.

SALMERON, R.A., 1963, Cern Report 63-20.

SHIBATA, S., NAGANO, M., MATANO, T., SUGA, K., and HASEGAWA, H., 1966, London Conference, 2, 672-675.

SOMOGYI, A.J., 1966, Ann. der Physik, 17, 221-232.

STERNHEIMER, R.M., 1959, Phys. Rev., 115, 137-142.

SWINSON, D.B., and PRESCOTT, J.R., 1966, London Conference, 2, 721-723.

SUESS, H.E., and UREY, H.C., 1956, Rev. Mod. Phys., 28, 53-74.

SURI, A.N., 1966, Ph.D. Thesis, University of Leeds.

TENNENT, R.M., 1967a, Proc. Phys. Soc., 92, 622-631.

TENNENT, R.M., 1967b, Calgary Conference (in the press).

THIELHEIM, K.O., and KARIUS, S., 1966, London Conference, 2, 779-782.

TOYODA, Y., SUGA, K., MURAKAMI, K., HASEGAWA, H., SHIBATA, S., DOMINGO, V., ESCOBAR, I., KAMATA, K., BRADT, H.V., CLARK, G., and LA POINTE, M., 1966, London Conference, 2, 708-711.

WALTON, A.B., 1966, M.Sc. Thesis, University of Durham.

WINN, M.M., WAND, R.H., ULRICHS, J., RATHGEBER, M.H., POOLE, P.C., NELSON, D., McCUSKER, C.B.A., JAUNCEY, D.L., CRAWFORD, D.F., and BRAY, A.D., 1965, Nuovo Cimento, 36, 701-732.

WOLFENDALE, A.W., 1963, 'Cosmic Rays', London : Newnes Ltd.

ZATSEPIN, G.T., NIKOLSKII, S.I., and KHRISTIANSEN, G.B., 1964, Jaipur Conference, 4, 100-126.

ACKNOWLEDGEMENTS

I am deeply indebted to Professor G. D. Rochester, F.R.S., for the privilege of working at Haverah Park under his supervision and for his interest at all times.

The constant encouragement, advice and help of Dr. K. E. Turver are gratefully acknowledged.

I wish to thank the other members of the Durham University group at Haverah Park, Professor A. J. Somogyi and Messrs. A. B. Walton, K. J. Orford, and G. C. Maslin for their contributions to the work presented in this thesis.

Professor J. G. Wilson and the members of the Leeds University group at Haverah Park are thanked for their cooperation and for the results of the analysis of showers detected by the 500 m array. Dr. J. K. Pidcock is thanked for the analysis of many showers from the 50 m array.

The ready assistance of the technical staff of the Physics Department of Durham University, especially Mr. W. Leslie and Miss A. M. Bevils, has been invaluable.

The Science Research Council is thanked for the provision of a Research Studentship.

I wish to thank my wife for her assistance in many ways, and particularly for drawing the figures for this thesis.

Mrs. J. Moore, who typed this thesis, is gratefully thanked.